ParisTech
INSTITUT DES SCIENCES ET TECHNOLOGIES
PARIS INSTITUTE OF TECHNOLOGY

TELECOM ParisTech

2013 ENST 0040

EDITE - ED 130

Doctorat ParisTech

T H È S E

pour obtenir le grade de docteur délivré par

TELECOM ParisTech

Spécialité « Electronique et Communication »

présentée et soutenue publiquement par

Wael GUIBENE

le 2 Juillet 2013

Contributions to Spectrum Sensing and Cognitive Radio Systems

Directeur de thèse : **Dirk SLOCK**

Jury
M. Raymond KNOPP, Professeur, Communication Systems, EURECOM, France
M. Jacques PALICOT, Professeur, Equipe SCEE, CentraleSupelec, France
M. Luc DENEIRE, Professeur, Equipe SIGNAL, Universite Nice-Sophia Antipolis, France
Mme. Aawatif HAYAR, Professeure, GREENTIC, Univ. Hassan II, Maroc
M. Oliver HOLLAND, Chercheur, CTR, King's College London, UK

TELECOM ParisTech
école de l'Institut Télécom - membre de ParisTech

THÈSE

Acknowledgements

I would like first to thank Prof. Dirk Slock, my supervisor, for accepting to pursue this Ph.D adventure with me. I am also grateful to Prof. Aawatif Hayar for being my first thesis supervisor and giving me the opportunity to start my Ph.D at EURECOM.
Also, I would like to thank my thesis jury members, Prof. Jacques Palicot and Prof. Luc Deneire for their time. I would also express my gratitude to Dr. Oliver Holland, Prof. Raymond Knopp and Prof. Awatif Hayar for being the examiners of my Ph.D defense.
I would also thank many friends at EURECOM and my colleges in the Mobile Communications Department for their support. I am also thankful to Prof. David Gesbert, head of department, for his time, his sympathy and his availability.
Many thanks also to the IT, secretariat and human resource departments for making it too easy to travel all around the world for conferences and for making life much easier at EURECOM.
I am also thankful to many people out of EURECOM circle, Professor Monia Turki from École Nationale d'Ingénieurs de Tunis for her valuable remarks and the fruitful cooperation we had and Professor Meriem Jaïdane for her encouragements. I would like also to thanks Dr. Chadi Khirallah from University of Edinburgh for the fantastic cooperation we had. I would also like to thank Dr. Hessam Moussavinik from Norwegian University of Science and Technology (NTNU) for the great collaboration we had when he was visiting researcher at EURECOM.
Finally, I would never thank enough my parents for their unconditional support, their love and their trust, but also my wife for being that patient and comprehensive, especially during the last months of the Thesis.

To my parents...

Sophia Antipolis, 2013
Waël Guibène

Contents

List of Figures

List of Tables

CHAPTER 1

Introduction

Motivation and Objectives

Over the last decades, we have witnessed a great progress and an increasing need for wireless communications systems due to customers' demand of more flexible, wireless, smaller, more intelligent and practical devices explaining markets invaded by smartphones, personal digital assistant (PDAs), tablets and netbooks. One area of focus for addressing this challenge is radio frequency (RF) spectrum. While almost all RF spectrum is allocated [1], most of it is either unused or underutilized [1]. The current spectrum allocation process for wireless communications is highly inefficient, leading to significant underutilization of spectrum in the face of explosive growth in demand. For example, in June 2010, Obama Administration ordered the National Telecommunications and Information Administration (NTIA) to work with the Federal Communications Commission (FCC) "to make available a total of 500 MHz of federal and nonfederal spectrum over the next 10 years, suitable for both mobile and fixed wireless broadband use" [2]. As a result, the NTIA, FCC, and other organizations are closely examining the current allocation and usage of RF spectrum to identify candidate spectrum bands for reallocation, sharing and enabling dynamic spectrum access (DSA).
Historically, cognitive radio (CR) was introduced by Mitola [3, 4], as one of the possible devices that could be deployed as users equipments and systems in wireless networks to enable dynamic spectrum access DSA and spectrum sharing. As originally defined, a CR is a self aware and "intelligent" device that can adapt itself to the wireless environment changes. Such device is able to detect changes in wireless network to which it is connected and adapt its radio parameters to the new opportunities that are detected.
Another interesting definition of cognitive radio systems was given by ITU-R in [5]: "a radio system employing technology that allows the system to obtain knowledge of its operational and geographical environment, established policies and its internal state; to dynamically and autonomously adjust its operational parameters and protocols according to its obtained knowledge in order to achieve predefined objectives; and to learn from the results obtained".
The main functions of Cognitive Radios are [6, 7]:

- Spectrum sensing: which is an important requirement towards CR implementation and feasibility as the CR detects the available spectrum opportunities (also called Spectrum

Holes or Spectrum White Spaces) as depicted in Figure (1.1). Three main strategies exist in order to perform spectrum sensing: Transmitter detection (involving PU detection techniques), cooperative detection (involving centralized and distributed schemes) and interference based detection.

- Spectrum management: which captures the most satisfying spectrum opportunities in order to meet both PU (primary users) and SU (secondary users) quality of service (QoS).
- Spectrum mobility: which involves mechanisms and protocols allowing frequency hopes and dynamic spectrum use.
- Spectrum sharing: which aims at providing a fair spectrum sharing strategy in order to serve the maximum number of SUs.

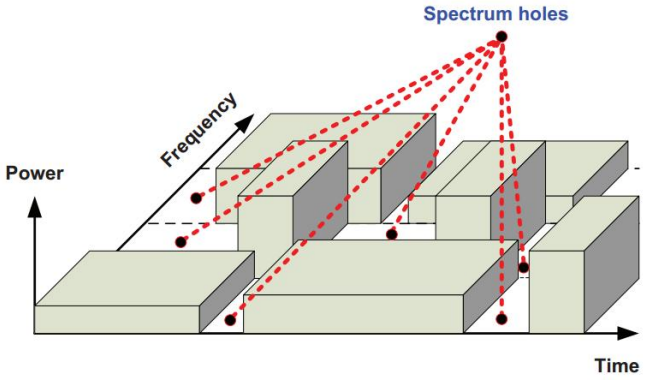

Figure 1.1: Spectrum Opportunities

Another system definition was given by FCC in [8]. In this definition, FCC considers a radio to be cognitive when it have the following capabilities:

- Frequency Agility: the ability of a radio to change its operating frequency to optimize use under certain conditions.
- Dynamic Frequency Selection: the ability to sense signals from other nearby transmitters in an effort to choose an optimum operating environment
- Location Awareness: the ability for a device to determine its location and the position of other transmitters, that would help selecting the appropriate operating parameters such as transmit power and frequencies allowed at that given location.

- Negotiated Use: incorporate a mechanism that would enable sharing of spectrum under the terms of a prearranged agreement between a licensed (primary) and non-licensed (secondary) users

- Adaptive Modulation: the ability to modify and adapt transmission characteristics and waveforms to exploit opportunities to use spectrum.

- Transmit Power Control: allows transmission at full power limits when necessary

The main objective of this work is to provide some contributions to the most important features enabling cognitive radio technology: spectrum sensing, spectrum awareness and network discovery through cooperative PU sensing and localization.

Structure and Contributions

The work presented within this thesis [1] fits in the context of spectrum sensing / spectrum awareness and network discovery mechanisms.
Chapter 1 is dedicated to recall some useful definitions and paradigms of cognitive radio. We start by presenting the goals and several issues of spectrum sensing then we introduce some state of the art sensing algorithms. Among those algorithms, we select some reference algorithms to be studied and simulated in terms of performance, receiver operating characteristic, energy efficiency curves as well as complexity study. Then, our contributions are presented as following:

- In **Chapter 2** [J1, C8-9, C14-15], we propose to study a novel multiband spectrum sensing technique based on a reconfigurable filter bank. The proposed algorithm locates some important frequencies in the RF spectrum characterized by transitions from free to used bands. PU transmission is thus located and sensing is done by means of enhanced energy detection algorithm.

- Similarly to what was presented by *Tian* and *Giannakis* in the context of wideband compressed sensing, in **Chapter 3** [C11-12], we present a wideband compressed sensing algorithm combining our frequency edge location algorithm to compressed sensing formalism. The main advantage in our approach is that contrarily to the wavelet approach of Tian *et al*, our frequency edge location algorithm is a one shot, online (operating frame by frame) non iterative algorithm.

[1] The work presented is funded by European projects: SACRA (spectrum and energy efficiency through multiband cognitive radio), SPECTRA (Spectrum and energy efficiency in 4G communication systems and beyond) and WHERE2 (Wireless Hybrid Enhanced Mobile Radio Estimators).

- In **Chapter 4** [C3, C7], we propose to address the problem of signal classification in heterogeneous cognitive systems. The approach is a two-step algorithm: first of all, by means of blind source separation, we separate the mixture of the received signal at the level of the CR and then, thanks to a hybrid architecture we are able to blindly discriminate the present standard in a sensed band (LTE, DVB-T or PMSE signals).

- In **Chapter 5** [C1], we propose to go further in the analysis of spectrum awareness by proposing another contribution for co-existence of different standards in the same band case. Such case occurs when the PU pops back in its bands while the SU is communicating. In this context we propose a Computer-Vision aided Cyclostationary Features Detection (CV-CFD) algorithm capable of detecting DVB-T or PMSE signals while an LTE system is transmitting in a considerably small time interval.

- In **Chapter 6** [J2, C5-6], we propose to focus on an other main enabling aspect of CR technology, which is location awareness. In this chapter, we analyze the equations related to spectrum sensing and PU location estimation with taking into consideration the hardware limitation that often CR terminals suffer from: Analog to Digital Converters acquiring signals at a sub-Nyquist rate. In this chapter we make the link between localization, spectrum sensing and compressed sensing. In this framework, we propose to study sensing/localization using Basis Pursuit (BP), Orthogonal Matching Pursuit (OMP) and Compressive Sampling Matching Pursuit (CoSaMP). The simulations results in a realistic network topology testify on the effectiveness of the proposed formalism.

Finally, in **Chapter 7** we conclude about the presented work, highlight its limitations and suggest new research directions.
The work conducted in this thesis lead to several disseminations:

Journals

J1- **W. Guibene**, M. Turki, B. Zayen and A. Hayar, *Spectrum sensing for cognitive radio exploiting spectrum discontinuities detection*, EURASIP JWCN, EURASIP Journal on Wireless Communications and Networking, Special Issue on 10 Years of Cognitive Radio, 2012.

J2- **W. Guibene**, and D. Slock, *Cooperative Spectrum Sensing and Localization in Cognitive Radio Systems*, Hindawi Journal of Sensors, Special Issue on Sensing Systems for Radio Context Awareness, *under review*.

Conferences

C1- **W. Guibene**,C.Khirallah, D. Slock, J.Thompson, *Computer Vision aided OFDM-based Standards Detection and Classification Technique for Cognitive Radio Systems*, ICASSP'13, The 38th International Conference on Acoustics, Speech, and Signal Processing (ICASSP), 26-31 May, Vancouver, Canada.

C2- **W. Guibene**, D. Slock, *Degrees of Freedom of Downlink Single- and Multi-Cell Multi-User MIMO Systems with Location based CSIT*, VTC-Spring'13, The 2013 IEEE 77th Vehicular Technology Conference (VTC-Spring), 2-5 June 2013, Dresden, Germany.

C3- **W. Guibene**, D. Slock, *Signal Classification in OFDM-based Cognitive Radio Systems*, ICT'13, The 20 International Conference on Telecommunications, The 20 International Conference on Telecommunications, 6-8 May 2013, Casablanca, Morocco.

C4- **W. Guibene**, C.Khirallah, D. Vukobratovic, D. Slock, J.Thompson, *Energy-Aware Multi-band Communications in Heterogeneous Networks*, ICT'13, The 20 International Conference on Telecommunications, 6-8 May 2013, Casablanca, Morocco.

C5- **W. Guibene**, D. Slock, *A Combined Spectrum Sensing and Terminals Localization Technique for Cognitive Radio Networks*, WiMob12, The 8th IEEE International Conference on Wireless and Mobile Computing, Networking and Communications, October 810, 2012, Barcelona, Spain.

C6- **W. Guibene**, D. Slock, *A Compressive Sampling Approach for Spectrum Sensing and Terminals Localization in Cognitive Radio Networks*, CAMAD'12, IEEE 17th International Workshop on Computer Aided Modeling and Design of Communication Links and Networks 2012, September 17–19, 2012, Barcelona, Spain.

C7- **W. Guibene**, D. Slock, *Signal Separation and Classification Algorithm for Cognitive Radio Networks*, ISWCS'12, The 9th International Symposium on Wireless Communication Systems, August 28-31, 2012, Paris, France

C8- A. Ben Jemaa, M. Turki, **W. Guibene**, *Enhanced Energy Detector Via Algebraic Approach for Spectrum Sensing in Cognitive Radio Networks*, CrownCom'12, 7th International Conference on Cognitive Radio Oriented Wireless Networks, June 18ï–20, 2012 Stockholm, Sweden.

C9- **W. Guibene**, M. Turki, A. Hayar and D. Slock, *A Complete Framework for Spectrum Sensing based on Spectrum Change Points Detection for Wideband Signals*, 2012 IEEE

75th Vehicular Technology Conference: VTC-Spring'12, 6-9 May 2012, Yokohama, Japan.

C10- **W. Guibene** and D. Slock, *Spectrum sensing for cognitive radio exploiting spectral masks*, CogART'11, International Conference on Cognitive Radio and Advanced Spectrum Management, October 26-29 October 2011, Barcelona, Catalonia, Spain.

C11- **W. Guibene**, H. Moussavinik and A. Hayar, *Combined compressive sampling and distribution discontinuities detection approach to wideband spectrum sensing for cognitive radios*, ICUMT'11, International Conference on Ultra Modern Telecommunications, October 5-7 2011, Budapest, Hungary.

C12- **W. Guibene** and A. Hayar, *Joint time-frequency spectrum sensing for cognitive radio*, CogART'10, 3rd International Workshop on Cognitive Radio and Advanced Spectrum Management, November 07-10 2010, Rome, Italy, **Best Student Paper Award**.

C13- H. Moussavinik, **W. Guibene**, A. Hayar, *Centralized collaborative compressed sensing of wideband spectrum for cognitive radios*, ICUMT'10, International Conference on Ultra Modern Telecommunications, October 18-20 2010, Moscow, Russia.

C14- B. Zayen, **W. Guibene** and A. Hayar, *Performance comparison for low complexity blind sensing techniques in cognitive radio systems*, CIP'10, 2nd International Workshop on Cognitive Information Processing, June 14-16 2010, Elba Island, Tuscany, Italy.

C15- **W. Guibene**, A. Hayar and M. Turki, *Distribution discontinuities detection using algebraic technique for spectrum sensing in cognitive radio networks*, CrownCom'10, 5th International Conference on Cognitive Radio Oriented Wireless Networks and Communications, June 9-11 2010, Cannes, France.

Project Deliverables

D1- SACRA D2.1 - Preliminary Report on Sensing and Access Techniques Design

D2- SACRA D2.2 - Specification of signal classification techniques for cognitive radios (Editor)

D3- SACRA D2.5 - Development and evaluation of energy efficient multiband spectrum sensing algorithms

D4- SACRA D3.1 - Cognitive RRM outer and inner loop architecture

D5- SACRA D3.4 - Cooperative and Cognitive RRM components and architecture for the SACRA scenarios

D6- SACRA D6.2 - Integration specification

D7- SACRA D6.3 - Report on the Implementation of selected algorithms

D8- ACROPOLIS D9.1 - Report on Spectrum Sensing

D9- WHERE-2 D3.6 - Location-aided PHY/MAC layer design for advanced cognitive radios

D10- SPECTRA D2.1 - Development and evaluation of energy efficient multiband spectrum sensing algorithms and provision of portable waveforms (Editor)

D11- SPECTRA D2.2 - Mixed-signals separation algorithms (Editor)

Part I

Spectrum Sensing Techniques for Cognitive Radio Systems

CHAPTER 2

Spectrum Sensing for Cognitive Radio Systems

2.1 Introduction

As previously stated, spectrum sensing is the first challenging task that have to be achieved by the cognitive terminal in order to build a local map of unused resources. In this chapter, we aim at presenting a deeper look to spectrum sensing in cognitive radio systems. We start by presenting spectrum sensing principles and challenges. We also present some well-known state of the art sensing techniques. There actually exist two big families of spectrum sensing techniques: coherent and blind techniques. In our work we focus on developing blind sensing techniques. Furthermore, we explicit some examples of feature spectrum sensing algorithms including the cyclostationary features detector and the autocorrelation based detector, and as example of blind sensing algorithms including the energy detector, the eigenvalue based detectors. We give in this chapter simulations related to the detectors in order to assess their performance in different channel conditions. These detectors will serve as reference detectors for our work.

2.2 Spectrum Sensing Challenges

Before getting into spectrum sensing techniques details, we give some challenges associated to spectrum sensing for CR:

Sensing Time Spectrum sensing is the phase during which the SU is supposed to decide about the PU presence/absence in its allocated band. The period of time, that is taken by the SU to perform this sensing task is called Sensing Time and is challenging for at least two reasons. In TDD systems, this period is a pure waste of resources for the SU transmission time as $Frame_{Time} = Sensing_{Time} + Transmission_{Time}$. Thus, the sensing time is supposed to be kept as small as possible in order to fully exploit the available resources. In the other hand, the decision rules (as explained in the next

sections) are function of sensing time and the longer the sensing period is, the more reliable the decision is. So here is a first dilemma for spectrum sensing [9].

Complexity Another challenging aspect is the computational complexity, as the more the spectrum sensing algorithm is computationally demanding, the hardest and more energy consuming it gets when implemented on real-time systems. That is why one of the challenges today towards implementing CR systems is to develop low complexity sensing techniques.

Cooperation In CR systems the problem of shadowing and fading is a prominent issue. As several nodes in the network could not receive enough power of the PU signal (in case of energy detection for example) and decide on its absence when it is actually present in its allocated band. To overcome this issue, multiple SUs can be coordinated to perform spectrum sensing cooperatively. Several recent works have shown that cooperative spectrum sensing can greatly increase the probability of detection in fading channels [10].

Other Challenges Some other challenges that need to be considered while designing effective spectrum sensing algorithm include: hardware requirements, presence of multiple SUs, degrees of knowledge about the PUs, coherence times, multi-path and shadowing, competition, robustness and power consumption [9].

2.3 Spectrum Sensing Goal

The received signal at time n, denoted by y_n, can be modeled as:

$$y_n = A_n s_n + e_n \tag{2.1}$$

where A_n is the transmission channel gain, s_n is the transmitted signal sent from the primary user (PU), and e_n is an additive noise.
In order to avoid interferences with the primary (licensed) system, the CR needs to sense its radio environment whenever it wants to access available spectrum resources. The goal of spectrum sensing is to decide between two conventional hypotheses modeling the spectrum occupancy:

$$y_n = \begin{cases} e_n & \mathcal{H}_0 : \text{Decide that received signal is only noise} \\ A_n s_n + e_n & \mathcal{H}_1 : \text{Decide that received signal is signal plus noise} \end{cases} \tag{2.2}$$

The sensed sub-band is assumed to be a white area if it contains only a noise component, as defined in $\mathcal{H}_0$; while, once there exist PU signals drowned in noise in a specific band, as defined in $\mathcal{H}_1$, we decide that the band is occupied. The key parameters of all spectrum

sensing algorithms are the false alarm probability P_F and the detection probability P_D. P_F is the probability that the sensed sub-band is classified as it contains a PU data while actually it is only a noise signal, thus P_F should be kept as small as possible. On the other hand, P_D is the probability of classifying the sensed sub-band as a PU data when it is truly present, thus sensing algorithms tend to maximize P_D.
In order to design the optimal detector based on Neyman-Pearson criterion, the aim is to maximize the overall P_D under a given overall minimal P_F. Based on these definitions, P_F is the probability of the spectrum detector sensing a user signal given the hypothesis H_0, and is given by:

$$P_F = P(\mathcal{H}_1 \mid \mathcal{H}_0) = P(\text{ PU is detected} \mid \mathcal{H}_0) \tag{2.3}$$

while P_D is the probability of the spectrum detector sensing a user signal under the hypothesis $\mathcal{H}_1$. P_D is given by:

$$\begin{aligned} P_D &= 1 - P_M = 1 - P(\mathcal{H}_0 \mid \mathcal{H}_1) \\ &= 1 - P(\text{ PU is not detected} \mid \mathcal{H}_1) \end{aligned} \tag{2.4}$$

where P_M indicates the probability of missed detection.
In order to decide about the presence or absence of a signal in a given sensed band, a decision threshold that is determined based on the required P_F needs to be known at the SU. The threshold γ for a given value of P_F is determined by solving the following equation:

$$P_F = P(y_n \text{ is present} \mid \mathcal{H}_0) = 1 - F_{\mathcal{H}_0}(\gamma) \tag{2.5}$$

where $F_{\mathcal{H}_0}$ denotes the cumulative distribution function (CDF) under $\mathcal{H}_0$.

2.4 Single Node Spectrum Sensing Techniques

As depicted in Figure (2.1), single node spectrum sensing techniques are divided into two families [6]:

Non Coherent Single Node Techniques Non coherent spectrum sensing techniques do not need any coordination, coherence, synchronization between the PU and the SU. Many techniques have been developed in this context, such as energy detection, eigenvalues based detection, model selection algorithms, etc. The main advantage of such technique is their potential blind behavior.

Coherent Single Node Techniques Some other techniques need a perfect synchronization between PUs and SUs in the network in order to perform sensing. Many techniques

have been proposed in the literature such as cyclostationary features detection (CFD), sparsity based CFD, matched filters, pilot based detection, etc. The main drawback of those techniques is the need of perfect synchronization in the network, but these techniques exploit some apriori PU statistics or features while performing sensing, which result in more performing techniques.

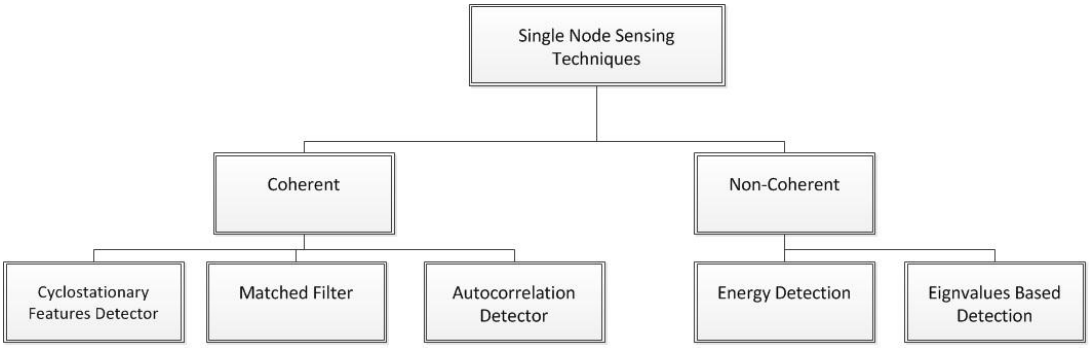

Figure 2.1: Classification of State of The Art Sensing Techniques

2.4.1 Non Coherent Techniques

Many blind techniques were presented in the state of the art. The most common technique is Energy Detector (ED) [11] which implementation is as simple as a radiometer. A second technique is Eigenvalues based Detection [13,14]. More recently, two hybrid detectors combining Energy Detection and Cyclostationary Features Detection (CFD) was proposed by [18,19,21]. The first detector [18] iteratively adjusts the ED threshold to converge towards the CFD performance. In the second algorithm [19], the CFD is used to estimate noise statistics and feed the ED threshold. The second detector is shown to outperform conventional CFD.
From these algorithms, we propose to give the mathematical details behind ED and CFD and to study their performance under different channels conditions.

2.4.1.1 Energy Detection

Energy detection is the most common method for spectrum sensing because of its non-coherency and extreme low complexity. Energy detector can be simply implemented like spectrum analyzer. The energy detector measures the received energy during a finite time interval and compares it to a predetermined threshold. That is, the test statistic of the energy detector

is [11]

$$\Upsilon_{ED}(\mathbf{x}) = \sum_{i=1}^{p} |x_i|^2 \tag{2.6}$$

The performance of the energy detector in additive white Gaussian noise (AWGN) is well-known, and can be written in closed form. The probability of false alarm is given by

$$P_{FA,ED} = 1 - G\left(\frac{2\gamma_{ED}}{\sigma^2}, p\right) \tag{2.7}$$

where G is the cumulative distribution function [12] of a χ^2 distributed random variable with $2p$ degrees of freedom, γ_{ED} is the detection threshold, and σ^2 is the noise variance [11].
The energy detector is a blind technique in the sense that it does not require any knowledge about the PU signal to be detected. On the other hand, for the same reason it does not exploit any potentially available knowledge about the signal. Moreover, the noise power needs to be known to set the decision threshold and control the false alarm probability. It is very common that the noise power levels vary depending on time and location. Consequently, there may be a need to estimate the noise power from a signal-free data set in order to obtain constant false alarm probability detector performance.

2.4.1.2 Eignevalues Based Detection

In [13] and [14], two sensing algorithms were suggested. The first is based on the ratio of the maximum eigenvalue to minimum eigenvalue. The second is based on the ratio of the average eigenvalue to minimum eigenvalue. Assume that the signal to be detected is highly correlated. Let $\mathbf{R}$ be the covariance matrix of the received signal. Then, under $\mathcal{H}_0$, all eigenvalues of $\mathbf{R}$ are equal. However, under $\mathcal{H}_1$ some eigenvalues of $\mathbf{R}$ will be larger than the others. Detector exploiting this property, called Eigenvalue Detector (EiD), was proposed in [13], and will be described briefly afterwards. Consider N observations $\mathbf{x}_n$ received in a sequence. We define the sample covariance matrix as:

$$\hat{\mathbf{R}} = \frac{1}{N}\sum_{n=1}^{N} \mathbf{x}_n \mathbf{x}_n^T \tag{2.8}$$

Let $\lambda_n|_{n=1,\ldots,N}$, be the eigenvalues of $\mathbf{R}$. There are two eigenvalue-based detectors proposed in [13]. The first detector uses the ratio of the largest eigenvalue to the smallest eigenvalue, and compares it to a threshold. That is, the test statistic of the first proposal of [13] is based on condition number

$$\Upsilon_{EiD}(\mathbf{x}) = \frac{\max \lambda_n}{\min \lambda_n} \tag{2.9}$$

The probability of false alarm of the EiD is given by:

$$P_{FA,EiD} = 1 - F_1\left(\frac{\gamma_{EiD}\left(\sqrt{N}-\sqrt{p}\right)^2 - \left(\sqrt{N-1}-\sqrt{p}\right)^2}{\left(\sqrt{N-1}-\sqrt{p}\right)\left(\frac{1}{\sqrt{N-1}}+\frac{1}{\sqrt{p}}\right)^{\frac{1}{3}}}\right) \quad (2.10)$$

where F_1 is the cumulative distribution function (CDF) of the Tracy-Widom distribution of order 1, N is the number of PU observations and p is the length of each observation. The distribution function is defined as

$$F_1 = \exp\left(-\frac{1}{2}\int_t^\infty \left(q(u) + (u-t)q^2(u)\right) du\right) \quad (2.11)$$

where $q(u)$ is the solution of the nonlinear Painleve II differential equation

$$q"(u) = uq(u) + 2q^3(u) \quad (2.12)$$

With the above expressions for the probability of false alarm, the expected detection performance can be evaluated.

2.4.2 Coherent Techniques

Many coherent techniques needing synchronization between PUs and SUs were presented in literature. First of all CFD [15, 17], where the objective is to detect the cyclic signature of the PU transmission. We may also autocorrelation detectors (ACD) [57] which estimate at some time lags non null properties of the digitally modulated signals. More recently, in [20], a compressed sensing (CS) based CFD algorithm was proposed. The goal was detect the cyclic frequencies by means of CS tools.
From the various coherent techniques, we propose to study CFD and ACD

2.4.2.1 Cyclostationary Features Detection

The most known feature sensing technique is the CFD [15], [17]. Cyclostationary processes are random processes for which statistical properties such as mean and autocorrelation change periodically as a function of time. Wireless communication signals typically exhibit cyclostationary properties at multiple cyclic frequencies that may be related to the carrier frequency, symbol, chip, code, or hop rates, as well as their harmonics, sums, and differences. These features can be exploited to design powerful sensing algorithms for cognitive radios. Cyclostationary Feature Detectors (CFD) have the potential to distinguish among the PU and SU signals as they exhibit cyclostationary features at different cyclic frequencies. Moreover,

random noise commonly does not possess cyclostationary properties. Cyclostationary feature detection (CFD) has received considerable amount of attention in the literature. Recent bibliography on cyclostationarity, including a large number of references on cyclostationarity based detection, is provided in [16]. The cyclic autocorrelation function at some lag l and some cyclic frequency α can be estimated from samples $\mathbf{x}$ by

$$\hat{r}_l(\mathbf{x}, \alpha) = \frac{1}{p-l} \sum_{n=0}^{p-l-1} x_{n+l} x_n^* e^{-j\alpha n} \qquad l \geq 0 \tag{2.13}$$

In order to detect cyclostationary features for a given signal, we make the choice of the statistical test proposed by Dandawate and Giannakis [15]. It has been shown in [15] that under hypothesis H_0, regardless of the distribution of the input data, the distribution of $T(\mathbf{x})$ converges asymptotically to a central χ^2 distribution with $2p$ degrees of freedom where p is an integer such as $p \geq 1$. This makes it possible to analytically calculate the probability of false alarm for large enough observation length T for a given threshold, leading to an asymptotically constant false alarm rate test. One can write under H_0:

$$\lim_{T \to \infty} \Upsilon_{CFD}(\mathbf{x}) = \chi^2_{2p} \tag{2.14}$$

Hence, the (asymptotic) probability of false alarm for this detector with threshold γ_{CFD} is given by

$$P_{FA,CD} = 1 - G\left(\frac{\gamma_{CFD}}{2}, K\right) \tag{2.15}$$

where $G(a, x)$ is the (lower) incomplete gamma function [12].
The main advantage of the cyclic autocorrelation function is that it differentiates the noise from modulated signal. Therefore, CFD can perform better than other detectors in discriminating against noise due to its robustness to the uncertainty in noise. However, it is computationally complex and requires significantly long observation time.

2.4.2.2 Autocorrelation based Detection

Many communication signals contain redundancy, introduced for example to facilitate synchronization by channel coding or to circumvent inter-symbol interference. This redundancy occurs as non-zero average autocorrelation at a certain time lag l. The autocorrelation function at l can be estimated from:

$$\hat{r}_l(\mathbf{y}) = \frac{1}{p-l} \sum_{n=0}^{p-l-1} y_{n+l}\, y_n^* \qquad l \geq 0 \tag{2.16}$$

Any signal, except white noise signal, will have non-zero autocorrelation function values at specific time lags larger than zero.
To detect the existence/non-existence of OFDM signals we can use functions of the autocorrelation lags, where the autocorrelation is based on (5.14). Therefore, the autocorrelation-based decision statistic is given by [57]

$$\Upsilon_{ACD}(\mathbf{y}) = \sum_{l=1}^{L} w_l \frac{\mathrm{Re}\{\hat{r}_l\}}{\hat{r}_0} \tag{2.17}$$

where the number of lags, L, is selected to be an odd number. The weighting coefficients w_l could be computed to achieve the optimal performance, and is given by:

$$w_l = \frac{L+1+|l|}{L+1} \tag{2.18}$$

With decision threshold γ_{ACD}, the probability of false alarm of this detector is

$$P_{FA,ACD} = Q\left(\gamma_{ACD}\left[\frac{\gamma_{ACD}^2}{p} + \frac{1}{2p}\sum_{l=1}^{L} w_l^2\right]^{-\frac{1}{2}}\right) \tag{2.19}$$

where Q is the generalized Marcum Q-function [12].

2.5 Assessing Performance and Energy Efficiency for Single Node Spectrum Sensing Techniques

2.5.1 Single Node Performance Evaluation

2.5.1.1 Evaluation Framework

In our evaluation framework we focus on the single node detection techniques. The primary system used is a DVB-T system. The standard is administered by the European Telecommunications Standards Institute (ETSI) [22]. In DVB-T, there are two modes in 8 MHz channel, 2K and 8K modes, which set the number of carriers in the OFDM symbol. In 2K and 8K modes there are actually 1,705 or 6,817 subcarriers and subcarriers are approximately 4 or 1 KHz apart, respectively. Three different modulation schemes (QPSK, 16QAM, 64QAM) can be used. As a digital transmission, DVB-T delivers data at the symbol rate in a series of discrete blocks. In DVB-T, a coded OFDM (COFDM) transmission technique including variable length guard interval is used. The choice of the DVB-T system is justified by the fact that many of the current and especially future wireless systems utilize the OFDM modulation format. In addition, one target is to study secondary use, i.e. spectrum sensing, of the spectrum in the UHF band, extended to TVWS (TV white space) where DVB-T is utilized in the

frequency range above 470 MHz. The simulation scenarios are generated by using different combinations of parameters given in Table 2.1. The simulated channel models are AWGN and Rayleigh channels. Two different scenarios with different properties are chosen to evaluate the

Bandwidth	8MHz
Mode	2K
Guard interval	1/4
Frequency-flat	Single path
Sensing time	1.5ms
Location variability	10dB

Table 2.1: Simulated DVB-T signal parameters

spectral detection performance, subject to provide different attributes so that the performance can be assessed under different conditions, aiming to provide fair conditions before making conclusions. OFDM is the modulation of choice for the two simulation scenarios to be used as evaluation tools in this chapter. In OFDM, a wideband channel is divided into a set of narrowband orthogonal subchannels. OFDM modulation is implemented through digital signal processing via to the FFT algorithm [23].

1. Scenario 1 uses a DVB-T OFDM signal in an AWGN channel. It is assumed that the detection performance in AWGN will provide a good impression of the performance, but it is necessary to extend the simulations to include signal distortion due to multipath and shadow fading.

2. Scenario 2 utilizes the same DVB-T OFDM signal as scenario 1, but to make the simulations more realistic, the signal is subjected to Rayleigh multipath fading and shadowing following a log normal distribution in addition to the AWGN. The maximum Doppler shift of the channel is 100Hz and the standard deviation for the log normal shadowing is 10dB. Since the fading causes the channel to be time variant, it is necessary to apply longer averaging than in scenario 1 to obtain good simulation results. Thus the number of iterations in the Monte Carlo simulation is increased from 500 to 1000.

2.5.1.2 Simulation Results

Two key metrics are considered in our evaluation, performance curves (P_D Vs. SNR at fixed P_{FA} and Sensing Period) and Receiver Operating Characteristic (ROC) curves (P_D Vs. P_{FA} at fixed SNR and Sensing Period). The performance curve is the answer to the question: up to which SNR region can we trust a given detector ? As for IEEE 802.22 compatible scenarios,

we will look at the performance for $P_D > 90\%$ and a $P_{FA} < 10\%$. Meanwhile the ROC curve is the answer to the question: is the detector compliant with the Neyman-Pearson criteria, i.e does it tend to maximize P_D while minimizing P_{FA} ?

Figure (2.2), reports the figures for the first evaluation scenario, i.e transmission over an AWGN channel. A very first remark could be that for our area of interest (i.e. $P_D > 90\%$), the detectors can be classified as following from the less to most performing: ED, EiD, ACD, CFD. In subfigure (a), we notice that the ED, EiD, ACD and CFD are trustable up to -5.5dB, -7.5dB, -10dB and -11dB respectively at $P_{FA} = 5\%$ and sensing time of 1.5 ms. Figure (b) show that at -10dB the only detectors that satisfy the Neyman-Peason criteria are the CFD and ACD. Figure (2.3), reports the figures for the second evaluation scenario, i.e transmission over

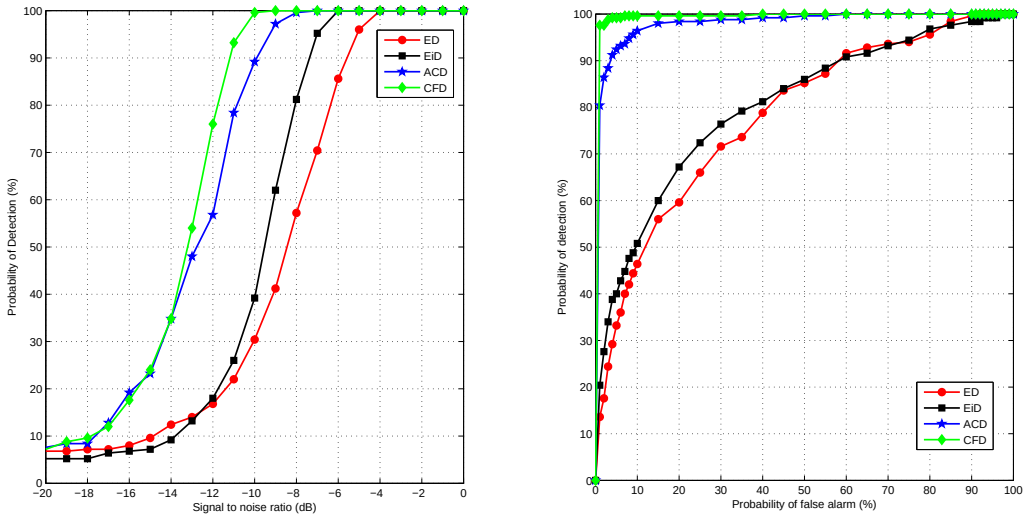

(a) (b)

Figure 2.2: (a) Probability of detection Vs. SNR at fixed $P_{FA} = 5\%$ and sensing period of 1.5 ms over an AWGN channel, (b) ROC curve for the SoTA detectors at SNR=-10 dB and sensing duration of 1.5 ms over an AWGN channel

---

an Rayleigh channel with multipath fading and shadowing following a log normal distribution in addition to the AWGN. In subfigure (a), we notice that the ED, EiD, ACD and CFD are trustable up to 0dB, -1dB, -4dB and -5dB respectively at $P_{FA} = 5\%$ and sensing time of 1.5 ms; which, compared to the scenario 1, is a consequent drop in the performance. Figure (b) show that almost no detector is satisfying the Neyman-Pearson, but still ACD and CFD are

outperforming ED and EiD .

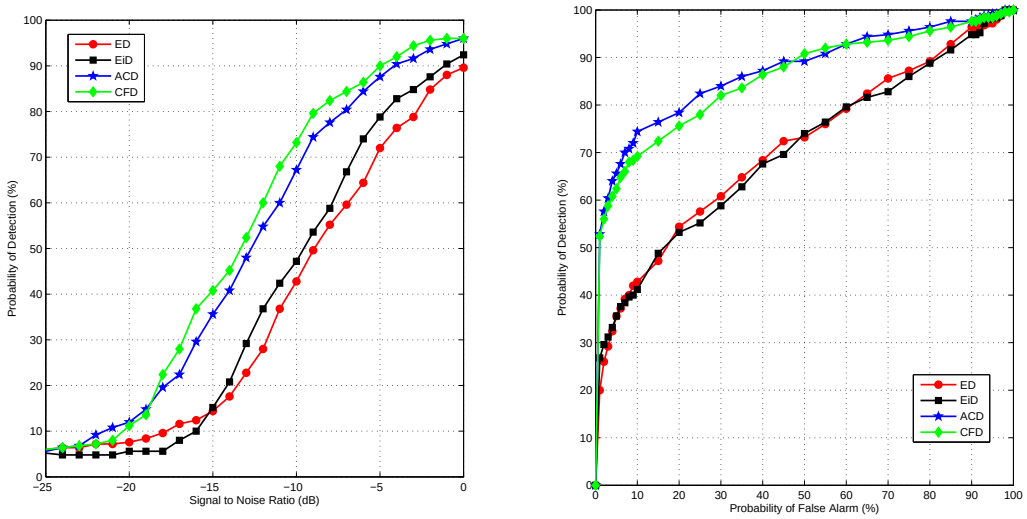

(a) (b)

Figure 2.3: (a) Probability of detection Vs. SNR at fixed $P_{FA} = 5\%$ and sensing period of 1.5 ms over a Rayleigh channel, (b) ROC curve for the SoTA detectors at SNR=-10 dB and sensing duration of 1.5 ms over a Rayleigh channel

2.5.2 Energy Efficiency

Algorithms complexity are measured in terms complex operations number that the detection algorithm has to perform in order to complete the decision statistics on the spectrum occupancy.

We summarize the number of multiplications required for each technique in the Table 2.2. Note that p refers to the number of samples and N to the size of covariance matrix. From this table, we find that the CFD, ACD and EiD detectors are the most complex among all. While ED is the least complex among them. For more information about the complexity study of spectrum sensing methods see [7].

Sensing Method	Complexity
CFD	$p^2 + O(p\log(p))$
ACD	$p + O(p\log(p))$
ED	p
EiD	$Np + O(N^3)$

Table 2.2: Theoretical complexity analysis [24]

2.5.2.1 Energy Consumption

The energy efficiency of the considered sensing detectors ED, ACD and CFD is computed assuming the use of ARM Cortex-A8 and Cortex-A9 processor cores. We use the published energy consumption figures for the Qualcomm Scorpion central processing unit (CPU) of these ARM processors that is featured in the Snapdragon mobile chipset range [25–27].
Based on the computation complexity values of the chosen sensing algorithm in Table 2.2, we can then use an embedded processors power usage to estimate the detector's energy-efficiency. For example, If we assume that Scorpion CPU can achieve this using one Single Instruction Multiple Data (SIMD) multiplication and one SIMD addition instruction, and that this is comparable to two Dhrystone instructions, then using the DMIPS/mW figures from Table 2.3, we can estimate how much energy is consumed per detection operation. Figure (2.4) reports the

Benchmark, DMIPS/MHz	2.1
Assumed clock rate	1.0GHz
Total DMIPS	2100
Typical power usage	350mW
Energy Efficiency, DMIPS/mW	6

Table 2.3: Qualcomm SCORPION CPU Details

simulations related to the energy efficiency of the various state of the art detectors. Here the results in Table 2.2 are confirmed, as we see that for example for non coherent techniques ED is more energy efficient than EiD; and also for the coherent techniques ACD is more energy efficient than CFD.

2.6 Cooperative Approaches

As previously stated, sensing can be can be achieved locally (by one SU) or collaboratively between different SUs. In the literature, cooperation is discussed as a solution to problems that arise in spectrum sensing due to noise uncertainty, fading, shadowing and hidden node

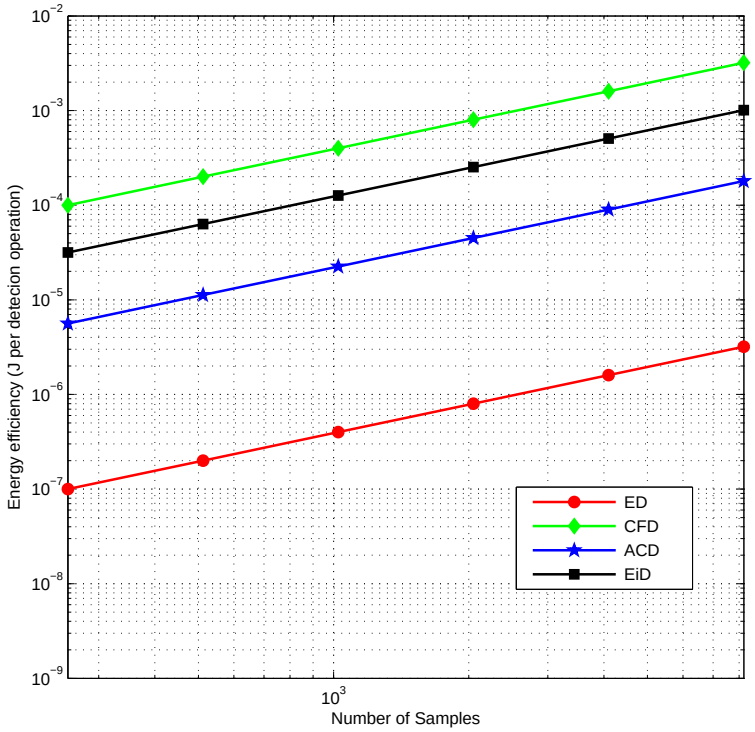

Figure 2.4: Energy efficiency of the SoTA Spectrum Sensing Algorithms

problems.

In Figure 2.5, SU 1 is shadowed by a high building over the sensing channel. In this case, the CR cannot reliably sense the presence of the PU due to the very low SNR of the received signal. Then, this CR assumes that the observed channel is vacant and begins to access this channel while the PU is still operating. To address this issue, multiple SUs can be coordinated to perform spectrum sensing cooperatively.

In addition to the advantages listed before, cooperative sensing decreases the probability of mis-detections and the probability of false alarms considerably. It can also mitigate the multi-path fading and shadowing effects, which improves the detection probability. However, the cooperation causes adverse effects on resource-constrained networks due to the additional operations and overhead traffic.

Cooperative sensing can be implemented in two ways: *centralized* or *distributed*.

Centralized Sensing In centralized sensing, a central unit collects sensing information from

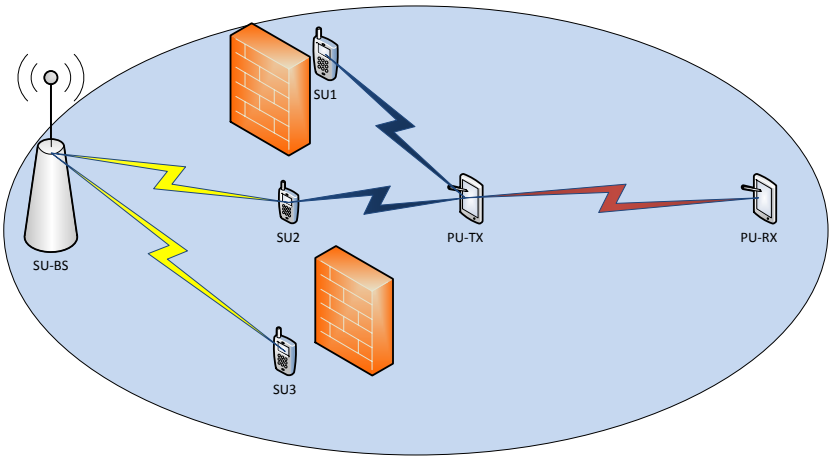

Figure 2.5: Cooperative spectrum sensing in cognitive radio networks: SU 1 is shadowed over the reporting channel and SU 3 is shadowed over the sensing channel.

SUs, identifies the available spectrum opportunities, and broadcasts this information to other SUs or directly controls the CR traffic.

The binary hypothesis testing results are gathered at a central place which is known as access point [28]. In [29], the sensing results are combined in a central node, termed as master node, for detecting TV channels/PMSE transmissions. Hard and soft information combining methods are investigated for reducing the probability of missed opportunity. The results presented in [29] show that soft information-combining outperforms hard information-combining method in terms of probability of missed detection.

Distributed Sensing In the case of distributed sensing, cognitive nodes share information among each other but they make their own decisions on part of the spectrum they can use. Distributed sensing is more advantageous in the sense that there is no need for a backbone infrastructure.

A distributed collaboration algorithm is proposed in [28]. The collaboration is performed between two SUs. The user closer to primary transmitter, which has better change of detecting the PU transmission, cooperates with a far away user. An algorithm for pairing SUs without a centralized mechanism is also proposed. In [30], a distributed sensing method is proposed where SUs share their sensing information among themselves. Only final decisions are shared in order to minimize the network overhead due

to collaboration.

2.7 Conclusion

This chapter presented the topic of spectrum sensing for CR and explained how spectrum sensing algorithms can be divided in the two groups of blind and coherent techniques. Some reference detectors have been presented. An intuitive explanation of the algorithms along with the important mathematical descriptions should provide the reader with a sound perspective of common blind and feature spectrum sensing algorithms. This is important as the following chapter will start analyzing the problems with these algorithms in the low signal to noise ratio region and also in multi-band context.

CHAPTER 3

Reconfigurable Filter Bank based Multi-band Detector

3.1 Introduction

This chapter presents a novel technique in spectrum sensing based on a new characterization of PU signals in wideband communications. First, we have to remind that in CR systems, the first task to be operated by the SU is sensing and identification of spectrum holes in the wireless environment. This chapter summarizes the advances in the algebraic approach. We present the results and the complete framework of the proposed technique based on reconfigurable filter bank based multi-band detector . Spectrum over a wide frequency band is decomposed into elementary building blocks of subbands that are well characterized by local irregularities in frequency. As a powerful mathematical tool for analyzing singularities and edges, the algebraic framework is employed to detect and estimate the local spectral irregular structure, which carries important information on the frequency locations and power spectral densities of the sensed subbands.

3.2 Filter Bank Sensing Architectures Background

In litterature, the multiband sensing was addressed in [39], [40], [41]. In this context, we consider a primary communication system (e.g., multicarrier modulation based) operating over a wideband channel that is divided into K non-overlapping narrowband subbands. In a particular geographical region and within a particular time interval, some of the K subbands might not be used by PUs and are available for opportunistic spectrum access as summarized in Figure (3.1). The detection problem on each subband k is a binary hypothesis testing problem as choosing between a hypothesis $\mathcal{H}_0$, which represents the absence of primary signals, and an alternative hypothesis $\mathcal{H}_1$, which represents the presence of primary signals.
The crucial task of spectrum sensing is to sense the K subbands and identify spectral holes for opportunistic use. To simplify, we assume that the upper-layer protocols, e.g. the medium access control (MAC) layer, can guarantee that all cognitive radios stay silent during the de-

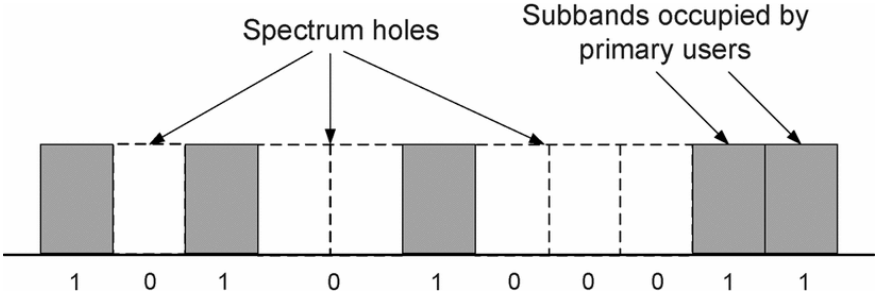

Figure 3.1: Example of multiband channel occupancy

tection interval such that the only spectral power remaining in the air is emitted by the primary users.

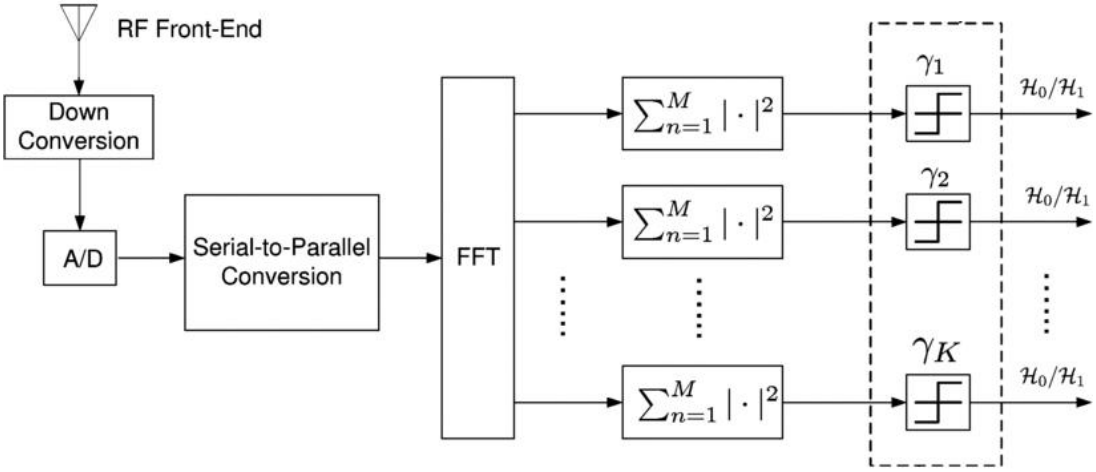

Figure 3.2: Multiband spectrum sensing in cognitive radio systems

3.3 Main Contributions

In order to clearly expose our contribution in the filter bank based sensing for the wideband scenarios, we summarize them as following:

- Our approach is going a step beyond the fixed boundaries in the SoTA filters, as the proposed scheme is able to dynamically detect these boundaries.

- The proposed filters in our scheme are adapted to the input signal and take into consideration noise reduction.

- Our suggested filter bank architecture can dynamically adapt itself to the input signal in order to track spectrum opportunities.

3.4 Model Assumptions

In this section, we propose to derive a pre-processing block for the formal ED that estimates and helps denoising the received signal spectrum. In order to enable efficient spectrum sharing, the first step is to locate the discontinuities in the spectrum in order to highlight the alternate use of spectrum as shown in Figure (3.1).

First of all, we suppose that the frequency range available in the wireless network is *B* Hz. *B* could be expressed as $B = [f_0, f_K]$. Saying that a wireless network is cognitive, means that it supports heterogeneous wireless devices that may adopt different wireless technologies for transmissions over different bands in the considered frequency range. A CR at a particular place and time needs to sense the wireless environment in order to identify spectrum holes for opportunistic use.

Since the spectrum usage in radio communications alternates between used and free bands, the spectrum of each transmission (seen as analytical function) can be viewed by sub-bands as continuous. Thus, by a direct application of Weierstrass Approximation Theorem [42], we can stipulate that over sub-band, sensed spectrum can be seen as a concatenation over the adjacent sub-bands of polynomial functions (a family of polynomials $\{p\}$) approximating each transmission.

We can express the whole spectrum, as perceived at the level of a CR trying to sense a wide-band of interest, say $[f_0, f_K]$, as following:

$$Y = \sum_{k=0}^{K-1} \chi_{[f_k, f_{k+1}]}(f) p_k(f - f_k) + E \tag{3.1}$$

where $\chi_{[f_k, f_{k+1}]}(f)$ denotes the indicator function for the frequency band $[f_k, f_{k+1}]$, that is if $f_k \leq f \leq f_{k+1}$ then $\chi_{[f_k, f_{k+1}]}(f) = 1$ and 0 otherwise; p_k is the polynomial approximating the spectrum over the band $[f_k, f_{k+1}]$ and E is the corrupting noise. Even though $\{f_k\}_{k=0,..K}$ are unknown, the model described in Equation (3.1) is still valid, it would be enough to sub-divide $[f_0, f_K]$ not in exact K actual sub-bands but in N uniform bands with a resolution of $b = \frac{f_K - f_0}{N}$. The only assumption that we will make at this level is that: ***over each band*** b***, one and only one actual change point*** f_k ***is present.***

3.5 Spectrum Discontinuities Detection Algorithm

With these new notations, Equation (3.1) can be re-written as:

$$\begin{aligned} Y &= \sum_{k=0}^{K-1} \chi_{[f_k,f_{k+1}]}(f)p_k(f-f_k) + E \\ &= \sum_{n=0}^{N-1} \chi_{[f_n,f_{n+1}]}(f)p_n(f-f_n) + E \\ &= X + E \end{aligned} \tag{3.2}$$

Where $X = \sum_{n=0}^{N-1} \chi_{[f_n,f_{n+1}]}(f)p_n(f-f_n)$, denotes the noise-free estimate of Y.
We also denote by $X_b(f) = X(f+b)$ for $f \in I_n^b = [0,b]$, which represent the restriction of the noise-free spectrum to I_n^b (keeping in mind that $b = \frac{B}{N}$).
We now can redefine the actual change point f_k relatively to I_n^b saying that:

$$\begin{cases} f_k^b = 0, & \text{if } X_b(f)\text{is smooth} \\ 0 < f_k^b \leq b, & \text{otherwise} \end{cases}$$

Now, in order to emphasize the spectrum discontinuity behavior, we proceed by deriving Equation (3.2) in the sense of distributions, we obtain:

$$\frac{d^P}{df^P} X_b(f) = [X_b(f)]^{(P)} + \sum_{j=1}^{P} \mu_{P-j}\delta(f-f_k^b)^{(j-1)} \tag{3.3}$$

where: $\mu_j \triangleq X_b(f)^{(j)}(f_k^{b^+}) - X_b(f)^{(j)}(f_k^{b^-})$ is the jump in the derivative at the change point frequency f_k^b for the j^{th} derivative of X_b. We note that in the case of absence of a change point f_k^b in I_n^b, $\mu_j = 0\ \forall j$, and $[X_b(f)]^{(P)}$ represents the regular P^{th} derivative of $[X_b(f)]$. In order to proceed clearly, for example we choose $P = 2$. Here, a second order derivative estimator is presented. Equation (3.3) thus becomes:

$$\frac{d^2}{df^2} X_b(f) = [X_b(f)]^{(2)} + \sum_{j=1}^{2} \mu_{2-j}\delta(f-f_k^b)^{(j-1)} \tag{3.4}$$

By making the assumption of the polynomials p being first order polynomials (Weierstrass approximation theorem: every continuous function defined on an interval $[a,b]$ can be uniformly approximated as closely as desired by a polynomial function) it will be annihilated after taking second order derivative, so the first term in (3.4) is annihilated and Equation (3.4) becomes:

$$\frac{d^2}{df^2} X_b(f) = \mu_1\delta(f-f_k^b)^{(0)} + \mu_0\delta(f-f_k^b)^{(1)} \tag{3.5}$$

In order to solve the equation, problem is transferred into operational domain (it is possible to solve the equation in Fourier domain too, but it is more complex than in operational domain). Here when we mean by operational domain or Laplace transform, the Laplace(Fourier domain). Thus Equation(3.5) becomes:

$$s^2\widehat{X}_b(s) - sX_b(0) - \dot{X}_b(0) = \mu_1 e^{-f_k^b s} + s\mu_0 e^{-f_k^b s} \tag{3.6}$$

where $\widehat{X}_b(s)$, $X_b(0)$ and $\dot{X}_b(0)$ are respectively the Laplace transform of $X_b(f)$, initial condition in 0 and the derivative of the initial condition in 0 of $X_b(f)$. Equivalently we can express (3.6) as:

$$e^{f_k^b s}(s^2\widehat{X}_b(s) - sX_b(0) - \dot{X}_b(0)) = \mu_1 + s\mu_0 \tag{3.7}$$

$$e^{f_k^b s}u(s) = \mu_1 + s\mu_0 \tag{3.8}$$

where $u(s) = s^2\widehat{X}_b(s) - sX_b(0) - \dot{X}_b(0)$.
By applying the differential operator $\frac{d^2}{ds^2}(.)$, we do obtain:

$$f_k^{b^2} e^{f_k^b s}u(s) + 2f_k^b e^{f_k^b s}u(s)^{(1)} + e^{f_k^b s}u(s)^{(2)} = 0 \tag{3.9}$$

$$f_k^{b^2} u(s) + 2f_k^b u(s)^{(1)} + u(s)^{(2)} = 0 \tag{3.10}$$

Finally back from $u(s)$ notation:

$$\begin{aligned} f_k^{b^2}(s^2\widehat{X}_b(s) - sX_b(0) - \dot{X}_b(0)) &+ \\ 2f_k^b(s^2\widehat{X}_b(s) - sX_b(0) - \dot{X}_b(0))^{(1)} &+ \\ (s^2\widehat{X}_b(s) - sX_b(0) - \dot{X}_b(0))^{(2)} &= 0 \end{aligned} \tag{3.11}$$

To end up with

$$\begin{aligned} f_k^{b^2}(s^2\widehat{X}_b(s) - sX_b(0) - \dot{X}_b(0)) &+ \\ 2f_k^b(s^2\widehat{X}_b(s) - sX_b(0))^{(1)} &+ \\ (s^2\widehat{X}_b(s))^{(2)} &= 0 \end{aligned} \tag{3.12}$$

Since only the initial condition remains unknown, we suggest to apply the differential operator $\frac{d^2}{ds^2}(.)$ to obtain:

$$f_k^{b^2}(s^2\widehat{X}_b(s))^{(2)} + 2f_k^b(s^2\widehat{X}_b(s))^{(3)} + (s^2\widehat{X}_b(s))^{(4)} = 0 \tag{3.13}$$

We remind that multiplication with s^l (in this case $l = 2$) in operational domain will result later in derivation in frequency domain, which will result in amplifying noise. We suggest at this level dividing by s^m so that the effect will be the strict inverse, and thus our algorithm will help eliminate noise with the only condition $m > 2$. Thus we obtain:

$$\frac{f_k^{b^2}(s^2\widehat{X}_b(s))^2}{s^m} + \frac{2f_k^b(s^2\widehat{X}_b(s))^{(3)}}{s^m} + \frac{(s^2\widehat{X}_b(s))^{(4)}}{s^m} = 0 \tag{3.14}$$

Since it remains no unknown parameter and/or factor, we transfer the solved equations back to the frequency domain. After some computational steps, we can easily show that:

$$\begin{aligned} L^{-1}(\frac{(s^2\widehat{X}_b(s))^{(\kappa)}}{s^m}) &= \int_0^b (\frac{\nu^{m-1}(b-\nu)^\kappa}{(m-1)!})^{(2)} X(f-\nu)d\nu \\ &= \int_0^\infty h_{\kappa-1}(\nu)X(f-\nu)d\nu \end{aligned} \tag{3.15}$$

where

$$h_{\kappa-1}(\nu) = \begin{cases} (\frac{\nu^{m-1}(b-\nu)^\kappa}{(m-1)!})^{(2)}, & \text{for } 0<\nu<b \\ 0, & \text{otherwise} \end{cases}$$

and $\kappa = 2, 3, 4$.

Finally, denoting $\phi_{\kappa-1} = L^{-1}(\frac{(s^2\widehat{X}_b(s))^{(\kappa)}}{s^m})$, in frequency domain, the actual change point over each sub-band b, is the one solving the Equation (3.14), that is:

$$f_k^{b^2}\phi_1 + f_k^b\phi_2 + \phi_3 = 0 \tag{3.16}$$

So we have shown that from the proposed model we obtain a simple filtering in order to locate and reconstruct the boundaries (spectrum change points) of occupied spectrum.

Adopting exactly the same approach, and starting by $P = 3$ and saying that p is 2^{nd} order, we obtain:

$$f_k^{b^3}\phi_1 + 3f_k^{b^2}\phi_2 + 3f_k^b\phi_3 + \phi_4 = 0 \tag{3.17}$$

where:

$$\begin{aligned} \phi_{\kappa-2} &= L^{-1}(\frac{(s^3\widehat{X}_b(s))^{(\kappa)}}{s^m}) \\ &= \int_0^\infty h_{\kappa-2}(\nu)X(f-\nu)d\nu \end{aligned} \tag{3.18}$$

where

$$h_{\kappa-2}(\nu) = \begin{cases} (\frac{\nu^{m-1}(b-\nu)^\kappa}{(m-1)!})^{(3)}, & \text{for } 0<\nu<b \\ 0, & \text{otherwise} \end{cases}$$

and $\kappa = 3, 4, 5, 6$

A third model can be derived with $P = 4$, thus p is 3^{rd} order polynomial series. We obtain:

$$f_k^{b^4}\phi_1 + 4f_k^{b^3}\phi_2 + 6f_k^{b^2}\phi_3 + 4f_k^b\phi_4 + \phi_5 = 0 \tag{3.19}$$

where:

$$\begin{aligned} \phi_{\kappa-3} &= L^{-1}(\frac{(s^4\widehat{X}_b(s))^{(\kappa)}}{s^m}) \\ &= \int_0^\infty h_{\kappa-3}(\nu)X(f-\nu)d\nu \end{aligned} \tag{3.20}$$

where

$$h_{\kappa-3}(\nu) = \begin{cases} \left(\frac{\nu^{m-1}(b-\nu)^{\kappa}}{(m-1)!}\right)^{(4)}, & \text{for } 0 < \nu < b \\ 0, & \text{otherwise} \end{cases}$$

and $\kappa = 4, 5, 6, 7, 8$.

In this Section, we only present the three first detection algorithms to be used for simulation parts. We derived a generalized form of this algorithm in [33,34].

Let's have a deeper look into Equations (3.16), (3.17) and (3.19). The change point in the spectrum f_k^b, relatively to I_n^b is solution to those equations. It is easy to see, that since by construction the ϕ_κ series are positive. Then, f_k^b satisfying equations (3.16), (3.17) and (3.19), is equivalent to say that over each band I_n^b, f_k^b annihilates $\psi_k(f) = \prod \phi_\kappa$. The last criteria is simpler to implement than equations (3.16), (3.17) and (3.19).

We recall at this stage that these equations were derived in a noise free environment. In noisy environments, in all equations, X is substituted with the noisy observation $Y = X + E$. Thus the criteria in equations (3.16), (3.17) and (3.19) would be an ε and not exactly 0.

3.6 Reconfigurable Filter Bank for Spectrum Sensing

Once the frequency boundaries in the wideband spectrum successfully detected, we construct adapted filters to those boundaries. Over each band $[f_k^b, f_{k+1}^b]$, we apply the corresponding window function given by $\psi_k(f) = \prod \phi_\kappa$.

The over all detector architecture is given in Figure (3.3). In this figure, the FFT of the received frame represents the input of our algorithm. As stated in the beginning, the over all band of interest is divided in N uniform bands with a resolution of $b = \frac{f_K - f_0}{N}$ and in a parallel way, we seek the frequency boundary f_k^b for each band if ever it exist. We map back the frequencies and apply $\psi_k(f)$ as a window on each band $[f_k^b, f_{k+1}^b]$. Finally, the used sensing technique is the conventional energy detector with a length of $f_{k+1}^b - f_k^b$ samples.

Each stage is called an algebraic detector and have as input the received frame FFT and as output a single frequency f_k^b if existing and a window function ψ_k.

Now, let us derive the key metrics of the proposed sensing algorithm. We resonate on a single frequency band, as for all others, the formulation is the same.

As stated previously, in spectrum sensing, a binary hypothesis testing is applied to decide on the presence or not of the PU in his original band $[f_k^b, f_{k+1}^b]$ and we obtain:

$$\mathcal{T}_k = \begin{cases} \sum_{f=f_k^b}^{f_{k+1}^b} |\psi_k(E_k(f))|^2 & \mathcal{H}_0 \\ \sum_{f=f_k^b}^{f_{k+1}^b} |\psi_k(X_k(f)) + \psi_k(E_k(f))|^2 & \mathcal{H}_1 \end{cases} \tag{3.21}$$

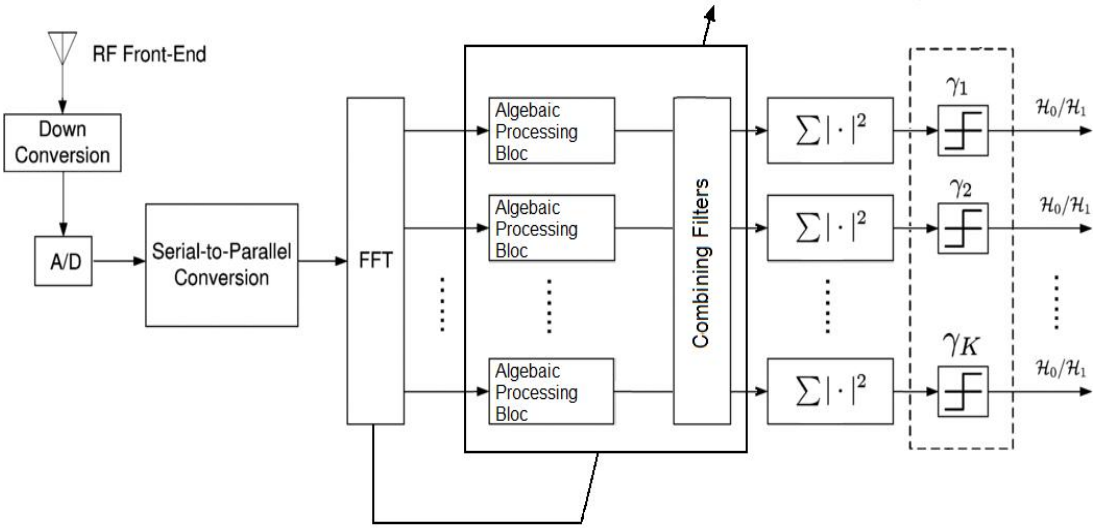

Figure 3.3: Proposed Reconfigurable Filter Bank Multi-band Detector

which can be written as:

$$\mathcal{T}_k = \begin{cases} \sum_{f=f_k^b}^{f_{k+1}^b} |E'_k(f)|^2 & \mathcal{H}_0 \\ \sum_{f=f_k^b}^{f_{k+1}^b} |X'_k(f) + E'_k(f)|^2 & \mathcal{H}_1 \end{cases} \tag{3.22}$$

This last formulation looks quite like the conventional energy detection formulation over an AWGN. what is left to do in order to use this formalism, is to find the relationship between $\sigma^2_{E_k}$ and $\sigma^2_{E'_k}$.

From [41], we have $\sigma^2_{E'_k} = G_k \sigma^2_{E_k}$ where G_k is the filter energy, i.e: $G_k = \sum_{f=f_k^b}^{f_{k+1}^b} |\psi_k(f)^2|$.

The test statistic $\mathcal{T}_k$ under $\mathcal{H}_0$ hypothesis can be rewritten as $\mathcal{T}_k = \eta G_k \frac{\sigma^2_{E_k}}{2}$ where η is following a χ^2 distribution since the real and imaginary parts of E_k follow i.i.d random process each. Following the central limit theorem, $\mathcal{T}_k$ follows asymptotically a normal distribution such as:

$$\mathcal{T}_k \approx \mathcal{N}(\delta_k s_k G_k \sigma^2_{E_k}, \delta_k s_k G_k^2 \sigma^4_{E_k}) \tag{3.23}$$

where $s_k = f_{k+1}^b - f_k^b + 1$ is the number of samples per channel and δ_k denotes the number of sub-bands for the k^{th} user. In our configuration, we assume a single user per sub-band and a single sub-band per user. Thus $\delta_k = 1$.

Finally, we obtain the performance metrics for our proposed detector function of the threshold γ_k:

- Probability of False Alarm:

$$\begin{aligned} P_{FA,k} &= \Pr\left(\mathcal{T}_k > \gamma_k | \mathcal{H}_0\right) \\ &= Q\left(\frac{\gamma_k - \delta_k s_k G_k \sigma_{E_k}^2}{\sqrt{\delta_k s_k} G_k \sigma_{E_k}^2}\right) \end{aligned} \tag{3.24}$$

- Probability of Detection:

$$\begin{aligned} P_{D,k} &= \Pr\left(\mathcal{T}_k > \gamma_k | \mathcal{H}_1\right) \\ &= Q\left(\frac{\gamma_k - \delta_k s_k G_k (\sigma_{E_k}^2 + \sigma_{X_k}^2)}{\sqrt{\delta_k s_k} G_k (\sigma_{E_k}^2 + \sigma_{X_k}^2)}\right) \end{aligned} \tag{3.25}$$

Where $P_{D,k}$, is obtained by processing the same way as $P_{FA,k}$ by characterizing the test statistic $\mathcal{T}_k$ under $\mathcal{H}_1$. For a constant false alarm rate (CFAR) case, where a target $P_{FA,k}$ is fixed, we obtain:

- Threshold γ_k expression:

$$\gamma_k = \left[Q^{-1}(P_{FA,k})\sqrt{\delta_k s_k} + \delta_k s_k\right] G_k \sigma_{E_k}^2 \tag{3.26}$$

- Probability of Detection:

$$P_{D,k} = Q\left(\frac{Q^{-1}(P_{FA,k})\sqrt{\delta_k s_k}\sigma_{E_k}^2 - \delta_k s_k \sigma_{X_k}^2}{\sqrt{\delta_k s_k}(\sigma_{E_k}^2 + \sigma_{X_k}^2)}\right) \tag{3.27}$$

where $Q(.)$ is the tail probability of the standard normal distribution, which can be expressed in terms of the error function $Q(x) = \frac{1}{2}(1 - erf(\frac{x}{\sqrt{(2)}}))$

3.7 Performance Evaluation

First, we assess the sensing performance of the proposed reconfigurable filter bank technique in single band detection. Then, we apply our sensing technique on several actual measurements to see the impact of spectral estimation using the proposed window function.
Three different scenarios, with different properties are chosen to evaluate spectral detection performance. All simulation scenarios follow the Monte Carlo principle, where detection results are obtained as the average of simulations number. For each iteration of the Monte-Carlo simulation, a test statistic is computed on the basis of the signal samples in one block, and a binary decision is made by comparing the test statistic to a predetermined detection

threshold. For the Monte Carlo simulation 1000 iterations are performed in the simulation. The threshold is computed for the detectors to have a probability of false alarm $P_{FA} = 0.05$.

Scenario 1: OFDM signal in AWGN channel: we consider a DVB-T OFDM signal in AWGN channel. Assuming that the detection performance in AWGN provide a good impression of the performance, but it is necessary to extend the simulations to include signal distortion due to multipath and shadow fading.

Scenario 2: OFDM signal in Rayleigh multipath fading with shadowing: this scenario uses the same DVB-T OFDM signal as scenario 1, but to make the simulations more realistic, the signal is subject to Rayleigh multipath fading and shadowing following a log normal distribution in addition to the AWGN. The maximum Doppler shift of the channel is 100 Hz and the standard deviation for the log normal shadowing is 10 dB.

Scenario 3: OFDM signal in Rician multipath fading with shadowing: the third simulation scenario uses also a DVB-T OFDM signal in Rician multipath fading with shadowing. The K-factor for the Rician fading is 10, which represents a very strong line of sight component. The maximum Doppler shift of the channel and the standard deviation for the log normal shadowing are the same as in the second scenario.

Figure (3.4) shows the proposed detection technique in the state of the art techniques. The important remark to remind at this point is that these reconfigurable filter bank techniques are belonging to the non-coherent detectors class. Our proposed techniques are energy detection-based. For the AD_1 the performance are close to the ED. For AD_2 the performance are comparable, and to certain extend, better than the EiD. The most interesting result, is for AD_3 which have comparable results to the ACD. The last result is remarkably interesting, as with an energy-based detection we can reach the performance of coherent detection techniques. Figures (3.5), (3.6), (3.7), report the simulation results of the proposed techniques compared to the energy detection for respectively scenarios 1 (AWGN Channel), 2 (Rayleigh Channel) and 3 (Rician Channel). Each of the figures report P_D Vs. SNR for ED, AD_1, AD_2, AD_3 at fixed $P_{FA} = 5\%$ and sensing period of 1.5ms. We also derive the ROC curve for the three first simulated detectors and energy detector at SNR=-10dB and sensing duration of 1.5ms for the different channels. These figures confirm the first tendency as in Figure (3.4), where by order of performance (from less to most) we have AD_1, ED, AD_2, AD_3.

In July 2008, EURECOM have performed data acquisition bands specified in Table (3.1):
The parameters on the acquisitions are:

1. 20480 samples
2. Complex I/Q samples
3. Resolution 12 bits.

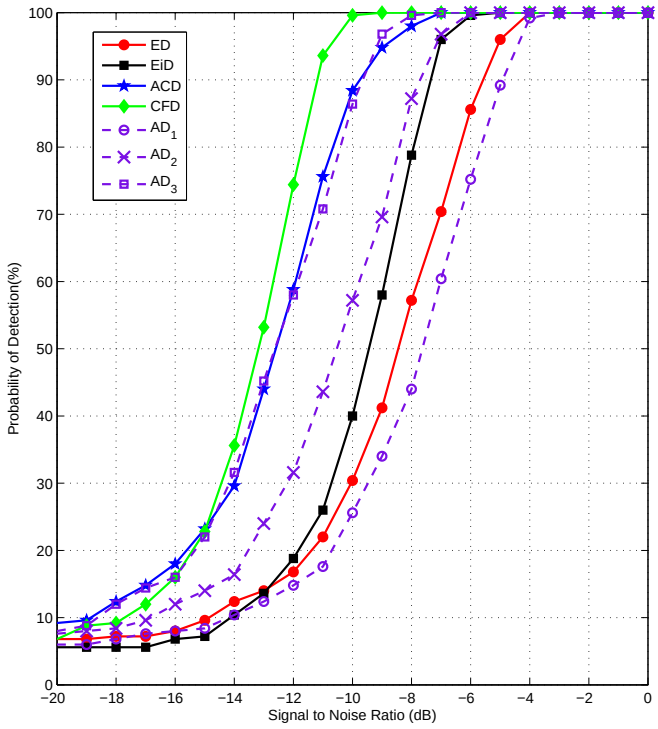

Figure 3.4: Probability of detection Vs. SNR at fixed $P_{FA} = 5\%$ and sensing period of 1.5 ms over an AWGN channel of the SoTA and Proposed Detector

For each frequency band, we have several acquisitions:

1. A reference one with the RF antenna connector connected to a signal generator which generates a sinusoid at the center frequency. The reference file is used for IQ balance correction

2. Other acquisitions where the RF antenna connector connected to a wide band antenna for real data acquisition.

Figure 3.8 shows the performance of the spectral estimator attached to the reconfigurable filter bank on (a) GSM signal at 1836 MHz, (b) GSM signal at 930 MHz and (c) DVB-T signal at 578 MHz. This figure is meant to highlight the capabilities of the filter bank to

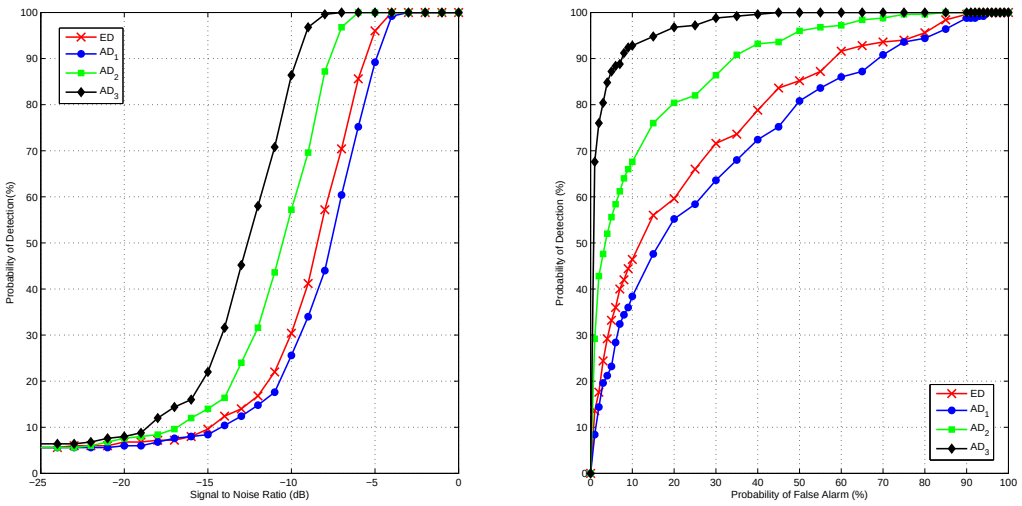

(a) (b)

Figure 3.5: (a) Probability of detection Vs. SNR at fixed $P_{FA} = 5\%$ and sensing period of 1.5 ms over an AWGN channel, (b) ROC curve for the three first simulated detectors and energy detector at SNR=-10 dB and sensing duration of 1.5 ms over an AWGN channel

reduce considerably the measurements noise and have "cleaner" signals where one can clearly distinguish occupied and free bands. This is also important as the enhanced ED have a more robust behavior towards noise, as it is considerably reduced. This noise reduction comes from the inner structure of the detector.

3.8 Conclusion

In this chapter, we derived a novel filter bank based sensing techniques for wideband cognitive radios. The first step was to locate in the sensed RF spectrum some specific frequencies carrying valuable information (vacant to occupied channel transmission). Secondly, we derived some adapted filters to these bands that helped us to reduce acquisition noise and enhance energy detection over the different bands. Finally, we showed through various simulation settings and actual data how performing and robust the proposed technique is.

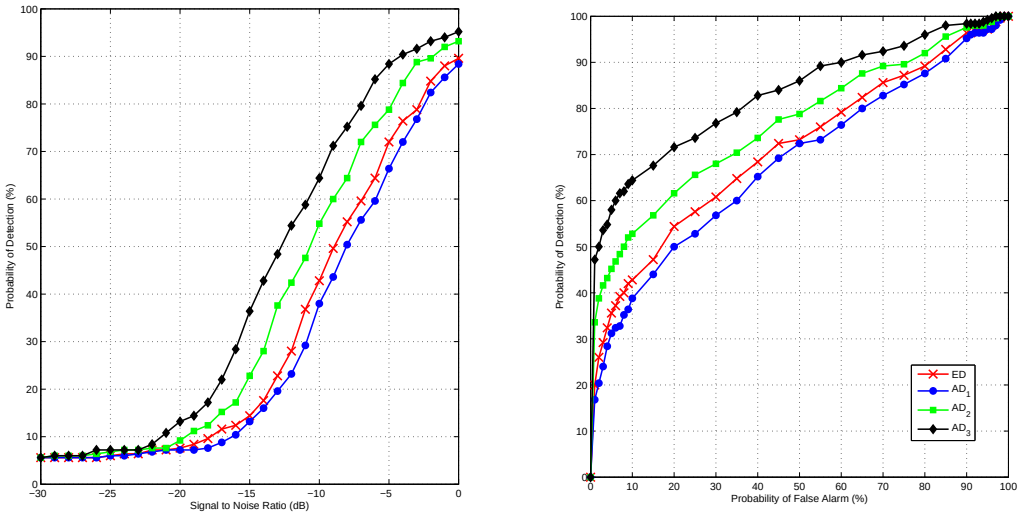

(a) (b)

Figure 3.6: (a) Probability of detection Vs. SNR at fixed $P_{FA} = 5\%$ and sensing period of 1.5 ms over a Rayleigh channel, (b) ROC curve for the three first simulated detectors and energy detector at SNR=-10 dB and sensing duration of 1.5 ms over a Rayleigh channel

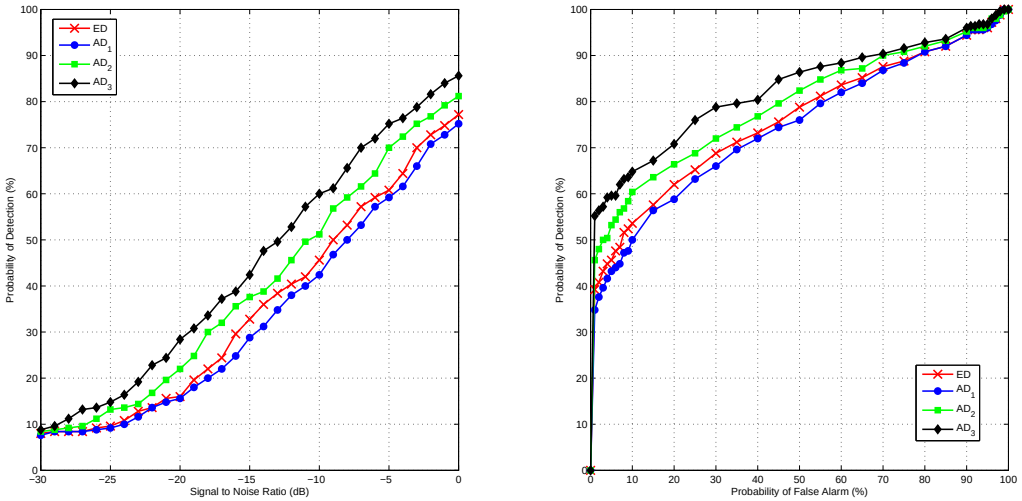

(a) (b)

Figure 3.7: (a) Probability of detection Vs. SNR at fixed $P_{FA} = 5\%$ and sensing period of 1.5 ms over a Rician channel, (b) ROC curve for the three first simulated detectors and energy detector at SNR=-10 dB and sensing duration of 1.5 ms over a Rician channel

Freq (in MHz)	Observations (thanks to a Spectral analyser)
578	DVB
930	GSM
1836	DSC
1875	DCS
2113	UMTS-FDD

Table 3.1: Performed data acquisitions

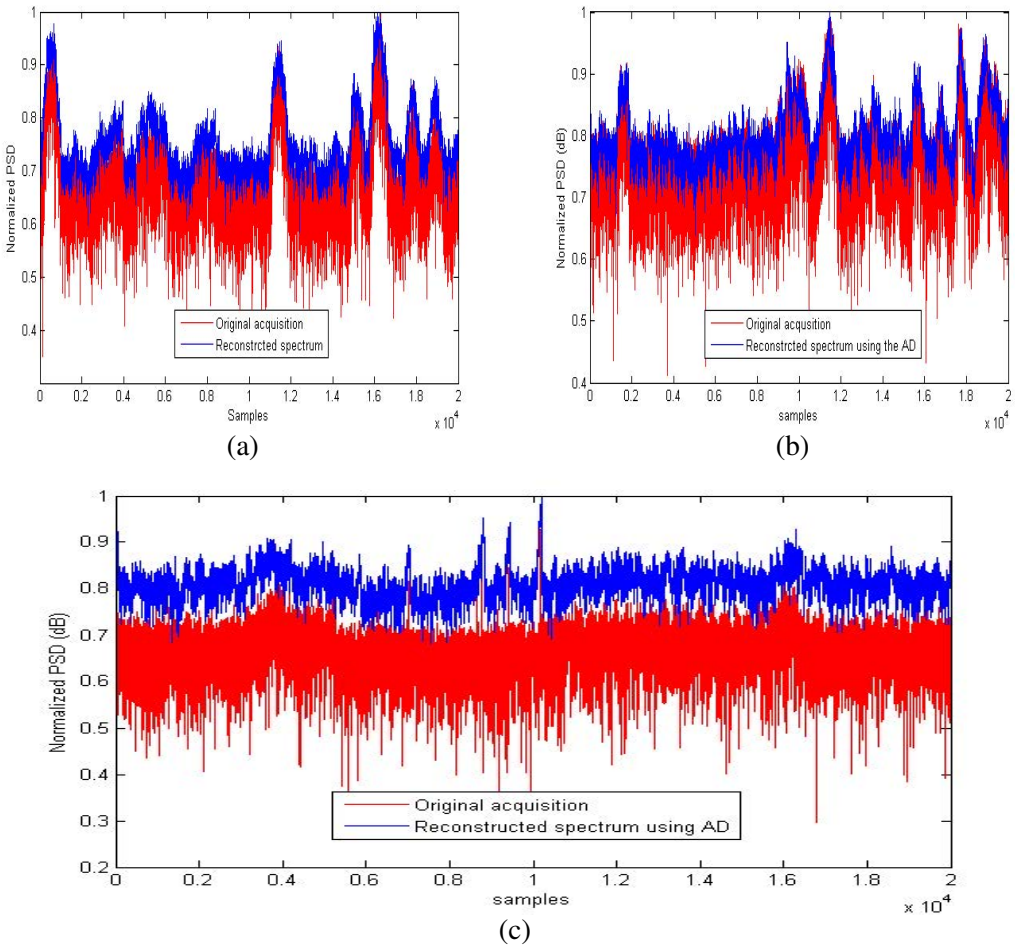

Figure 3.8: Performance of the spectral estimator attached to the reconfigurable filter bank on (a) GSM signal at 1836 MHz, (b) GSM signal at 930 MHz and (c) DVB-T signal at 578 MHz

CHAPTER 4

Compressed Sensing for Wideband Cognitive Radios

4.1 Introduction

Recently, compressed sensing/compressive sampling (CS) has been considered as a promising technique to improve and implement cognitive radio (CR) systems. In wideband radio one may not be able to acquire a signal at the Nyquist sampling rate due to the current limitations in Analog-to-Digital Converter (ADC) technology [43]. Compressive sensing makes it possible to reconstruct a *sparse* signal by taking less samples than Nyquist sampling, and thus wideband spectrum sensing is doable by CS. A sparse signal or a compressible signal is a signal that is essentially dependent on a number of degrees of freedom which is smaller than the dimension of the signal sampled at Nyquist rate. In general, signals of practical interest may be only nearly sparse [43]. And typically the wireless signals in open networks are sparse in the frequency domain since depending on location and at some times the percentage of spectrum occupancy is low due to the idle radios [3, 48].

In CS a signal with a sparse representation in some basis can be recovered from a small set of nonadaptive linear measurements [49]. A sensing matrix takes few measurements of the signal, and the original signal can be reconstructed from the incomplete and contaminated observations accurately and sometimes exactly by solving a simple convex optimization problem [43, 44]. In [45] and [46] conditions on this sensing matrix are introduced which are sufficient in order to recover the original signal stably. And remarkably, a random matrix fulfills the conditions with high probability and performs an effective sensing [47, 49].

Apart from reconstructing the original signal, detection is more required and interesting in the context of cognitive radio. Generally, for detection purposes it is not necessary to reconstruct the original signal, but only an estimate of the relevant sufficient statistics for the problem at hand is enough. This leads to less required measurements and lower computational complexity [50]. We are interested to skip the estimation of the original signal and directly use the measurements for detection purpose, and so reduce the complexity of the system as much as possible.

In [48] a wavelet-based detection approach using CS to identify the spectrum holes is intro-

duced. To find the frequency band boundaries they derive a convex optimization formulation that the solution gives the band boundaries of the spectrum without requiring to reconstruct the original signal.
In this chapter we develop a combined compressive sampling and spectrum discontinuities detection technique based on algebraic method for the sensing task of identifying the spectrum holes. The proposed algebraic detector is a linear detector and we would like to feed the algorithm directly with the compressed measurements. For this purpose we find a proper sensing matrix that gives the possibility of feeding the algebraic detector with the measurements directly.

4.2 Combined Compressive Sampling and Spectrum Discontinuities Detection

In order to actualize sensing in wide spectrum and to reduce the complexity and power consumption at CR nodes, sampling at a smaller rate than Nyquist rate, while reconstruction or detection of signal is accurately possible, is a prominent key. Hence, (CS) becomes a promising solution in realization of cognitive radio. CS enables us to do the sampling at a smaller rate than Nyquist rate, sometimes much smaller, and accurately reconstruct the *sparse* signal, or perform detection or estimation.
The first step of cognitive radio is to sense the spectrum and identify the spectrum holes, or in other words, detect the occupied frequency bands. Typically the wireless signal in open access networks is sparse in the frequency domain since depending on location and at some times the percentage of spectrum occupancy is low due to the idle radios [3, 48]. For example, we can model the spectrally sparse wideband signals as

$$s(t) = \sum_{j=0}^{N-1} \beta_j e^{i2\pi jt/N}, t = 0, \cdots, N-1 \tag{4.1}$$

where N is very large but the number of nonzero coefficients β_j is much less than N. In this sense we can say that the signal is spectrally sparse [47]. Therefore, we would like to implement spectrum sensing in the context of cognitive radio by performing compressed sensing combined with distribution discontinuities detection. To avoid signal reconstruction burden we find a sensing matrix that enables the algebraic detector properly works while accepting the compressed samples directly as input.

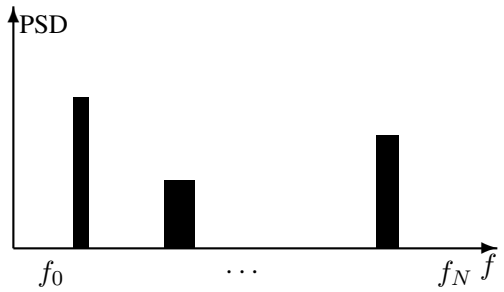

Figure 4.1: An example of power spectral density vs. the frequency of a spectrally sparse wideband signal. PSD stands for power spectral density and f is frequency.

4.2.1 Compressed Sensing

Let $x \in \mathbb{R}^N$ be a signal with expansion in an orthonormal basis Ψ as

$$x(t) = \sum_{j=0}^{N-1} \alpha_j \psi_j(t), \quad t = 0, \cdots, N-1 \tag{4.2}$$

where Ψ is $N \times N$ matrix with the waveforms ψ_j as rows. To use convenient matrix notations we can write the decomposition as $x = \Psi\alpha$ or equivalently, $\alpha = \Psi^* x$ where Ψ^* denotes conjugate transpose of Ψ. A signal x is sparse in the Ψ basis if the coefficient sequence α is supported on a small set. We say that a vector α is S-sparse if its support $\{j : \alpha_j \neq 0\}$ is of cardinality less or equal to S [43]. Consider that we would like to recover all the N coefficients of x, vector α, from measurements y about x of the form

$$y_m = \langle x, \phi_m \rangle = \sum_{n=0}^{N-1} \phi_{mn} x[n], m = 0, \cdots, M-1 \tag{4.3}$$

or

$$y = \Phi x = \Phi\Psi\alpha = \Theta\alpha \tag{4.4}$$

where we are interested in the case that $M \ll N$, and the rows of the $M \times N$ sensing matrix Φ are incoherent with the columns of Ψ. Then it is shown that signal x can accurately and sometimes exactly be recovered, considering that the recovered signal $x^\star$ is given by $x^\star = \Psi\alpha^\star$, and $\alpha^\star$ is the solution to the convex optimization program

$$\min_{\tilde{\alpha} \in \mathbb{R}^N} ||\tilde{\alpha}||_{l_1} \text{ subject to } \Phi\Psi\tilde{\alpha} = \Theta\tilde{\alpha} = y \tag{4.5}$$

where $||\tilde{\alpha}||_{l_1} := \sum_{j=1}^{N} |\tilde{\alpha}_j|$. The compressed sensing (CS) theory states that there exists a measuring factor $c > 1$ such that only $M := cS$ incoherent measurements y are needed to

recover x with high probability. We also have to mention that except l_1-minimization solution other methods such as greedy algorithms exist for recovering the sparse signal [44,50].
In case of noisy measurements, i.e., $y = \Phi x + e$, where e is noise with $||e||_{l_2} \leq \varepsilon$, [44] shows that solution to

$$\min_{\tilde{\alpha} \in \mathbb{R}^N} ||\tilde{\alpha}||_{l_1} \text{ subject to } ||\Theta\tilde{\alpha} - y||_{l_2} \leq \varepsilon \tag{4.6}$$

recovers the sparse signal with an error at most proportional to the noise level. Also, [44] discuss the conditions for stable recovery from noisy measurements.
We are interested in doing the spectrum holes detection using algebraic approach *directly* from the compressed measurements without reconstructing the original signal itself. For this reason we must find out the appropriate sensing matrix according to the detection technique. The proposed detection technique is a linear algebraic algorithm. This technique uses the Fourier transform of the observed signal to detect the occupied frequency bands in the observed spectrum. Therefore the compressed measurements of the observed signal must keep the linearity and properties of the original signal in order to apply the detection algorithm successfully on the compressed measurements. To find the sensing matrix we start by looking at the Fourier transform of the signal $x \in \mathbb{R}^N$.

$$X_l = \sum_{n=0}^{N-1} x[n] \exp(-\omega l n), l = 0, \cdots, N-1 \tag{4.7}$$

where $\omega = \frac{2\pi i}{N}$ and i is the imaginary unit. The Fourier transform of the measured signal is

$$Y_k = \sum_{m=0}^{M-1} y[m] \exp(-\omega k m), k = 0, \cdots, M-1. \tag{4.8}$$

From (4.4) we replace $y[m]$ and we have

$$Y_k = \sum_{m=0}^{M-1} (\sum_{n=0}^{N-1} \phi_{mn} x[n]) \exp(-\omega k m), k = 0, \cdots, M-1 \tag{4.9}$$

where ϕ_{mn} denotes the element of Φ at the cross of row m and column n. Then by linearity properties we have

$$Y_k = \sum_{n=0}^{N-1} \sum_{m=0}^{M-1} \phi_n[m] \exp(-\omega k m) x[n], k = 0, \cdots, M-1 \tag{4.10}$$

where $\phi_n[m]$ denotes the m^{th} element of the n^{th} column vector of Φ, ϕ_n, and we see that

$$\sum_{m=0}^{M-1} \phi_n[m] \exp(-\omega k m) = \hat{\Phi}_{n_k}, k = 0, \cdots, M-1 \tag{4.11}$$

that is the Fourier transform of the n^{th} column vector of Φ, $\hat{\Phi}_n$. Then from (4.10) and (4.11)

$$Y_k = \sum_{n=0}^{N-1} \hat{\Phi}_{n_k} x[n], k = 0, \cdots, M-1. \tag{4.12}$$

And, as we said, in order to feed the detection algorithm directly by the compressed measurements we seek that

$$Y_k(\omega) = aX_l(\omega), k \in \{0, \cdots, M-1\}, l \in \{0, \cdots, N-1\} \tag{4.13}$$

where $a > 0$ is a constant. From (4.12) and to satisfy (4.13) we find that

$$\hat{\Phi}_{n_k} = a \exp(-\omega z n), z \in \{1, \cdots, N\}, k = 0, \cdots, M-1 \tag{4.14}$$

and therefore from inverse Fourier transform we have

$$\phi_n = a\delta(n-z), z \in \{1, \cdots, N\} \tag{4.15}$$

which means that any row vector of the sensing matrix is a Dirac function, that is, only one column of each row is nonzero.

Now that the general format of the sensing matrix is clear, we should find a way to generate it. The Φ^T matrix can be generated by randomly selecting M columns of an identity matrix I_N. Φ is given by transpose of Φ^T, and we define $a = 1$ to make sure that the columns of the sensing matrix are unit-normed. So the sensing matrix Φ that we achieved has a form like this

$$\Phi \sim \begin{bmatrix} 0 & 1 & 0 & \cdots & 0 & 0 & 0 & 0 \\ \vdots & \vdots & \vdots & \vdots & \vdots & \vdots & \vdots & \vdots \\ 0 & 0 & 0 & \cdots & 0 & 1 & 0 & 0 \end{bmatrix}_{M \times N}. \tag{4.16}$$

This form of sensing matrix gives us the opportunity to use the compressed measurements directly as input to the algebraic detection algorithm and thus avoiding the computation complexity of reconstructing the original signal. Following, the algebraic detection technique with compressed measurements as the input to the algorithm is explained.

4.2.2 Algebraic Detection Based on Compressive Sampling

The algebraic detection (AD) is a new approach based on advanced differential algebra and operational calculus. In this method, the primary user's presence is rather casted as a change point detection in its transmission spectrum. In this approach, the mathematical representation of the spectrum of the compressed measurements, i.e., the observed signal Y_n in frequency domain, is assumed to be a piecewise P^{th} polynomial signal expressed as following:

$$Y_n = \sum_{k=1}^{K} \mathcal{Y}_k[n_{k-1}, n_k](f) \times p_k(n - n_{k-1}) + E_n \tag{4.17}$$

where $\mathcal{Y}_k[n_{k-1}, n_k]$ is the characteristic function, p_k is a polynomial series of order P, E_n is the additive corrupting noise, K is the number of subbands defined in the frequency range of observation interest, and $n = \frac{f}{f_s}$ is the normalized frequency, where f_s is the sampling frequency and f is the signal frequency.
Let us define the clean version of the received signal S_n as:

$$S_n = \sum_{k=1}^{K} \mathcal{Y}_k[n_{k-1}, n_k](f) \times p_k(n - n_{k-1}) \tag{4.18}$$

And let b, the frequency band, be such that one and only one change point occurs in the interval $I_b = [n_{k-1}, n_k] = [\nu, \nu + b]$, $\nu \geq 0$. Denoting $S_\nu(n) = S(n + \nu)$, $n \in [0, b]$ as the restriction of the signal in the interval I_b and redefine the change point n_ν relatively to I_b such as:

$$\begin{cases} n_\nu = 0 & \text{if } S_\nu \text{ is continuous} \\ 0 < n_\nu \leq b & \text{otherwise} \end{cases} \tag{4.19}$$

Then, the primary user presence on a sensed sub-band is equivalent to find $0 < n_\nu \leq b$ on that band. The AD gives the opportunity to build a whole family of spectrum sensing detectors, depending on a given model order P. Depending on this model order, we can show that performance of the AD is increasing as the order P increases.
The proposed algorithm is implemented as a filter bank which composed of P filters mounted in a parallel way. The impulse response of each filter is:

$$h_{k+1,n} = \begin{cases} \frac{(n^l(b-n)^{P+k})^{(k)}}{(l-1)!}, 0 < n < b \\ 0, otherwise \end{cases} \tag{4.20}$$

where $k \in [0 \cdots P-1]$ and l is chosen such that $l > 2 \times P$. The proposed expression of $h_{k+1,n}$, $k \in [0 \cdots P-1]$ is determined by modeling the spectrum with a piecewise regular signal in frequency domain and casting the problem of spectrum sensing as a change point detection in the primary user transmission. Finally, in each detected interval $[n_{\nu_i}, n_{\nu_{i+1}}]$, we compute the following equation:

$$\lambda_{k+1} = \sum_{m=n_{\nu_i}}^{n_{\nu_{i+1}}} W_m h_{k+1,m} X_m \tag{4.21}$$

where M is the number of samples of the observed signal, W_m is the weight for numeric integration defined by:

$$\begin{cases} W_0 = W_M = 0.5 \\ W_m = 1 \quad \text{otherwise} \end{cases} \tag{4.22}$$

In order to infer whether the primary user is present in its interval, a decision function is computed as following:

$$Df = \| \prod_{k=0}^{P} \lambda_{k+1}(n_\nu) \| \tag{4.23}$$

The decision is made by comparing the threshold Th to the mean value of the decision function over the detected intervals.

4.3 Simulations

4.3.1 Single Node Spectrum Sensing

In this section we investigate the performance of the proposed algorithm in comparison with the energy detector (ED). First we consider a frequency band in the range of $[50, 250]$MHz, in order to compare the compressive sensing using the algebraic method and the wavelet approach introduced in [48]. The signal is fully described in [48]. During the observed burst of transmissions in the network, there 6 bands, with frequency boundaries at:
$n_{\nu_{n=0}}^{6} = [50, 120, 170, 200, 220, 224, 250]$ MHz.
Comparing with the wavelet approach, in the algebraic detection technique change points are detected only in one shot, while in the wavelets approach, many detections have to be conducted and fused to make a final decision.
Figure 4.2 shows the algebraic detection performance on this signal. Now, comparing the pro-

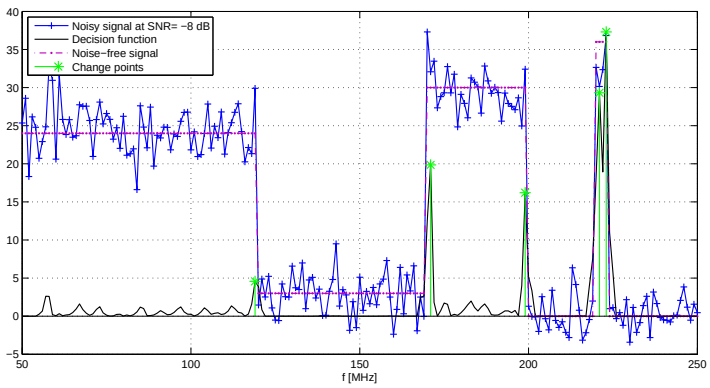

Figure 4.2: Edge detection using the algebraic technique. The signal in red is the original signal, the one in blue is the noisy observation with SNR=-8dB. The black signal is the computed decision function and the green stars are the detected change points.

posed compressed sensing algorithm to the reference algorithm, let us give some key notes on

the ED. ED is the most common method for spectrum sensing because of its non-coherency and low complexity. The energy detector measures the received energy during a finite time interval and compares it to a predetermined threshold. That is, the test statistic of the energy detector is:

$$\sum_{m=1}^{M} \| y_m \|^2 \tag{4.24}$$

where M is the number of samples of the received signal y.
Traditional ED can be simply implemented as a spectrum analyzer. A threshold used for primary user detection is highly susceptible to unknown or changing noise levels. Even if the threshold would be set adaptively, presence of any in-band interference would confuse the energy detector.
In order to achieve realistic and well founded simulations, DVB-T signals based on DVB-T 2K recommendations are used as the signals to be sensed. This choice can be justified by the fact that almost all licensed primary networks are DVB-T and secondary users are CR deployed in these networks. The signal parameters are given in Table 4.1. Figure 4.3

Bandwidth	8MHz
Mode	2K
Guard interval	1/4
Channel models	AWGN
Frequency-flat	Single path
Sensing time	1.5ms

Table 4.1: The transmitted DVB-T primary user signal parameters

shows the performance of the following simulated detectors: energy detector (ED), first order algebraic detector (AD_1), AD_1 with compression rate of $M/N = 20\%, 30\%, 40\%$ and 50% and a second order algebraic detector (AD_2) with $M/N = 50\%$. We note that ED, AD_1 and $AD_2^{50\%}$ all have the same complexity and the figure 4.3 shows that $AL_2^{50\%}$ have a much better performance than ED and at low SNRs it is outperforming AD_1.
Another key metric in the sensing problems is the receiver operating characteristics (ROC) curve which helps giving an idea about the reliability of the proposed technique. For instance we plot the ROC curve at $SNR = -25dB$ for ED, AD_1 and $AL_2^{50\%}$.
Figure 4.4 shows how reliable the compressed sensing technique is, as the detector operates at high probability of detection under a low false alarm rate.

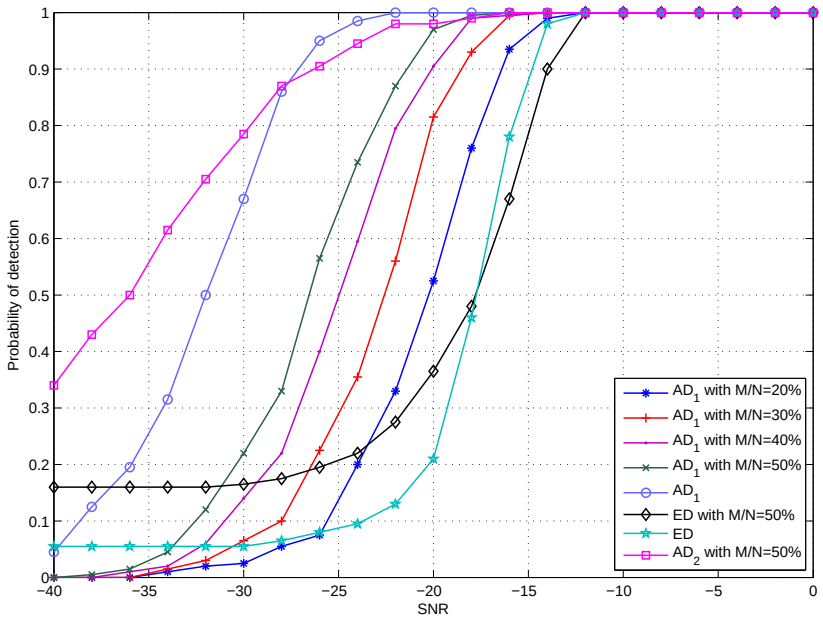

Figure 4.3: P_D vs. SNR at P_F=0.05; AD$_P$:Algebraic detection of order P; ED: Energy detector; $\frac{M}{N}$:Compression ratio.

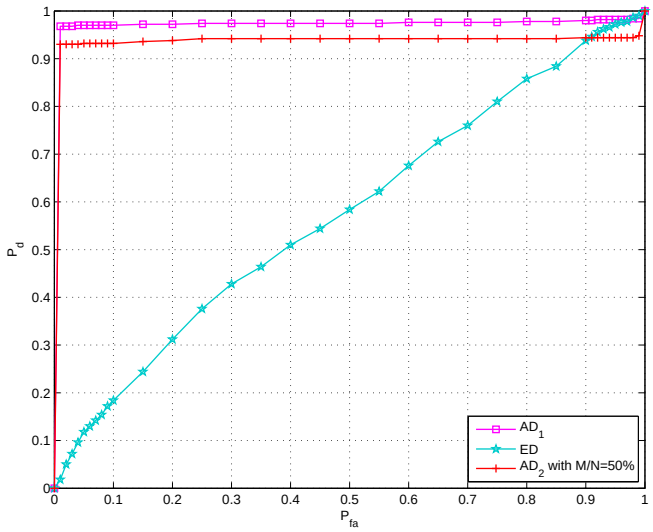

Figure 4.4: ROC curve at SNR=$-25dB$; AD$_P$:Algebraic detection of order P; ED: Energy detector; $\frac{M}{N}$:Compression ratio.

4.3.2 Cooperative Sensing

We consider collaborative radios group with size of $1, 5, 10, 20$ radios. For each group size, compressed collaborative detection with different compression ratios, $\frac{M}{N} = \{10\%, 20\%, 30\%\}$, is simulated and compared to the ED detector with single radio and no compression. Collaborative ED is not simulated due to timing issues and since the comparison is still valid with single radio as will be seen.

Figure 4.5 shows the performance of energy detector (ED) with no compression and first order algebraic detector AD_1 with different compression ratios for collaborative groups of size $1, 5, 10$ and 20 radios.

We note that only performance of a single radio with compression ratio of 10% is not as good as performance of ED with single radio and no compression. And for the rest of examples the performance is better. This is where the complexity of the compressed sensing, i.e., $\frac{M}{N}$, is much lower than ED, i.e., N. Collaboration among radios greatly improve the detection performance. Also, we note that when the number of collaborations increases the compression ratio at each radio can be decreased in order to achieve a specific probability of detection P_D.

Figure 4.6 shows the probability of detection that is achievable by different number of collaborative radios for a compressed sensing ratio of $\frac{M}{N} = 10\%$ at SNR=$-20dB$ and $P_F = 0.05$. These results are obtained with Algebraic detection of order $P = 1$, and using order $P = 2$

improves the performance dramatically where complexity increases to $2M$ from M. But, still, for example for $\frac{M}{N} = 10\%$, complexity is much less than complexity of ED, i.e., N. For $\frac{M}{N} = 50\%$ the complexity of compressive sensing technique is same as ED while the performance is much better comparing to ED.
As a final word, we can say that the collaborative compressed sensing can decrease the complexity and energy consumption of cognitive radio networks remarkably due to the low sampling rate required for each radio while it makes the cognitive network robust to fading.

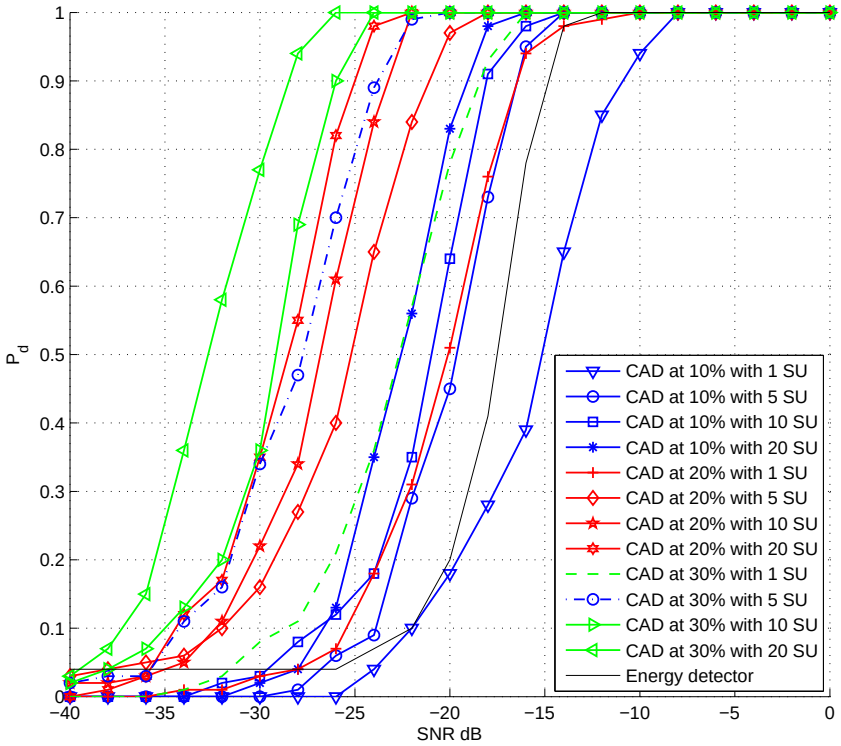

Figure 4.5: Probability of detection, P_D, vs. SNR at $P_F = 0.05$. CAD: Compressed sensing with Algebraic detection of order $P = 1$. SU: secondary users/collaborative radios.

4.4 Conclusion

We present in this work a new sensing technique which combines compressive sampling and algebraic method to detect spectrum holes. In a first step, we designed a compressed sensing matrix which keeps the linear properties of the sampled primary signal. Then, we applied the compressed measurements to algebraic detector to localize spectrum discontinuities and iden-

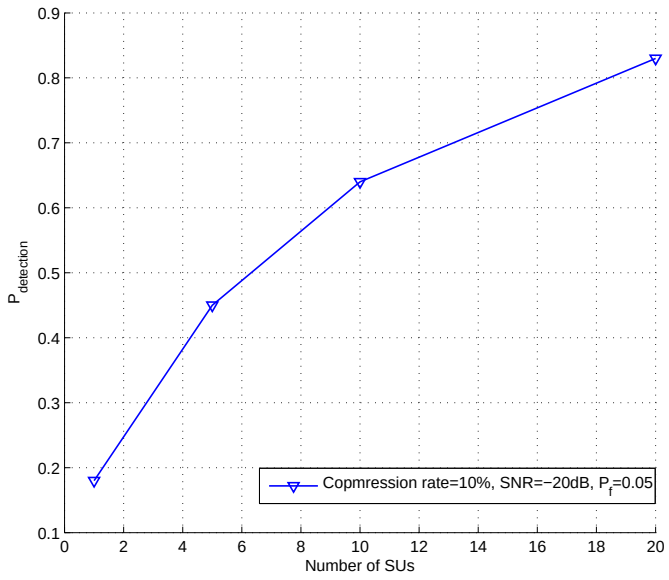

Figure 4.6: Probability of detection, P_D, vs. number of collaborative radios (SUs) with compressed sensing of ratio $\frac{M}{N} = 10\%$ and Algebraic detection of order $P = 1$, at SNR=$-20dB$ and $P_F = 0.05$.

tify spectrum holes. The analysis of the complexity of the proposed technique shows that it can be dramatically reduced when the model order of the algebraic detector increases. The performance comparison at different sampling rates shows that the new designed scheme achieves better performance than energy detector while preserving a low computational complexity.

Part II

Spectrum Awareness for Cognitive Radio Systems

CHAPTER 5

Spectrum Awareness for OFDM-based Cognitive Radio Systems

5.1 Introduction

The presented work in this chapter fits in the context of spectrum sensing/spectrum sharing framework for CR networks and more precisely single node detection/ standard identification. Related to this work, many statistical approaches for the spectrum sensing part were developed. As previously stated, one of the most performing sensing techniques is the cyclostationary features detection [7,17]. The main advantage of the cyclostationarity detection is that it can distinguish between noise signal and PU transmitted data. Indeed, noise has no spectral correlation whereas the modulated signals are usually cyclostationary with non null spectral correlation due to the embedded redundancy in the transmitted signal. The reference sensing technique is the energy detector [7], as it is the easiest to implement and the less complex detection technique. In the other hand, some papers have been dedicate to the signal identification part [51–53] and decision making [54,55] where the main focus was to identify what standard is being used by the PUs rather than simply detecting their presence. In this Chapter, we present a robust classification technique based on mixed signals separation and parallel spectrum sensing techniques in order to combine the sensing / classification features of the CR.

5.2 Targeted Scenarios

The goal of this chapter is to derive a classification scheme for different systems and signals coexisting in the TV White Spaces (TVWS). The transmitters considered in several CR networks (example for SACRA/SPECTRA projects) are identified and characterized below:

1. A DVB-T Primary User (PU) which uses OFDM Modulation. As shown later, there are several DVB-T configurations, depending on

   (a) the bandwidth (5 MHz, 6 MHz, 7 MHz, 8 MHz) of the channel being used,

(b) the modulation (QPSK/QAM/16-QAM/64-QAM) used by the subcarriers from the OFDM symbol,

(c) the useful symbol and guard periods: system characteristics have been predefined by standards, and they are fixed known values for the useful T_U and guard T_G period (the latter is also called cyclic prefix period).

2. An LTE Secondary User (SU) which uses OFDM Modulation (in DL) and SC-FDMA (in UL) combined with BPSK/QAM/16-QAM/64-QAM. System characteristics with fixed symbol and guard periods (T_U and T_G) have been predefined by 3GPP standardization activities.

3. A PMSE PU which uses QPSK Modulation (400 KHz Bandwidth) or FM Modulation (200 KHz). Excepting the bandwidth, the system characteristics are not very well defined for PMSE. These devices will further be discussed in latter sections.

In Figure (5.1), terminal UE5 is connected to a base station operating through the licensed band (2.6GHz), eNB3, and may be authorized to use resources in another band (DD/TVWS) to communicate with a second base station, eNB1. This use case is based on the spectrum aggregation concept, introduced in LTE-Advanced standard. The terminal is thus operating in a heterogeneous network, with OFDM LTE-A, OFDM DVB-T and PMSE signals cohabitating in the network. From this coexistence came the need to classify each standard in order to enable the opportunistic use of the TVWS bands. The due tasks of the CR are thus, mixed signals separation and then classification of each separated signal.

5.3 Proposed Algorithm for Signal Separation in Cognitive Radio Networks

Let M be the number of terminals in the proposed CRS architecture and N be the number of source signals.
The received wideband signal can be written as following:

$$x(t) = A \,.\, s(t) + n(t) \tag{5.1}$$

where $x(t)$ is a M-dimensional vector of the observed signals. $s(t)$ is a N-dimension vector corresponding to the source signals transmitted by the cognitive radios. The matrix A is $M \times N$, and denotes the mixing matrix. And $n(t)$ is the additive white noise vector having the same size as $x(t)$ Now, in order to proceed with the blind source separation (BSS) problem, and in order to adopt an independent component analysis (ICA) algorithm we have first to filter the wideband signal in a band of interest, modulate it to baseband, decorrelate,

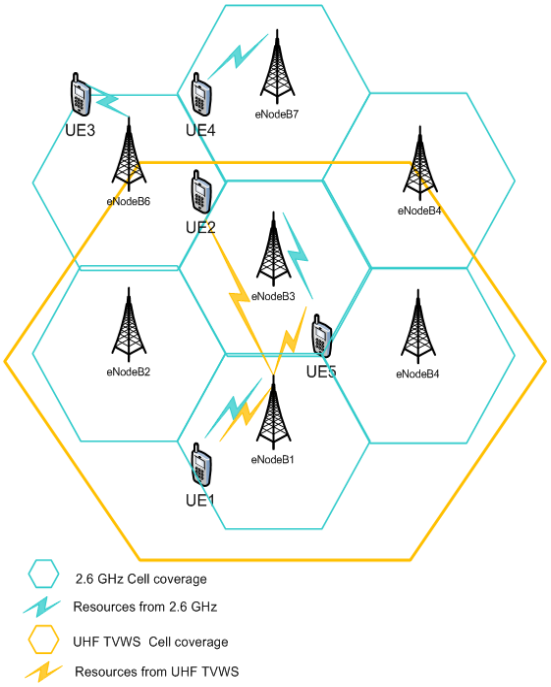

Figure 5.1: Targeted wide-band cognitive radio network scenario

center its data, proceed with the FastICA and finally demodulate back the signal to its original frequency band.

1. Filtering:
   In order to be able to separate the source signals from the mixture present in each subband, we need to analyse each subband separately. Thanks to the frequency edge location algorithm, we can sub-divide the wideband signal and thus obtain the frequency borders. By choosing two consecutive frequencies from the frequency set $\{f_n\}$, we can construct a filter h_{B_n} where $B_n = f_n - f_{n-1}$ is frequency support and $f_{nm} = (f_n - f_{n-1})/2$ is the center frequency.
   Then in order to filter the signals between f_{n-1} and f_n, we get x_{in}: observed signal on each CR given by:
   $$x_{in} = x_i * h_{B_n}, \quad i = 1, 2, .., M \tag{5.2}$$
   where * denotes the convolution operation.

2. Signal Modulation:
   As we intend to use some Blind Signal Separation (BSS) processing, and as it is gen-

erally done in BSS, we modulate high frequency signals back to base band frequency. Thus we get:

$$x_{inL} = x_{in} * h_{Modn}, \;\; i = 1, 2, .., M \tag{5.3}$$

where, x_{inL} is the modulated signal on each terminal and h_{Modn} represents the modulation carrier according to the estimated frequency edge. From this modulation process, we finally get a baseband signals matrix

$$X_{nL} = [x_{1nL}^T \;\; x_{2nL}^T ... \;\; x_{mnL}^T ... \;\; x_{MnL}^T]^T$$

3. Signals decorrelation and centering:
   In order to proceed with BSS and ICA analysis of mixute, we have to make sure that the vector X_{nL} is uncorrelated and zero mean. Thus we proceed as following:
   Centering Phase:
   $$\widetilde{X}_{nL} = X_{nL} - E[X_{nL}] \tag{5.4}$$
   now that the matrix $\widetilde{X}_{nL}$ is a zero-mean matrix, we can proceed to make it a non correlated matrix as classically done in BSS and ICA preprocessing. We also chose to ensure at the output of this process a unity variance for the uncorrelated matrix components.
   Whitening Phase:
   $$\widehat{X}_{nL} = E \,.\, D^{\frac{-1}{2}} \,.\, E^T \,.\, \widetilde{X}_{nL} \tag{5.5}$$
   where E is the orthogonal matrix of eigenvectors of $E\{\widetilde{X}_{nL} \,.\, \widetilde{X}_{nL}^T\}$. $D = diag(d_1, ..., d_M)$ is the diagonal matrix containing the eigenvalues of $E\{\widetilde{X}_{nL} \,.\, \widetilde{X}_{nL}^T\}$.

4. Separation Technique:
   Now that the matrix containing mixture signals is well conditioned, we can proceed to the signal separation step. In FastICA, which is one of the most used techniques for signals separation, the source signals in baseband, $\widehat{S}$, can be derived from the modulated, whitened, centered signal using a separation matrix, say W, as described by the following equation:
   $$\widehat{S} = W^T \,.\, \widehat{X}_{nL} \tag{5.6}$$
   In order to briefly describe the separation process, we initially choose an M-dimential weight vector, say w_{init}. Afterwards, the vectors has to be computed and updated in order to converge to W. The first component is computed at the first iteration by:
   $$\begin{aligned} w_1^+ &= E\{\widehat{X}_{nL} \,.\, g(w_{init}^T \,.\, \widehat{X}_{nL})\} \\ &- E\{g'(w_{init}^T \,.\, \widehat{X}_{nL})\} \,.\, w_{init} \end{aligned} \tag{5.7}$$

then we normalize w_1 as following:

$$w_1 = \frac{w_1^+}{\|w_1^+\|} \tag{5.8}$$

where $g(\ .\ )$ is a non quadratic function that usually is chosen among: gaussian, hyperbolic tangent or a cubic function.
If w_1 does not converge, we proceed with equation (5.8) until $|w_1^T\ .\ w_{init}|$ gets as close as possile to 1.
Now, that w_1 converged,we get by successive iteration the $N-1$ (N and M are not necessarely equal) missing vectors of separation matrix. The k^{th} is computed at the k^{th} iteration by:

$$\begin{aligned} w_k^+ &= E\{\widehat{X}_{nL}\ .\ g(w_{k-1}^T\ .\ \widehat{X}_{nL})\} \\ &- E\{g'(w_{k-1}^T\ .\ \widehat{X}_{nL})\}\ .\ w_{k-1} \end{aligned} \tag{5.9}$$

then we normalize w_k as following:

$$w_k = \frac{w_k^+}{\|w_k^+\|} \tag{5.10}$$

Therefore, after all these computations, we obtain the matrix $W = [w_1^T\ ,\ w_2^T\ ....\ , w_N^T]$.
Now, having an estimate of the matrix W, we can compute the source signals and recontract S from the observed mixture from 5.6:

$$\widehat{S} = W^T\ .\ \widehat{X}_{nL}$$

where $\widehat{S} = [\widetilde{s}_{1nL}^T\ \ \widetilde{s}_{2nL}^T ...\ \ \widetilde{s}_{inL}^T ...\ \ \widetilde{s}_{NnL}^T]^T$, is the separated signals matrix. Given this notation, $\widetilde{s}_{inL}^T$ denotes the separated baseband signal vector.

5. Demodulation:
As a final step, we modulate $\widehat{S}$ back to its original subbands via the demodulation filter h_{demodn} constructed from the knowledge of h_{Modn}. and thus we get:

$$\widetilde{s}_{in} = \widetilde{s}_{inL} * h_{demodn},\ \ i = 1, 2, .., N \tag{5.11}$$

where $\widetilde{s}_{in}$ denotes the recovered signal vector on the frequency support delimited by f_{n-1} and f_n. And finally denoting, $\widetilde{S} = [\widetilde{s}_{1n}^T\ \ \widetilde{s}_{2n}^T ...\ \ \widetilde{s}_{in}^T ...\ \ \widetilde{s}_{Nn}^T]^T$, we do obtain the recovered signals matrix on each subband $[f_{n-1}\ ,\ f_n]$.

5.4 The Standards Classification Scheme

5.4.1 Conventional Spectrum Sensing for CRS

In order to model the spectrum sensing problem, let's suppose that the detector receives signal $y_n = A_n s_n + e_n$, where A_n models the channel, s_n is the transmit signal sent from primary

user and e_n is the additive noise. The goal of spectrum sensing, as depicted in Figure (5.2), is to decide between two conventional hypotheses modeling the spectrum occupancy H_0 and H_1 modeling respectively, the decision by the detector of PU signal absence and presence. In order to make such a decision, the detector implements a scalar test statistic Λ function of the input signal y_n. This test statistic is to be compared to a threshold level γ function of the SNR and the probability of false alarm P_{FA} and we thus obtain:

$$\begin{cases} \text{if } \Lambda = \mathfrak{F}(y_n) \geq \gamma & \text{decide } \mathrm{H}_1 \\ \text{if } \Lambda = \mathfrak{F}(y_n) < \gamma & \text{decide } \mathrm{H}_0 \end{cases} \tag{5.12}$$

In the proposed classification scheme, we proposed to mount as many parallel detectors as the number of standards we would like to discriminate. In this work for example, we would like to focus on two OFDM-based standards (LTE, DVB-T) and PMSE signals (for wireless microphones), therefore the classifier would have 3 stages.

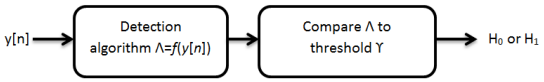

Figure 5.2: Spectrum Sensing Principles

5.4.2 Robust Signal Classifier for CRS

In this section, we briefly present each signal to be classified and the corresponding test statistic and threshold to be applied for the each detection stage. Since we are considering three standards, the proposed classifier has to implement three stages as presented in Figure (5.3) and explained afterwards.

5.4.2.1 LTE signals detection

The algorithm we are adopting is fully described in [58]. To sum-up, the algorithm is based on the fact that LTE signals exhibit reference signals-introduced second-order cyclostationarity with the cyclic autocorrelation function (CAF), $R_y^\alpha(\tau) \neq 0$ at cyclic frequency $\alpha = 0$ and delay $\tau = D_F$ (D_F is the frame duration) for all transmission modes. This property exhibited by FDD downlink LTE-OFDM transmissions can thus be used to detect presence of LTE signals. The CAF of the received signal, y_n, is estimated from N_s samples at the delay τ and the CF (cyclic frequency) α and we form the following vector: $\widehat{R}_y^\alpha = [\mathrm{Re}(R_y^\alpha(\tau))\mathrm{Im}(R_y^\alpha(\tau))]$ in order to compute the test statistic given by:

$$\Lambda_{LTE-CFD} = N_s \widehat{R}_y^\alpha \widehat{\Sigma}^{-1} (\widehat{R}_y^\alpha)^t \tag{5.13}$$

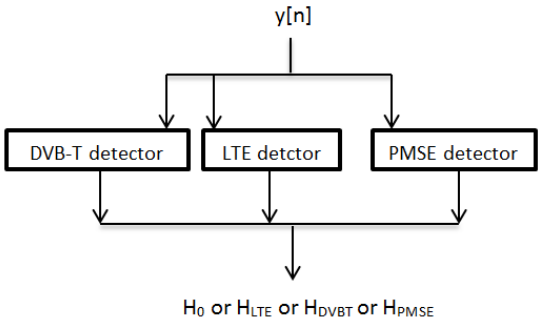

Figure 5.3: Proposed Standard Classification Scheme

where $\widehat{\Sigma}$ is the estimate of the $\widehat{R}_y^{\alpha}$ covariance matrix.
The test statistic $\Lambda_{LTE-CFD}$ has now to be compared to some threshold value λ to make the decision. As previously stated, this threshold is function of the probability of false alarm P_{FA}. In our case, and given the test statistic, a possible definition of P_{FA} could be: the probability of deciding that the tested frequency α is a CF at delay τ when this is actually not. frequency is a CF at delay, or : $P_{FA} = \Pr(\Lambda_{LTE-CFD} \geq \lambda | \mathrm{H}_0)$. keeping in mind that $\Lambda_{LTE-CFD}$ is following a chi-squared distribution [59], the threshold λ is obtained from the tables of the chi-squared distribution for a given value of P_{FA} probability.

5.4.2.2 DVB-T signals detection

For the detection of DVB-T signals, a robust algorithm to be applied could be the autocorrelation based detector (AD). Let us remind the mathematical formulation of AD. It is based on the fact that many communication signals contain redundancy, introduced for example to facilitate synchronization, by channel coding or to circumvent inter-symbol interference. This redundancy occurs as non-zero average autocorrelation at some time lag l. The autocorrelation function at some lag l can be estimated from:

$$\hat{r}_l(y) = \frac{1}{p-l} \sum_{n=0}^{p-l-1} y_{n+l}\, y_n^* \qquad l \geq 0 \tag{5.14}$$

where p is the length of the PU signal in samples. Any signal except for the white noise case will have values of the autocorrelation function different from zero at some lags larger than zero, although some might be exactly zero depending on the zero crossings. In [56], authors have proposed an autocorrelation-based detector for DVB-T OFDM signals. This detector is limited to the case when the PU is using DVB-T. To detect the existence/non existence of signal

we use functions of the autocorrelation lags, where the autocorrelation is based on Equation (5.14). Therefore, the autocorrelation-based decision statistic is given by [57]

$$\Lambda_{DVBT-AD}(y) = \sum_{l=1}^{L} w_l \frac{\mathrm{Re}\{\hat{r}_l\}}{\hat{r}_0} \tag{5.15}$$

where the number of lags, L, is selected to be an odd number. The weighting coefficients w_l could be computed to achieve the optimal performance, and is given by:

$$w_l = \frac{L+1+|l|}{L+1} \tag{5.16}$$

5.4.2.3 PMSE signals detection

For the PMSE signal, we opt for a wireless-microphones oriented detector the Teager-Kaiser energy detector for narrowband wireless microphone as presented in [60]. The PMSE signal as transmitted from the PMSE equipment can be modeled by:

$$x(t) = A\cos(2\pi f_0 t + \frac{\kappa_f}{s_m}\int_{\tau} s(\tau)d\tau) \tag{5.17}$$

where where f_0 is the carrier frequency, κ_f the frequency deviation of the FM modulation, and $s(t)$ the modulating signal having an amplitude of s_m. The signal $x(t)$ has a power $\sigma_x^2 = A^2/2$. And the received signal over an AWGN is :

$$y(t) = x(t) + n(t) \tag{5.18}$$

In order to derive the test statistic of this detector, The Teager-Kaiser energy operator Ψ is used to extract directly the energy from the instantaneous signal and is expressed by:

$$\Psi[y(k)] = \Psi[x(k)] + \Psi[n(k)] + 2\Psi[x(k), n(k)] \tag{5.19}$$

and since the noise and the signal are uncorrelated, $\Psi[x(k), n(k)] = 0$. and the test statistic is the average value of Teager-Kaiser energy operator applied to $y(k)$, expressed as:

$$\Lambda_{PMSE-TKED} = E\langle\Psi[y(k)]\rangle \tag{5.20}$$

$$= E\langle\Psi[x(k)]\rangle + \sigma_n^2 \tag{5.21}$$

For this detector, we will use a Monte-Carlo simulation to derive the desired threshold function of the P_{FA}.

5.4.2.4 Combining rule for Classification

So far, the choice made for each detectors was based on the criterion that each sensing technique should be suitable for only one standard. That is why the choice for DVB-T was the autocorrelation detector (DVBT-AD) that highlights the DVB-T characteristics among the other standards; and for LTE we opted for the second order cyclostationary feature detector (LTE-CFD); and finally for PMSE signal we used the Teager-Kaiser energy operator (PMSE-TKED) that is convenient for narrowband signals. In order to combine the outputs of these standard-dedicated detectors, we will fuse the data from different stages of OFDM-based techniques as in Equation (5.22).
In Equation (5.22), for the two first decisions, we won't focus on TKED output, as if it is an LTE or DVB-T signal it has an output energy greater than the threshold, so its output is $\mathcal{H})_1$. We will focus rather on the outputs of the CFD and the AD in order to discriminate between LTE and DVB-T respectively. We will focus on TKED only when the CFD and AD give both null hypothesis testing results $\mathcal{H}_0$.

$$\begin{cases} \text{if } \frac{\Lambda_{DVBT-AD}}{\gamma_{AD}} \geq 1 \text{ and } \frac{\Lambda_{LTE-CFD}}{\gamma_{CFD}} < 1 & \text{decide } \mathcal{H}_{DVB-T} \\ \text{if } \frac{\Lambda_{LTE-CFD}}{\gamma_{CFD}} \geq 1 \text{ and } \frac{\Lambda_{DVBT-AD}}{\gamma_{AD}} < 1 & \text{decide } \mathcal{H}_{LTE} \\ \text{if } \frac{\Lambda_{PMSE-TKED}}{\gamma_{TKED}} \geq 1 \text{ and } \frac{\Lambda_{DVBT-AD}}{\gamma_{AD}} < 1 \text{ and } \frac{\Lambda_{LTE-CFD}}{\gamma_{CFD}} < 1 & \text{decide } \mathcal{H}_{PMSE} \end{cases} \tag{5.22}$$

5.5 Simulations and Results

5.5.1 Simulation Settings

We define two scenarios to evaluate the proposed solution:

- **Scenario 1:** In this scenario, we use DVB-T and LTE OFDM signals plus a QPSK wireless microphone as PMSE signal over an AWGN channel. It is assumed that the detection performance in AWGN will provide a good impression of the performance, but it is necessary to extend the simulations to include signal distortion due to multipath and shadow fading.

- **Scenario 2:** In this case, we use the same signals as Scenario 1, but to make the simulations more realistic, the signal is subjected to Rayleigh multipath fading and shadowing

following a log normal distribution in addition to the AWGN. The maximum Doppler shift of the channel is 100Hz and the standard deviation for the log normal shadowing is 10dB.

The simulation parameters used in this section for the DVB-T signals are are given in Table 5.1 [61, 62], while LTE signals are of bandwidth 10 MHz and using short cyclic prefix (CP). For more details on LTE parameters see ref [63], [64] and [65] for LTE specifications and simulations. And as far as PMSE signals are concerned a QPSK narrowband signal was considered for the simulation of wireless microphones.

Bandwidth	8MHz
Mode	2K
Guard interval	1/4
Channel	AWGN
Classification time	25ms

Table 5.1: The chosen DVB-T primary user signal parameters

5.5.2 Simulation Results

Figures (5.4) and (5.5), report the results of the two simulated scenarios. A general remark that could be made is that the DVB-T classification outperforms LTE and PMSE. That is fully comprehensible as for DVB-T the detection is made using the autocorrelation function of the whole signal, but for LTE we only made it for the RS (reference signals) which makes the correlation length lower than the DVB-T one; and this gets worst for PMSE as the signal itself is a narrowband one ($Bandwidth \leq 400KHz$). In Figure (5.4), the classification is done over an AWGN channel for 25 ms acquisition which is meant to give a first overview of the classifier performance and in Figure (5.5), for the same period the classification scheme is tested under a more realistic channel model, a Rayleigh multipath fading and shadowing following a log normal distribution in addition to the AWGN. The maximum Doppler shift of the channel is 100Hz and the standard deviation for the log normal shadowing is 10dB.

5.6 Conclusion

In this Chapter we presented a novel robust classification scheme. The use-case considered was a heterogenous network configuration projects case which, without any loss of generalities can be extended to any other cognitive network scenario. The robustness of the proposed classifier resides in the choice of the sensing algorithm for each standard. Here the AD was

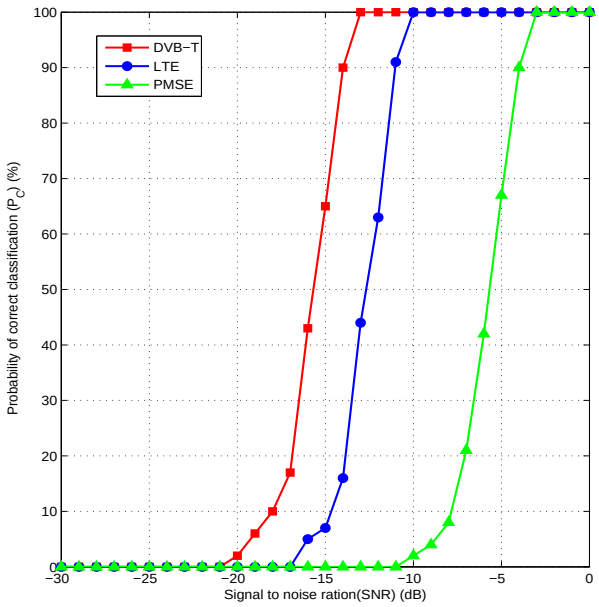

Figure 5.4: Probability of correct classification (P_C) Vs. Signal to Noise Ratio (SNR) for a Probability of False Alarm $P_{FA} = 10^{-3}$ and classification period of 25 ms: Scenario 1

chosen for DVB-T because it was assumed to be the best detector exploiting the OFDM DVB-T properties and so is the choice for CFD for OFDM LTE standard, but since the PMSE signals are quite hard to model in terms of statistics, we opted for the exploitation of the narrowband property of those signals.

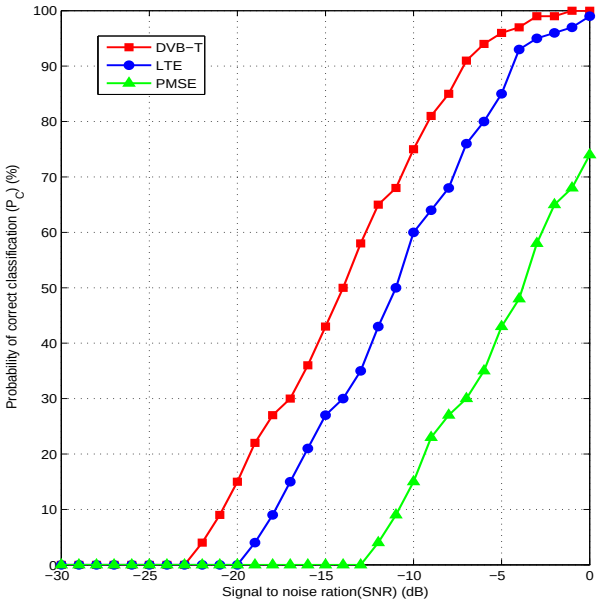

Figure 5.5: Probability of correct classification (P_C) Vs. Signal to Noise Ratio (SNR) for a Probability of False Alarm $P_{FA} = 10^{-3}$ and classification period of 25 ms: Scenario 2

CHAPTER 6

A Computer Vision OFDM-based Signal Classification Approach for Cognitive Radio Applications

6.1 Introduction

The first goal of this chapter is to identify classification methods for different systems with specific parameters and signal characteristics and operating in the TV White Spaces. The transmitters considered in our scenario are identified and characterized below:

1. A DVB-T Primary User (PU) which uses OFDM Modulation. As shown later, there are several DVB-T configurations, depending on
   (a) the bandwidth (5 MHz, 6 MHz, 7 MHz, 8 MHz) of the channel being used,
   (b) the modulation (QPSK/QAM/16-QAM/64-QAM) used by the subcarriers from the OFDM symbol,
   (c) the useful symbol and guard periods: system characteristics are predefined by standards, and they are fixed known values for the useful T_U and guard T_G period (the latter is also called cyclic prefix period).
2. An LTE Secondary User (SU) which uses OFDM Modulation (in DL) and SC-FDMA (in UL) combined with BPSK/QAM/16-QAM/64-QAM. System characteristics with fixed symbol and guard periods (T_U and T_G) are predefined by 3GPP standardization activities.
3. A PMSE PU which uses QPSK Modulation (400 KHz Bandwidth) or FM Modulation (200 KHz). Excepting the bandwidth, the system characteristics are not very well defined for PMSE. These devices will further be discussed in latter sections.

The second goal of this chapter is to define the specifications for the signal classification algorithms to be used by the cognitive radios. The purpose of classification in the CRS context is

to discriminate between multiple systems transmitting at the same time, in the same frequency band. From all the possible discrimination scenarios (i.e., between SUs, between SUs and PUs, between PUs), we have further selected only one (i.e., between SUs and PUs), which seems to be the most relevant one.

Even if the coexistence between SUs (SU/SU coexistence) is a very interesting case, the LTE coexistence should be addressed only for the inter-operator coexistence context. This statement is justified by the fact that intra-operator coexistence could easily be managed by a higher entity which deals with resource management (the eNodeBs are connected through the X2 interfaces and can easily deal with the intra-operator resource allocation), so the operator will use his own frequency spectrum without employing any classification techniques. Therefore, only the inter-operator coexistence could justify the classification, but it is out of scope of this work.

The coexistence of different PUs (PU/PU coexistence) seems to be not very realistic because, by definition, a PU occupies a licensed frequency band and 2 given PUs are not sharing the same licensed frequency band.

Regarding the coexistence between SUs and PUs (i.e., SU/PU coexistence), we assume that the SU should leave the opportunistic spectrum band once the PU starts transmitting. However, since the SU performs detection before opportunistically accessing the spectrum, the only valid classification scenario is when the PU is not present (or is not detected), the SU system starts communicating in the TVWS, and at a given unknown time, a PU starts retransmitting or starts transmitting for the first time. In this scenario, the SU system has to perform classification in order to discriminate signals coming from its own system and PU transmissions.

The classification is therefore necessary for a SU in order to discriminate between its own network and a PU that started to use the same spectrum at a given time, and without any quiet period made by the SU system.

6.2 Cyclostationarity for LTE, DVB-T and PMSE

The autocorrelation function $R_{rr}\left(t,\tau\right)$ of the received signal $r\left(t\right)$, in our considered scenarios $r\left(t\right) = r_{LTE}(t) + r_{DVBT}(t) + n(t)$ or $r\left(t\right) = r_{LTE}(t) + r_{PMSE}(t) + n(t)$, with $n(t)$ the white additive Gaussian noise, $r_{LTE}(t)$the received LTE signal from own secondary system, while $r_{DVBT}(t)$ and $r_{PMSE}(t)$are representing the incumbent PU signals, can be represented by Fourier series expansion as

$$R_{rr}\left(t,\tau\right) = \sum_{\alpha\in\psi} R_{rr}^{\alpha}\left(\tau\right)\exp\left(j2\pi\alpha t\right)$$

where α is a cyclic frequency, ψ is the entire set of cyclic frequencies, and $R_{rr}^{\alpha}\left(\tau\right)$ is the Fourier coefficient, also called Cyclic Autocorrelation Function (CAF). The CAF of the second

order autocorrelation function can be written as

$$R_{rr}^{\alpha}(\tau) = \lim_{T\to\infty} \frac{1}{T} \int_{-\frac{T}{2}}^{\frac{T}{2}} r(t) r^*(t-\tau) \exp(-j2\pi\alpha t)\, dt = \\ = \lim_{T\to\infty} \frac{1}{T} \int_{-\frac{T}{2}}^{\frac{T}{2}} r^*(t) r(t+\tau) \exp(-j2\pi\alpha t)\, dt$$

When we refer to CAF we usually refer to the second order CAF described by the previous equation, but in its time-discrete form is : $R_{rr}^{\alpha}(d) = \frac{1}{N_r} \sum_{n=0}^{N_r-1} r^*(n) r(n+d) \exp(-j2\pi\alpha n \Delta t)$. Here the delay d is normalized by the sampling frequency Δt, and N_r represents the number of available samples.

The Generalized Likelihood Ratio Test (GLRT) algorithm for cyclostationary features detection (CFD) is computing the covariance matrix $\sum_r \alpha$ as in [59]. Based on this covariance matrix, the method further computes the test statistic $N \cdot \underline{r}_{rr}^{\alpha}(\tau) \cdot \left(\sum_r(\alpha)\right)^{-1} \cdot \underline{r}_{rr}^{\alpha}(\tau)^T$, where $\underline{r}_{rr}^{\alpha}(\tau) = [Re\left(R_{rr}^{\alpha}(\tau)\right), Im\left(R_{rr}^{\alpha}(\tau)\right)]$. The test statistic is then compared to a threshold γ [66], computed with the help of the following equation:

$$P_{FA,t\arg et} = 1 - \Gamma(1, \gamma/2).$$

where Γ is the incomplete gamma function. In our simulations we have considered the target false alarm probability used for signal classification $P_{FA,t\arg et} = 0.1$.

The table below presents examples of the cyclic frequencies adequate for the most common types of secondary and primary user signals [67]:

Type of Signal	Cyclic Frequencies	(First) τ
OFDM	k/T_S, $k = \pm$ 0,1,2,...	$\pm\, T_U$
FM	$\pm\, 2f_0$	Does not matter
QPSK	k/T_S, $k = \pm$ 0,1,2,...	$\pm$ (1/2)T_S *for k=1*

Table 6.1: Cyclic frequencies for different signal types

For an OFDM signal, the peaks in the Cyclic Autocorrelation Function (CAF) are dependent on T_U and total symbol duration which is T_S=T_U+T_{CP}. The CAF will exhibit peaks for τ=$\pm T_U$ and α= *k/*(T_U+T_{CP}), *k*=$\pm$ 0,1,2, etc. For a sum of multiple OFDM signals with different parameters (different T_U and different T_S), multiple distinct peaks should appear on the cyclic autocorrelation function. Therefore, in general, cyclostationary detection may also be used for signal classification.

For normal cyclic prefix (LTE) there are 2 types of guard periods: for the first symbol T_{CP}/T_U=10/128; and for the rest of the symbols T_{CP}/T_U =9/128. The LTE cyclic prefix is very small, thus decreasing the cyclostationary properties.

For PMSE QPSK, the bandwidth is BW=400 KHz (or 600 KHz). The symbol period is T_S=(1+Roll-Off-Factor)/BW if Nyquist filter is being used. Our cyclostationary tests are con-

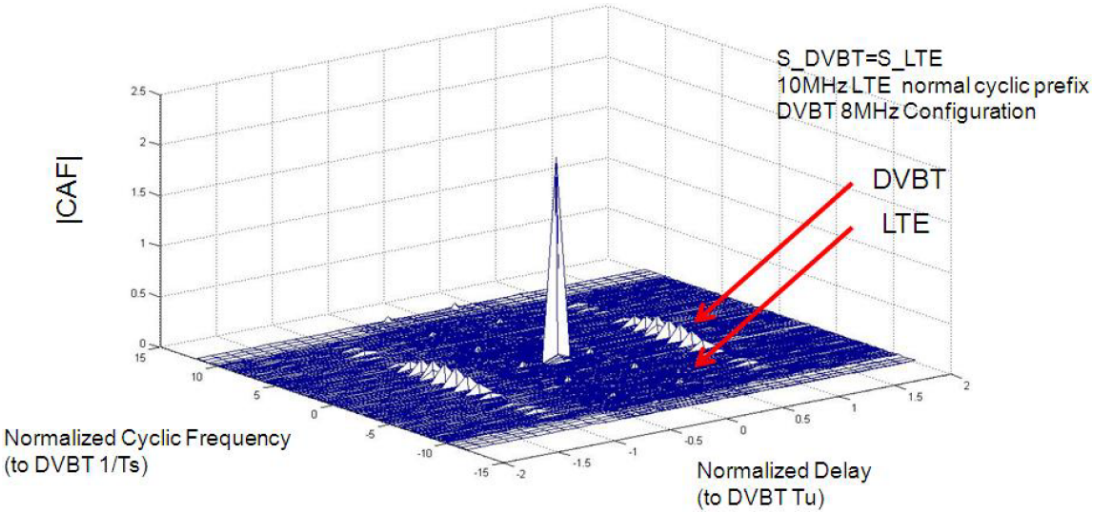

Figure 6.1: DVB-T and LTE signal classification using CAF

sidering different roll-off factors. The cyclic frequencies are appearing for multiple of $1/T_S$. The cyclic peaks are present for delays $\tau = \pm T_S/2$ (depending on the configuration);
For PMSE FM, the bandwidth BW=200 KHz. The PMSE system has to be carefully calibrated with respect to Carlson formula and required PMSE spectrum mask, meaning that a modulation index m=1.69 has to be used. Cyclic frequencies are present at $\pm 2f_0$ (residual carrier frequency in the considered band). It is important to mention that FM exhibits cyclostationary peaks for delays $\pm 1/2f$ when sinusoidal modulated signal is being used. This explains the presence of the secondary lobes.

6.3 DVB-T Signal Classification when LTE System is Transmitting

In Figure (6.1), we show that CAF DVB-T and CAF LTE characteristics are different. For LTE we have considered a 10 MHz system configuration with normal cyclic prefix, while for DVB-T we have considered an 8 MHz – 2k mode. The figure is showing that DVB-T classification is possible when LTE system is transmitting. In Table 6.2, using two different values for the Noise Figure (NF) and the 10 MHz LTE configuration, we have derived two values of SNRmin for DVB-T:

- -18.86 dB if the NF = 7 dB

	Signal Bandwidth	Pmin	Filter Bandwidth	Noise Density (KT)	NF	SNRmin
DVB-T	7.6 MHz	-114 dBm	8 MHz=69 dBHz (for subband splitting)	-174 dBm/Hz	7 dB	-16 dB
DVB-T	7.6 MHz	-114 dBm	3.84x4=15.36 MHz=71.86 dBHz	-174 dBm/Hz	7 dB	-18.86 dB
DVB-T	7.6 MHz	-114 dBm	3.84x4=15.36 MHz=71.86 dBHz	-174dBm/Hz	3 dB	-14.86 dB

Table 6.2: DVB-T SNRmin requirement for classification, under 10 MHz LTE system configuration

- -14.86 dB if the NF = 3 dB.

Figure (6.2) shows that 50 ms time is not sufficient for DVB-T classification when LTE is transmitting, if the NF is too high. However, for systems with 3 dB NF, the SNR required might be reached in cases when SNR LTE is sufficiently low. However, Figure (6.3) clearly shows that 250 ms classification time is sufficient for DVB-T classification when LTE is transmitting (SNR LTE is 0dB), for both NF=3dB and NF=7dB .

6.4 Computer Vision aided Signal Classification

6.4.1 Computer Vision Tools

The proposed approach uses two non-linear image processing tools to enhance the accuracy of PU signals detection at the SU side. Those tools are:

- **Morphological Reconstruction (MR)**. MR involves the use of non-linear image processing tools (e.g., erosion and dilation) to reconstruct an original image "marker" of unknown information about its features into a new image "mask" of parts that can be easily extracted and represented by meaningful information [68]. Moreover, the use of MR will smooth out spurious points that may cause false detections [69].
- **Extraction of connected components**. The detection of OFDM signals that belong to different standards involve searching the generated "mask" for objects/regions that

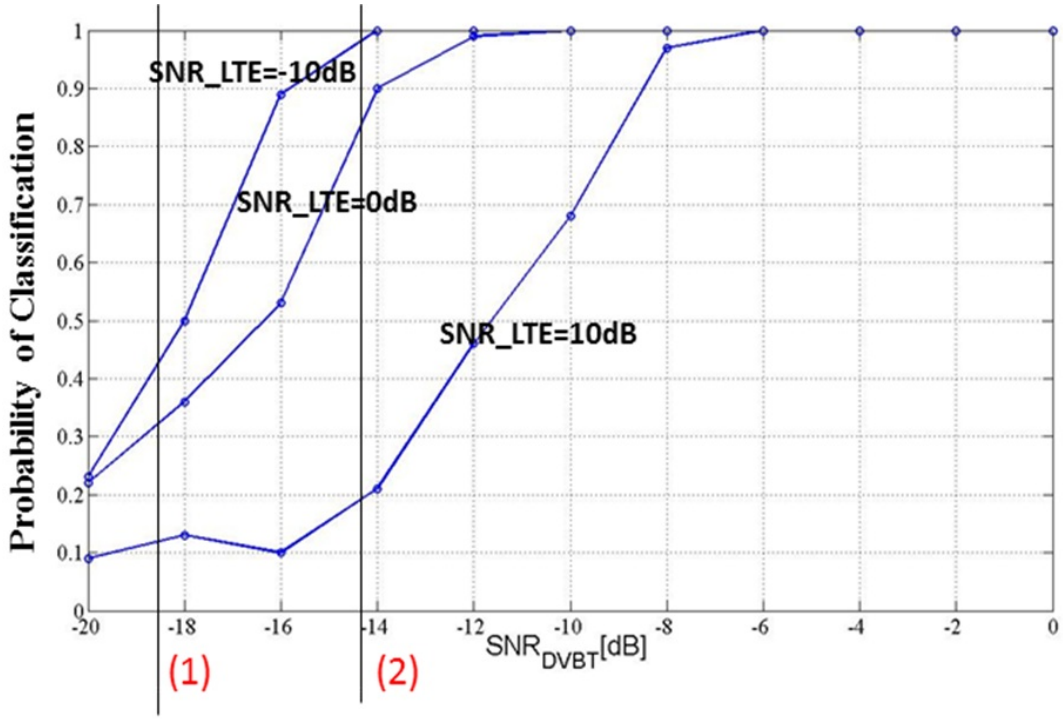

Figure 6.2: DVB-T classification, when LTE system is communicating, for 50 ms classification time

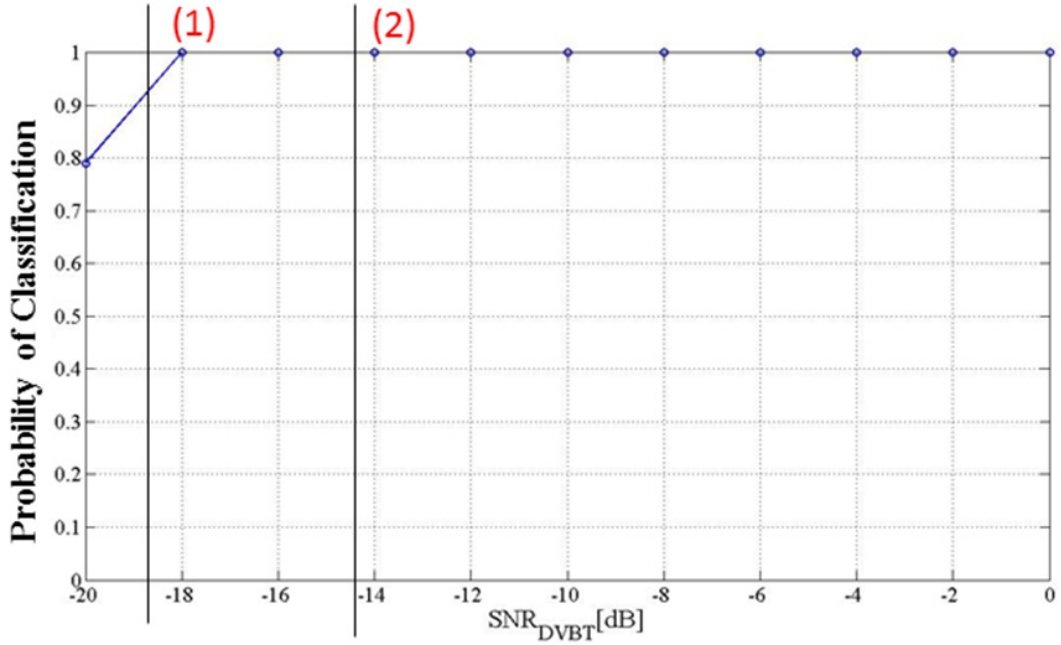

Figure 6.3: DVB-T classification, when LTE system is communicating, for 250 ms classification time

share specific features of the different OFDM standards. For example Figure (6.6) and Figure((6.7) demonstrate the "marker" image and the morphologically reconstructed "mask" image using an 8 point-connectivity region search [68].

6.4.2 Computer Vision aided Cycolstationary Features Detection

Figure (6.4) shows a block diagram of the proposed CV-CFD detection scheme. First, the autocorrelation function of the sensed input signal $y(t)$ is computed then processed using two non-linear image processing tools. A suitable threshold value is calculated based on the output image energy and that is how the final signal detection decision is made. For example,

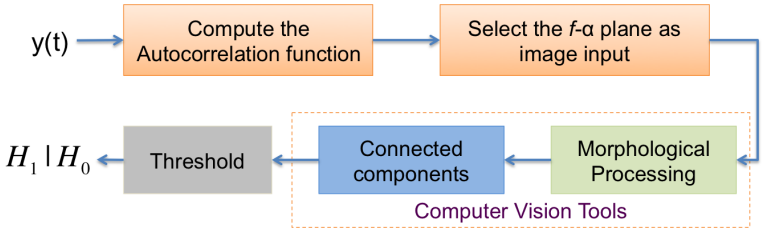

Figure 6.4: Signal detection flow.

Figure (6.5) shows the autocorrelation function of a noise free DVB-T signals. The locations of the autocorrelation peaks are specific to the DVB-T standards. This feature can be used to improve the detection of those signals in presence of other OFDM-based signals such as LTE or WiMAX that have their autocorrelation peaks at different locations [56]. Extracting the (f, α) plane from Figure 6.5, we obtain for the "marker" DVB-T signal at SNR = -5dB in Figure (6.6). The peaks location correspond to the highly contrasted regions in that plane, we can observe four regions in the (f, α) plane that the CV techniques help to emphasize compared to the remaining parts of the image. Figure 6.6 is considered as the input of the computer vision algorithms. The output is shown in Figure 6.7. Finally, the threshold value is calculated from the energy present in the new image,Figure (6.7), looking at the expected peak positions for specific wireless standards in the image provided by the CV tools. The x- and y-axis in Figures (6.6) and (6.7) represent the frequency f and the cyclic frequency α, respectively.

6.4.3 CV-CFD as a Sensing Technique

In this section we simulate the detection of two OFDM-based DVB-T systems using three spectrum sensing detectors. The combined CV-CFD, conventional CFD, and ED. The simulation parameters used for the DVB-T signals are given in Table 6.3:

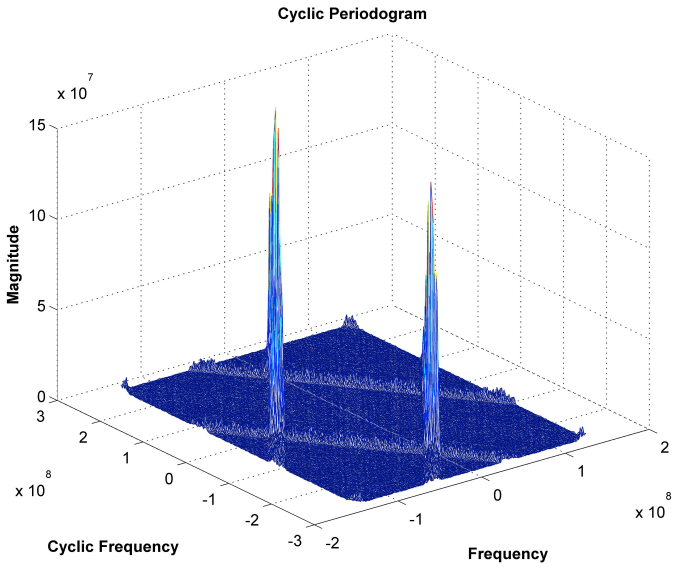

Figure 6.5: Cyclic Autocorrelation Function for DVB-T signal example computed according to Equation (5.14)

Bandwidth	8MHz
Mode	2K
Guard interval	1/4
Channel	AWGN
Sensing time	1.5ms

Table 6.3: The chosen DVB-T primary user signal parameters

Figure 6.8 shows the signal detection performance for the conventional CFD and the computer vision aided cyclostationary features detector (CV-CFD) for DVB-T. This figure clearly shows the significant CV-CFD performance compared with that of the conventional CFD. For example, in Figure 6.8, a performance gain of 5 dB is achieved at $P_{FA} = 0.05$, for DVB-T. In Figure 6.8, a performance gain of 5 dB is achieved at $P_{FA} = 0.05$. In addition, the proposed CV-CFD offers the best performance at low SNR conditions.

6.4.4 Improving Classification through Computer Vision

We use exactly the same formalism as in Section (5.3), but using the novel improvements in the CFD. For the classification of DVB-T while LTE is transmitting, we obtain the curve reported

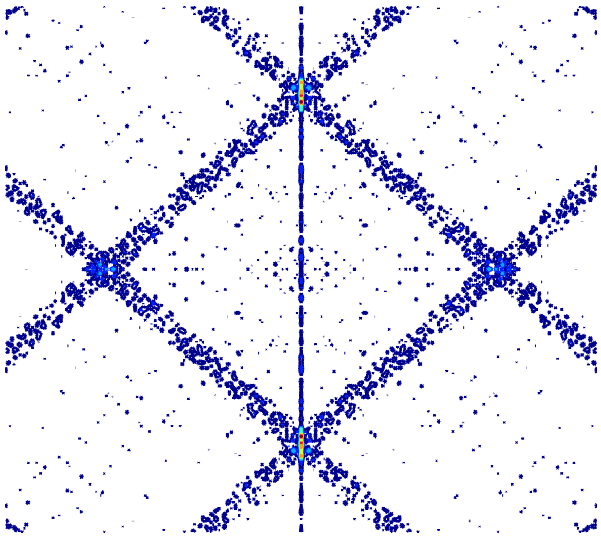

Figure 6.6: Original "marker" image of the DVB-T signal for the (f, α) plane at SNR = -5dB

in Figure (6.9) where 125 ms are enough this time in order to meet standards specifications for DVB-T signals classification.

6.5 Conclusion

The objective of this study was to detect while receiving and decoding data (very strong constraint), but in this case the choice of the sensing time will not affect the Quality of Service. The advantage of using classification instead of QP is that the classification time can be (theoretically) as long as possible.
Our conclusion is also that the requirements proposed by FCC for sensing can be adapted to classification. Please also note that the classification requirement depends on the following parameters:

- Sensing time;
- NF (Noise Figure of the amplification chain from LTE Rx);
- LTE configuration – which gives the sampling frequency being used and the detection BW size;

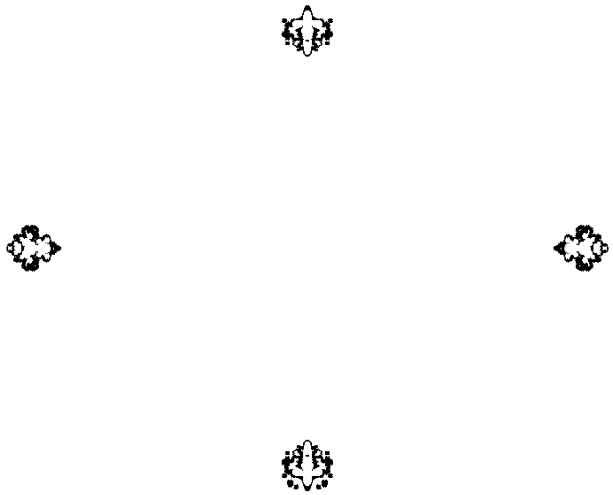

Figure 6.7: The "mask" image of Figure 6.6 for the (f, α) plane at SNR = -5dB.

- The amount of DVB-T/PMSE captured in the analyzed BW.

For 10 MHz Bandwidth (Very Wide Band), classification time is considerably shortened from 250 ms to 125 ms in order to meet the system requirements for DVB-T sensing.

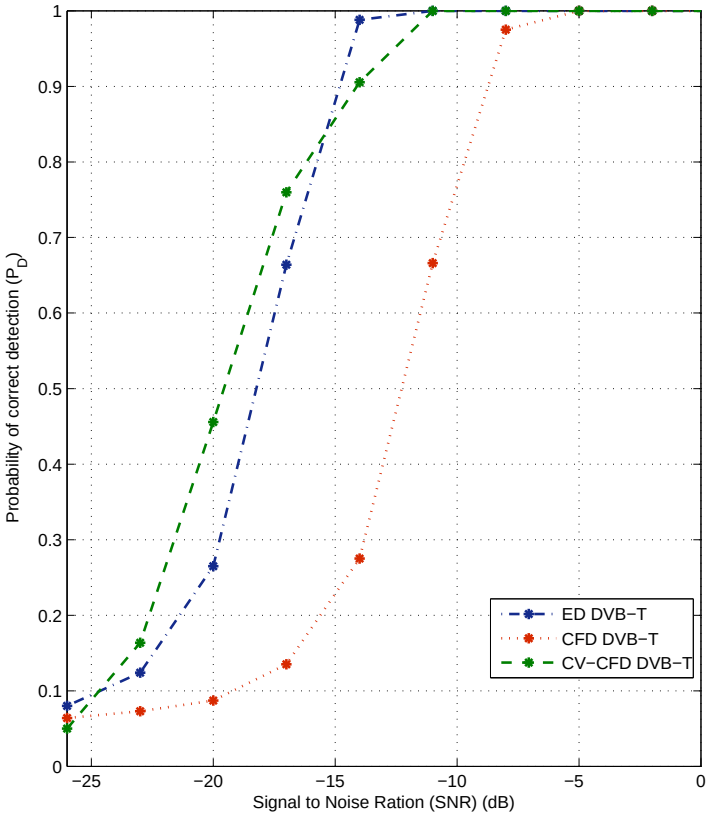

Figure 6.8: Probability of correct detection (P_D) versus signal to noise ratio (SNR) in dB at P_{FA} = 0.05. and sensing time of 1.5 ms

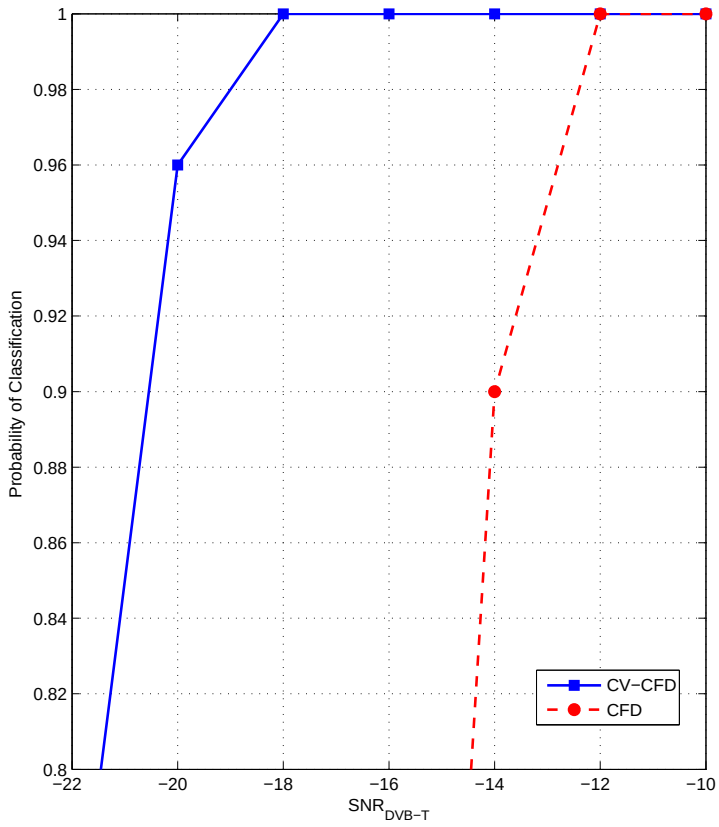

Figure 6.9: DVB-T classification, when LTE system is communicating, for 125 ms classification time

Part III

Location Aided Cognitive Radio Systems

CHAPTER 7

Cooperative Spectrum Sensing and Localization in Cognitive Radio

7.1 Introduction

Cognitive radio is a smart wireless communication concept that is able to promote the efficiency of the spectrum usage by exploiting the free frequency bands in the spectrum, namely spectrum holes [3, 4].
Detection of spectrum holes is of the first steps of implementing a cognitive radio system and is called spectrum sensing.
The major problem that arises in wideband radio, is the fact that one may not be able to acquire a signal at the Nyquist sampling rate due to the current limitations in Analog-to-Digital Converter (ADC) technology [43]. Compressive sensing makes it possible to reconstruct a *sparse* signal by taking less samples than Nyquist sampling, and thus wideband spectrum sensing is doable by Compressed Sensing (CS).
Another step towards the feasibility and a real implementation of cognitive radio systems is the problem of location awareness [70, 71]. This problem arises when we do consider a realistic scenario in hybrid overlay/underlay systems, when these spectrum opportunities permit cognitive radios to transmit below the primary users tolerance threshold. In this case, the cognitive radio, have to estimate robustly the primary users locations in the network in order to adjust its transmission power function of the estimated location in the network. The knowledge of position information in CRS is also an enabler of location based beamforming as shown in [73] and also as shown in ICT-WHERE2 project, a whole framework of location-aided PHY/-MAC layer design for advanced cognitive radios [74] with novel concepts of spectrum sensing techniques based on location information [75], to multi-cell multi-user MIMO systems with location based CSIT [76].
In our approach[1], we propose to analyze all these arisen problems. During the problem for-

[1] Part of the work presented in this chapter was accepted and presented in WIMOB 2012 [70], 8th IEEE International Conference on Wireless and Mobile Computing, Networking and Communications and CAMAD 2012 [71], IEEE 17th International Workshop on Computer Aided Modeling and Design of Communication Links and Networks

mulation and when analyzing more deeply the equations related to each question apart, we will make the link between the formulation of spectrum sensing, location awareness and the hardware limitation by describing those problems in a unique compressed sensing formalism.

7.2 Compressed Sensing Framework

In this section, we are considering sparse signals /vectors reconstruction.
A given d-dimensional vector is assumed to be s-sparse if it has s or fewer non zero coordinates, that is to say:

$$x \in \mathbb{R}^d, \quad ||x||_0 \triangleq |\text{supp}(x)| \leq s \ll d \tag{7.1}$$

where we denote by $||.||_0$ the quasi norm and for $1 \leq p < \infty$, $||.||_p \triangleq \sum_{i=1}^{d}(|x_i|^p)^{1/p}$ is the usual p-norm. In real world, we won't encounter perfect sparse signals, but signals whose coordinates satisfying a power law decay, that's to say x satisfy the following equation:

$$|x_i^*| \leq Ri^{(-1/q)} \tag{7.2}$$

where x^* is a non increasingly rearranged version of x, R is some positive constant and q is satisfying $0 < q < 1$. Sparse vectors recovery algorithms tend to reconstruct sparse vectors from a small set of measurements. Each of these measurements can be viewed as an inner product between a given vector, say $\phi_i \in \mathbb{R}^d$ and the vector $x \in \mathbb{R}^d$. Collecting the m measurement in a single matrix, we thus build an $m \times d$ measurement matrix, say $\mathbf{\Phi} = [\phi_1 ... \phi_m]$.
Theoretically speaking, recovering x from its measurement $u = \mathbf{\Phi}x \in \mathbb{R}^m$ is equivalent to solving the l_0-minimization problem:

$$\min_{z \in \mathbb{R}^d} ||z||_0 \quad \text{subject to} \quad \mathbf{\Phi}z = u \tag{7.3}$$

If x is s-sparse and $\mathbf{\Phi}$ is one-to-one[2] on all $2s$-sparse vectors, then the solution of Equation (7.3) must be the signal x. Indeed, say z is a solution and given the fact that x is an obvious solution, then $z - x$ must be a kernel of $\mathbf{\Phi}$. But $z - x$ is a $2s$-sparse vector and given the assumption that $\mathbf{\Phi}$ is one-to-one, $z = x$. Thus, theoretically speaking the l_0-minimization is a perfect solution to the reconstruction problem. Unfortunately it is shown in literature [79] that the l_0-minimization is a NP-Hard problem and numerically unfeasible.
This problem can be overcome by means of Compressed Sensing (CS). A first approach is to use Basis Pursuit (BP) algorithm in order to relax the l_0-minimization to an l_1-minimization formalism. BP requires stronger hypothesis on $\mathbf{\Phi}$, so it has not only to verify injection on

[2] A matrix is told to be one-to-one if it is representing an injective transformation from one space to another

sparse vectors property, but it has been shown that the relationship between m, d and s is given by: $m = s \log O(1)d$. l_1 minimization often relies on linear programming, and since there is no linear bound for such techniques, BP approaches are quite slowly convergent techniques. The second approach is to use greedy algorithms such as Orthogonal Matching Pursuit (OMP) [80], Stagewise Orthogonal Matching Pursuit (StOMP) [81], or Iterative Thresholding [82,83]. Those approaches are based on the iterative computation of the signal's support. As for BP, m, d and s are linked parameters such as: $m = O(s \log d)$. Once the support S of the signal computed, x is reconstructed from the measurement vector u as $x = (\mathbf{\Phi}_S)^\dagger u$, where $\mathbf{\Phi}_S$ is the restriction of $\mathbf{\Phi}$ to the columns indexed by S and $.^\dagger$ is the pseudo-inverse operator[3]. The main advantage of greedy approaches is their convergence time, as they are faster than BP, but they lose in stability compared to BP. Another class of CS algorithms recently emerged in order to shorten the gap between greed algorithms and BP. From these algorithms, we may cite Regularized Orthogonal Matching Pursuit (ROMP) [85] and Compressive Sampling Matching Pursuit (CoSaMP) [84]. These two algorithms provide a similar guarantees of stability as BP with the same iterative property of fast convergence as greedy algorithms.

7.3 Reconstruction Algorithms

In our work, we will consider one algorithm per class to be studied for spectrum sensing and localization purposes. We will thus introduce first of all BP, then OMP and finally CoSaMP that will be used afterwards for the target applications.

7.3.1 Basis Pursuit

Since the problem as formulated in Equation (7.3) is an NP-hard problem and numerically unfeasible, let's introduce a first approach to solve this problem. One may consider first, a mean square approach to solve the problem.

$$\min_{z \in \mathbb{R}^d} ||z||_2 \quad \text{subject to} \quad \mathbf{\Phi} z = u \tag{7.4}$$

Since the minimizer, say x^*, must satisfy $\mathbf{\Phi} x^* = u = \mathbf{\Phi} x$, x^* must be in the subspace $K = x + \ker\mathbf{\Phi}$. Actually, x^*, as defined in Equation (7.4) is the exact contact point between the smallest Euclidian ball centered at the origin and the subspace K. As shown in Figure (7.1), in the mean square approach there is no need to have x^* coinciding with the actual signal x. This is due to the fact that Euclidian geometry ball is not a good detector of sparsity.

[3] Recalling that for a given matrix A, $A^\dagger = (A^* A)^{-1} A^*$

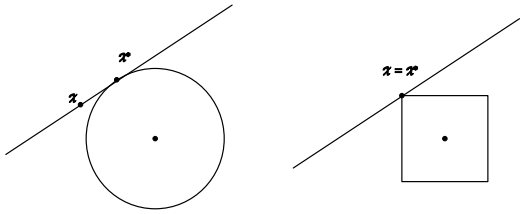

Figure 7.1: The minimizers to the mean square (left) and l_1 (right) approaches.

In this case, in order to solve Equation (7.3), we may opt for an l_1 approach. In this case, x^* would meet the contact point between the l_1 ball (also named octahedron) centered at the origin and the subspace K.
A first idea could be relaxing the problem into an l_1 minimization:

$$\min_{z \in \mathbb{R}^d} ||z||_1 \quad \text{subject to} \quad \mathbf{\Phi} z = u \tag{7.5}$$

Authors in [45] have proved that for measurement matrices satisfying a certain quantitative property called Restricted Isometry Property, l_0 and l_1 become equivalent.

7.3.2 Orthogonal Matching Pursuit

OMP is based on subgaussian measurement matrices to reconstruct sparse signals. If $\mathbf{\Phi}$ is verifying such condition (subgaussian property), then $\mathbf{\Phi}^*\mathbf{\Phi}$ is close to identity. In this case, a non-zero coordinate of x would maximize the observation $y = \mathbf{\Phi}^*\mathbf{\Phi}x$, and that's how we iteratively reconstruct the support of x. OMP is shown to be fast but not as stable as BP.
Algorithm (1) give the pseudocode for OMP implementation.
Once the support I of the signal x is found, the estimate $\widehat{x}$ can be reconstructed as: $\widehat{x} = \mathbf{\Phi}_I^{\dagger} u$. The algorithm simplicity allows a fast reconstruction as it iterates s times and over each iteration, it selects one among d elements in $O(d)$ time and multiplies by $\mathbf{\Phi}^*$ in a $O(md)$ time period and finally solves a least squares problem in $O(s^2 d)$. So the cost of such technique is $O(smd)$ operations.

7.3.3 Compressive Sampling Matching Pursuit

As far as the CoSaMP algorithm is concerned, the sampling operator $\mathbf{\Phi}$ is supposed to satisfy the Restricted Isometry Property [4] and each s coordinates of signal $y = \mathbf{\Phi}^*\mathbf{\Phi}x$, also called proxy signal, are close in terms of Euclidian norm to the s corresponding coordinates of x.

[4] For more information and a complete description of RIP please refer to [87]

Algorithm 1 Orthogonal Matching Pursuit (OMP) pseudocode

Require: Measurement matrix $\mathbf{\Phi}$, measurement vector $u = \mathbf{\Phi}x$, sparsity level s

1: **Initialize:** As a first step, initialize $I = \varnothing$ and the residual $r = u$
repeat s times:

2: **Identify:** Select the largest coordinate λ of $y = \mathbf{\Phi}^* r$ in absolute value. Break ties lexicographically.

3: **Update:** Add the coordinate λ to the index set: $I \leftarrow I \bigcup \lambda$ and update the residual according to:

$$\widehat{x} = \arg\min_{z} \parallel u - \mathbf{\Phi}_{|_I} z \parallel_2; \quad r = u - \mathbf{\Phi}\widehat{x} \tag{7.6}$$

4: **return** Index set $I \in 1, ..., d$

The algorithm operates according to the following steps:

1. **Identification**: The algorithm takes the residual as a proxy and locates its highest coordinates.

2. **Support merging**: At the iteration k, the set of recently identified coordinates is merged withe the set from iteration $k - 1$

3. **Estimation**: Based on the set of coordinates, the algorithm performs a least square to determine an approximation of the target signal

4. **Pruning**: In the estimated signal from least squares, the algorithm retains only the highest coordinates.

5. **Sample updating**: The samples are updates so that they integrate the residual part.

Algorithm 2 Compressive Sampling Matching Pursuit (CoSaMP) pseudocode

Require: Measurement matrix $\mathbf{\Phi}$, measurement vector $u = \mathbf{\Phi}x$, sparsity level s

1: **Initialize:** Set $a^0 = 0$, $v = u$, $k = 0$.
Repeat the following steps while increasing k until achieving halt criterion.

2: **Signal Proxy:** Set $y = \mathbf{\Phi}^* v$, $\Omega = \text{supp}y_{2s}$ and merge the support $T = \Omega \bigcup \text{supp}a^{k-1}$

3: **Signal Estimation:** Solving a least squares problem, set: $b_{|_T} = \mathbf{\Phi}_T^{\dagger} u$ and $b_{|_{T^c}} = 0$

4: **Prune:** Preparing the next iteration, set $a^k = b_s$

5: **Sample Update:** Update the samples by: $v = u - \mathbf{\Phi}a^k$

6: **return** s-sparse reconstructed vector $\widehat{x} = a$

7.3.4 Compressed Sensing for Spectrum Sensing and Primary Users Localization

In this chapter, we will use the above framework in order to solve two major issues enabling CR: spectrum sensing and terminals localization. In order to do so, we will tend in our analysis to express the upcoming equations as following:

$$y = \mathbf{\Phi} x \tag{7.7}$$

where $y \in \mathbb{R}^M$ is the measured entity, $\mathbf{\Phi} \in \mathbb{R}^{M \times N}$: the measurement matrix and $x \in \mathbb{R}^N$ the K-sparse vector to be reconstructed.
According to Restricted Isometry Property definition, $\mathbf{\Phi}$ would verify the RIP if: $M \geq O(K \log(N/K))$.

7.4 System Model

In the considered system model, we will suppose that we do dispose of N_{ch} available channels in a wideband wireless network. Over a large geographic area, let N_p be the number of deployed primary users using a different channel each. In this large area, we disperse N_c cognitive radios that will cooperate to locate PUs in the network and detect their channels usage and states. The measures made by these cognitive terminals will then be sent to the fusion center. In order to enable SUs transmissions, the secondary network have to be aware of the availability and the state of each channel. Thus, SUs have to estimate which channels are occupied and to identify the PUs transmission powers and locations.
For our system, we adopt the path loss model, given by:

$$L(f, d) = P_0 + 20 \lg(f) + 10n \lg(d) \qquad [dB] \tag{7.8}$$

where: P_0 is a constant related to antennas gain; f is the channel frequency; n is the path loss exponent; d is the distance separating the transmitting and receiving nodes and $\lg(.) = \log_{10}(.)$
In our case, we dispose of N_{ch} channels, thus f would be assumed the central frequency of each band, i.e $f \in \{f_0, f_1 ..., f_{N_{ch}-1}\}$.
Let's keep in mind that the path loss is related to the unknown channel and location of the PU. The received signal power is a combination of the unknown transmit power with the path loss expressed in Equation(7.8).
Our task is to infer from the received signal at the cognitive terminals all these unknown, but valuable, information about the primary users.

7.5 Compressed Sensing For Cognitive Radio Applications

7.5.1 Spectrum Sensing

For discrete signals, the time domain samples t are used to construct the spectrum in frequency domain using directly the DFT transform:

$$f = \mathbf{F}t \tag{7.9}$$

where $\mathbf{F}$ is the normalized DFT matrix.
As stated previously, the sparsity in this context may come from the inability of the ADC to acquire signals at a Nyquist rate. The time samples t are thus acquired at a sub-Nyquist rate which may result in a sparse vector.
We will thus directly apply the CS formalism with the different introduced algorithms to reconstruct the original time domain transmitted signal and spectrum sensing will be achieved using energy detection.

7.5.2 Location Estimation based on Compressed Sensing

Once spectrum reconstructed and spectrum sensing achieved, more information can be derived while looking deeper into channels occupied by primary users.
Let's assume that in a certain wide area, PUs are located at coordinates (xp_m, yp_n); where $xp_m \in \{0, \Delta xp, ...(M-1)\Delta xp\}$ are M possible x axis positions (abscissæ) of the PUs [5]; $yp_m \in \{0, \Delta yp, ...(N-1)\Delta yp\}$ are N possible y axis positions (ordinates) of the PUs; Δxp and Δyp are respectively the resolutions over x and y axis. Here, we do impose and suppose to the PU coordinates to be in discrete $M \times N$ dictionary (which, actually, is always true). It is good to remind at this level that the exact positions of the N_p PUs $\{(xp_i, yp_i)\ ; i \in [1..N_p]\}$ are unknown to our problem.
The N_c CRs positions in the network are located at positions: $\{(a_i, b_i)\ ; i \in [1..N_c]\}$ (on which we do not impose being in a finite set, even if they necessarily are).
For the k^{th} CR, sensing the i^{th} channel, the contribution of the PU located at the (xp_m, yp_n) position on the received PSD is:

$$\begin{aligned} R_{k,i}(m,n) &= P(m,n,i) \times 10^{L(f_i, d(m,n,k))/10} \\ d(m,n,k) &= \sqrt{(xp_m - a_k)^2 + (yp_n - b_k)^2} \end{aligned} \tag{7.10}$$

where $P(m,n,i)$ is the power transmitted by a PU using the i^{th} channel, located at (xp_m, yp_n); f_i is the center frequency of the i^{th} channel; $d(m,n,k)$ represents the distance between the k^{th} CR and the the PU located at (xp_m, yp_n).

[5] When we say $xp_m \in \{0, \Delta xp, ...(M-1)\Delta xp\}$, that does not mean that there are M PUs, but it means that N_p primary users abscissæ (for ordinates as well) do actually have a finite "dictionary"

The total received power over all the existing PUs, i.e over the $M \times N$ possible positions of the PUs, can be formulated as following:

$$\begin{aligned} Y_{k,i} &= \sum_m \sum_n R_{k,i}(m,n) \\ Y_{k,i} &= \sum_m \sum_n 10^{L(f_i,d(m,n,k))/10} \times P(m,n,i) \\ Y_{k,i} &= \overrightarrow{L}^T(k,i)\overrightarrow{P}(i) \end{aligned} \tag{7.11}$$

where $\overrightarrow{P}(i)$ is the vector containing the transmission power of the over all $M \times N$ grid over the i^{th} channel; and $\overrightarrow{L}(k,i)$ is the path loss vector computed according to Equation(7.8) from all PU possible positions at the level of the k^{th} CR, on the i^{th} channel.

$$\begin{aligned} &\overrightarrow{L}(k,i) = 10^{\overrightarrow{L}_{dB}(k,i)/10} \\ &\text{and :} \\ &\overrightarrow{L}_{dB}(k,i) = [L(f_i,d(0,0,k)), L(f_i,d(1,0,k)), \\ &..L(f_i,d(m,n,k)), ..L(f_i,d(M,N,k))]^T \end{aligned} \tag{7.12}$$

Let's denote by $\overrightarrow{Y}_k = [Y_{k,1}..Y_{k,N_{ch}}]^T$, the received signal power vector at the level of the k^{th} CR over the N_{ch} available channels. This according to Equation(7.11), and adopting the previous notation can be expressed as:

$$\overrightarrow{Y_k} = \mathbf{L_k}\overrightarrow{P} \tag{7.13}$$

where $\overrightarrow{P}$ is the vector containing the transmission power of the $M \times N$ grid of PU locations over the N_{ch} available channels of the N_C deployed CRs:

$$\overrightarrow{P}_k = [\overrightarrow{P}^T(i_1), \overrightarrow{P}^T(i_2), .., \overrightarrow{P}^T(i_{N_C})]^T \tag{7.14}$$

The matrix $\mathbf{L_k}$, is the fading gain matrix grouping at the level of the k^{th} CR the loss path contributions of the $M \times N$ PU positions. The j^{th} row of $\mathbf{L_k}$ is:

$$\mathbf{L_k}(j) = [\overrightarrow{0}, \overrightarrow{0}, ..., \overrightarrow{L}^T(k,j), \overrightarrow{0}, .., \overrightarrow{0}] \tag{7.15}$$

Combining all the equations describing the N_C CR system, we do obtain:

$$\overrightarrow{Y} = \mathbf{L}\overrightarrow{P} \tag{7.16}$$

Where $\overrightarrow{Y} = [\overrightarrow{Y_1}^T, ..., \overrightarrow{Y_{N_C}}^T]^T$ and $\mathbf{L} = [\mathbf{L_1}, ..., \mathbf{L_{N_C}}]$
The equation we ended with in Equation(7.16), reminds us of Equation (7.7) of the CS formalism we introduced previously: as $\overrightarrow{P}$ is an unknown but sparse vector because over the $M \times N$ area we've been considering, only N_P PUs are deployed in this area.
The two stages, spectrum sensing and localization, seem then to be attached to the same CS framework we've introduced before.

7.5.3 Joint Spectrum Sensing and Primary User Localization

We've shown till now that both problems: sensing and localization can separately be solved using CS formalism. It is now easy for us to combine these two operations.
The joint framework, would consider this dual sensin/localization problem as a 3D image reconstruction from sparse observation. The x and y axis of this unknown image are the PU location information and the z axis would represent the sensed channel occupancy information and the value of a given pixel at (x, y, z) is the reconstructed transmit power.

7.6 Simulations and Results

For our analysis, we suggest a realistic network simulation. In the considered CRS we deploy 5 PUs and 3 SUs. The 3 deployed CRs are attempting to communicate opportunistically and thus will perform the sensing and localization task.
A hexagonal cellular system functioning at 1.8GHz with a secondary cell of radius $R = 1000m$ and a primary protection area of radius $R_p = 600m$ is considered. Secondary transmitters may communicate with their respective receivers of distances $d < R_p$ from the BS. We assume that the PUs and the SUs are randomly distributed in a two-dimensional plane as shown in Figure 7.2. The BS is placed at the center $(0, 0)$. The distance, $d(m, n, k)$, from the k-th SU to the PU (m, n) is given by

$$d(m, n, k) = \sqrt{(xp_m - a_k)^2 + (yp_n - b_k)^2} \tag{7.17}$$

where (x_{p_m}, y_{p_n}) are the coordinates of the PU and (a_k, b_k) the coordinates of the k-th CR. The channel gains are based on the COST-231 Hata model [86] including log-normal shadowing with standard deviation of 10dB, plus fast-fading assumed to be i.i.d. circularly symmetric with distribution $\mathcal{CN}(0, 1)$. The basic path loss for the COST-231 Hata model is in dB in an urban area at a distance d is:

$$\begin{aligned} L(f, d) = 46.3 + 33.9 \log_{10}(f_c) - 13.82 \log_{10}(h_b) - \\ A_M + (44.9 - 6.55 \log_{10}(h_b)) \log_{10}(d) + C_M \end{aligned} \tag{7.18}$$

where f_c is the carrier frequency equal to 1.5GHz and h_b is the base antenna height equal to 50 meters. The distance d is computed using the formula (7.17). C_M is 0dB for medium sized cities and suburbs and is 3dB for metropolitan areas. In the simulations, we use $C_M = 0$dB. The A_M is defined for urban environment as:

$$A_M = 3.20 \left(\log_{10}(11.75 h_m)\right)^2 - 4.97 \tag{7.19}$$

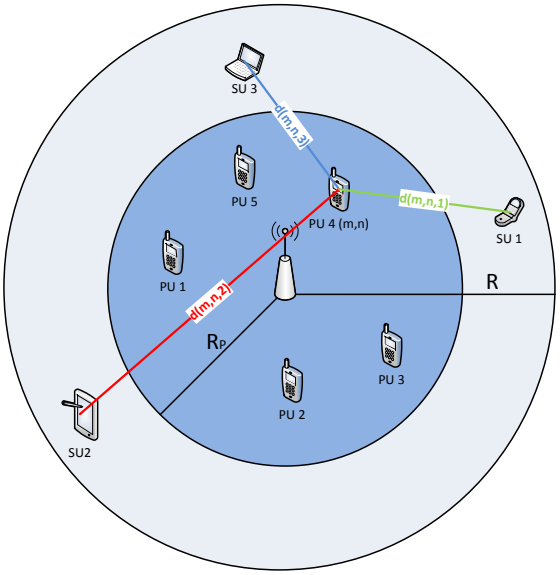

Figure 7.2: Two-dimensional plane of the cognitive radio system topology with five primary users and three secondary users.

where h_m is the mobile antenna height equal to 10 meters. The shadowing variations of the path loss can be calculated from the log-normal distribution

$$g(x \mid \sigma) = \frac{1}{\sigma\sqrt{2\pi}} \exp\left(\frac{-x^2}{2\sigma^2}\right) \tag{7.20}$$

where σ is the variability of the signal equal to 10dB. The shadowing variation is computed using the Matlab® function $randn$. Shadowing reflects the differences in the measured received signal power with relation to the theoretical value calculated by path loss formulas. Averaging over many received signal power values for the same distance, however, yields the exact value given by path loss.
Furthermore, for channels distribution, we suppose that the total number of available channels is in [1,2,..,20] channels and each of the five PUs is communicating over a single different channel.

7.6.1 Simulation Results

Figures (7.3) and (7.4) give an example of spectrum reconstruction MSE at 50% sparsity for the simulated algorithms and the impact of sparsity level on spectrum reconstruction MSE.

The very fist remark that we can give here is that the simulation results are in line with the theoretical aspects related to BP, OMP and CoSaMP. As we explained at the very beginning, performance related to BP is expected to overcome OMP, which is the case in Figure (7.3) and CoSaMP is shown both in theory and simulations to outperform OMP, but it is still not as efficient as BP.
Figure (7.4) is assessing the impact of sparsity level on spectrum reconstruction MSE. Here we clearly see that results are coherent with the definition we gave of sparsity, saying that "a d-dimensional vector is assumed to be s-sparse if it has s or fewer non zero coordinates". According to this definition, the more sparse the vector is, the largest its support is, so the less the reconstruction MSE would be, which is perfectly in line with the results reported in figure (7.4).

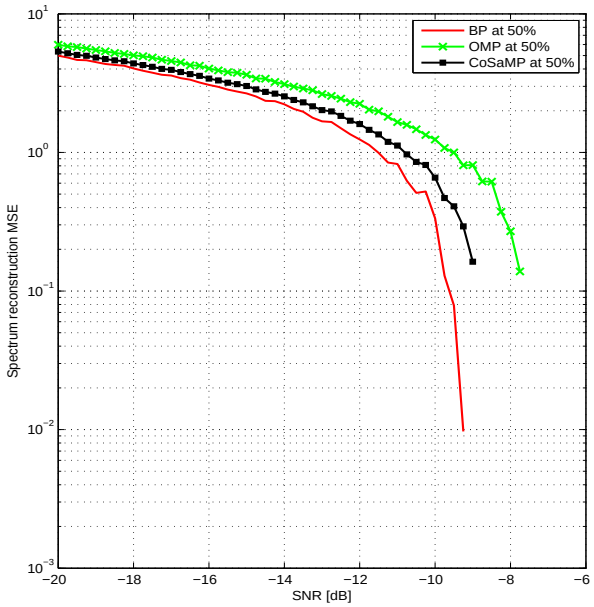

Figure 7.3: Example of Spectrum Reconstruction MSE at 50% sparsity level for BP, OMP, CoSaMP

Figures (7.5) and (7.6) give an example of PU location estimation at 50% sparsity for the simulated algorithms and the impact of sparsity level on PU location estimation error at 0 dB. Figure (7.5) gives an overview of PU location estimation error at 50% sparsity level for BP, OMP and CoSaMP. Here we validate again the previous results, as the tendency of BP outperforming CoSaMP and OMP is confirmed. The same for Figure (7.6), where we clearly see the

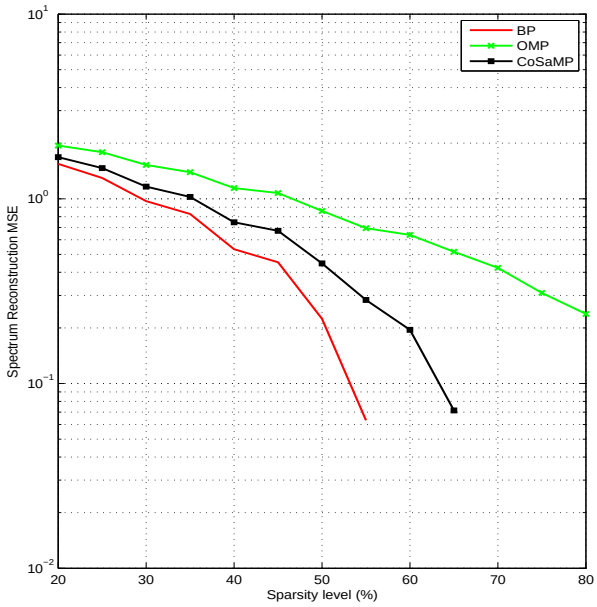

Figure 7.4: Impact of sparsity on spectrum reconstruction MSE at 0 dB

more signal is sparse (in the sense the more we have non-zero entries), the more robust the PU localization is.

Assuming a 15 meters limit of “good localization" bound, Figure (7.5), show that the idea of cooperative localization could be exploited up to -3 dB, -2 dB, and 1 dB for BP, CoSaMP and OMP respectively. These performance are obtained for totally autonomous GPS free techniques and with absolutely no need of extra overhead data exchange in the network.

7.7 Conclusion

This work presents a first look towards a combined spectrum sensing and localization task. These two tasks are fundamental in order to enable cognition in wireless networks. With the combination of the two tasks, we also considered a realistic data acquisition constraint, which is sparsity due to the ADC technology limits. Simulation results of the proposed technique show promising and interesting results for compressed sensing techniques applied to this formalism.

The formalism that we derived in this chapter is the starting point of a whole location aided

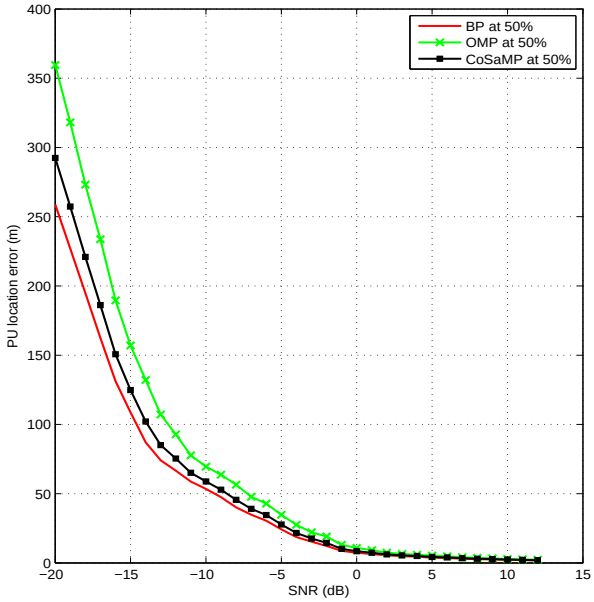

Figure 7.5: Error on PU location estimation at 50% sparsity level for BP, OMP, CoSaMP

cognitive radio framework we are developing within the FP7 WHERE-2 project. In this framework, once the radio map is built thanks to the sensing and localization asks, the CRs are thus able to communicate in the available bands in the available directions and thus the proposed framework is a key enabler of SDMA (Space Division Multiple Access) systems. And this formalism can also be exploited for the D2D (device to device) communication, as the CRs can communicate directly with each others while the fusion center can play the role of the control entity in the network.

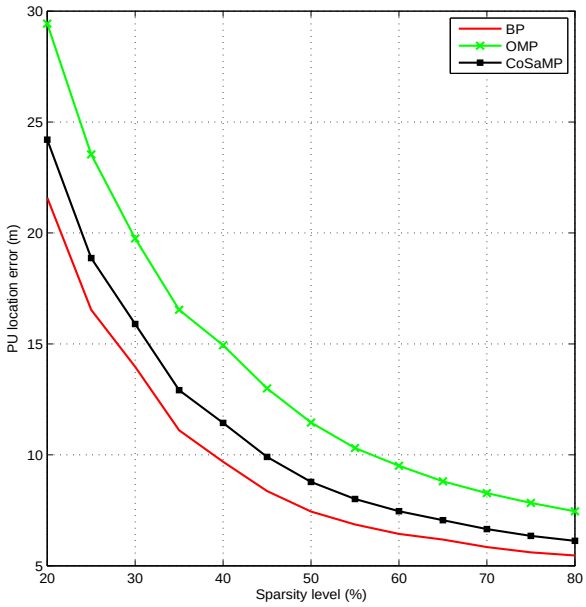

Figure 7.6: Impact of sparsity on PU location estimation at 0 dB

CHAPTER 8

Conclusions and Future Directions

8.1 Summary

In this work, we addressed several aspects related to cognitive radio technology:

- First of all, we presented a novel multiband detector that is blindly capable to locate the edges of the PU communication in the RF spectrum and thus allowing a more efficient use of the spectrum by exploiting all its fragmented parts, guard intervals, etc.. The proposed architecture is also interesting as the proposed filters take into account noise reduction and thus allow multiple applications of the proposed framework. We have shown through various simulation scenarios and actual measurements how efficient and performing the proposed enhanced energy detector attached to this framework is.

- The second contribution is also related to wideband compressed spectrum sensing. The improvement compared to the state of the art techniques resides in the fact that the proposed frequency edge location algorithm is a non-iterative, one shot and online algorithm. The performance of this technique was compared to the state of the art technique and shows some improvements.

- The third contribution is related to spectrum awareness. In this contribution we derived a novel classification technique in heterogeneous cognitive radio scenario. This classifier is based on mixed signal separation and multiple parallel sensing techniques for DVB-T, LTE and PMSE signals. Each detector was selected in order to optimize the detection relatively to a given standard. A fusion rule was derived as a combination of likelihood ratios to highlight at each time a unique standard.

- Another contribution to spectrum awareness was proposed as an interdisciplinary technique of signal classification inheriting some image processing tools. We have derived several applications of the proposed technique. First of all, as a spectrum sensing technique, and we've shown how performing this technique is, with improvements of nearly 50% compared to the CFD original technique. A second application was for signal classification. Here the targeted usecase is detecting the PU system (DVB-T, PMSE) while SU is transmitting (LTE). We have shown how performing the proposed technique is in

terms of reducing classification period while taking into account standard recommendations in terms of noise level.

- The last presented contribution is a network discovery-like mechanism for cognitive radio systems based on compressed sensing (CS). In this chapter, we formulated spectrum sensing and localization of PU transmitters in a CS formalism. Sparsity is exploited in both ways: for spectrum sensing, sparsity is due to the fact that ADC are generally not able to acquire signals at Nyquist rate and this incomplete/inaccurate signal acquisition can be recovered by means of compressed sensing. A second aspect of sparsity is considered for localization. Indeed when building the PU transmitters map by means of path loss model, the derived matrix characterizing PU transmissions is a sparse matrix in the sense that only few inputs are non null. We can thus apply the same CS algorithms to recover these positions.

8.2 Limitations

Although some interesting results were presented in the contributions, some limitations also exist.

- In the first contribution, we clearly see that the enhancement of the conventional filter bank spectrum sensing come with an extra cost. This is due to the computation of the frequency boundaries and the extra filters we are deriving in order to help noise reduction. The energy efficiency is also lost when we use high order polynomials in the per-band spectrum model.

- In the CS formalism that was presented, the limitation is in the form of the derived matrix, as it very specific for this application and context and also we are loosing too much in generality because the CS matrix is deterministic.

- The mixed signal separation and classification algorithm proposed in Chapter 5 is based on FastICA algorithm which is an iterative, time consuming time, energy consuming task and offline operation. The major other assumption made here is that the cognitive terminal have enough degrees of freedom to perform this separation.

- In Chapter 6, it is true that the required time for classification is divided by two almost, which is a great improvement, but still the complexity introduced by the Computer Vision tools used is also significant and time consuming.

- In Chapter 7, the used framework is obviously a LOS configuration where the PU is in its protection area and the cognitive terminals avoid transmitting in the PU bands. The

problem is that in real world systems, PUs and SUs are not distributed in this way. Still some use cases of D2D or M2M communications could exploit this framework. The other problem is that Primary transmitters are supposed to be fixed infrastructures so, how an open issue is how to further exploit this framework to meet at least pedestrian mobility ?

8.3 Future Directions

Still some issues and some ideas can complete the presented work:

- ***Spectrum Sensing***: The future of spectrum sensing in cognitive radio systems is energy efficient blind techniques which will be complimentary to geolocation data-bases based spectrum sensing. For these hybrid architectures, we have an ongoing work of blind model selection algorithm using Variational Bayes.

- ***Spectrum Awareness***: Some issues are still left open in spectrum awareness especially in reducing detection time of incumbent transmission. In the proposed techniques there is some improvement in the detection time but at the price of adding complexity to the over all system.

- ***Towards Green Communications***: Another interesting direction that is bringing Cognitive Radio into the spot lights again is (Cognitive) Green Communications. PHY Layer algorithms in addition to MAC mechanisms are studied subject to the energy consumption minimization. This aspect is quite interesting to see as these constraints of energy saving (especially in the user equipment side) are the key parameters toward seeing cognitive terminals invading markets in a near future.

Bibliography

[1] Shared Spectrum Company, General Survey of Radio Frequency Bands 30 MHz to 3 GHz, September 23, 2010 1

[2] U.S. Department of Commerce ,Plan and Timetable to Make Available 500 Megahertz of Spectrum for Wireless Broadband, October 2010 1

[3] S. Haykin, Cognitive radio: brain-empowered wireless communications, Selected Areas in Communications, IEEE Journal on, vol. 23, no. 2, pp. 201220, 2005. 1, 43, 44, 85

[4] J. Mitola and G. Maguire, Cognitive radio: making software radios more personal, Personal Communications, IEEE, vol. 6, no. 4, pp. 13 18, 1999. 1, 85

[5] ITU-R SM.2152-Definitions of Software Defined Radio (SDR) and Cognitive Radio System (CRS), September 2009 1

[6] I.F. Akyildiz , W.-Y. Lee , M.C. Vuran , S.Mohanty, NeXt generation/dynamic spectrum access/cognitive Radio Wireless Networks: A Survey, Computer Networks Journal (Elsivier) 2006. 1, 13

[7] T. Ycek, H.Arslan A Survey of Spectrum Sensing Algorithms for Cognitive Radio Applications IEEE Communications Surveys and Tutorials 2009, pages 116-130. 1, 21, 57

[8] FCC Docket 05-57 2

[9] A. Ghasemi and E.S. Sousa. Spectrum sensing in cognitive radio networks : Requirments, challenges and design trade-offs. IEEE Communications Magzine, pages 3239, Apr. 2008. 12

[10] S. M. Mishra, A. Sahai and R.W. Brodersen. Cooperative sensing among cognitive radios. IEEE Int. Conf. Communications, 4 :16581663, Jun. 2006. 12

[11] H. Urkowitz. Energy detection of unknown deterministic signals. Proceeding of the IEEE, 55(5) :523531, 1967. 14, 15

[12] M. Abramowitz and I.A. Stegun. Handbook of Mathematical Functions with Formulas, Graphs, and Mathematical Tables. 10th ed. Washington, D. C. : U.S. National Bureau of Standards, 1972 15, 17, 18

[13] Y. Zeng and Y.C. Liang. Eigenvalue-based spectrum sensing algorithms for cognitive radio. IEEE Transactions on Communications, 57(6) :17841793, Jun. 2009. 14, 15

[14] T. J. Lim, R. Zhang, Y. C. Liang and Y. Zeng. Glrt-based spectrum sensing for cognitive radio. In IEEE GLOBECOM, Nov. 30-Dec. 4 2008. 14, 15

[15] A.V. Dantawate and G.B. Giannakis. Statistical tests for presence of cyclostationarity. IEEE Transactions on Signal Processing, 42(9) :23552369, Sept. 1994. 16, 17

[16] W. A. Gardner, A. Napolitano and L. Paura. Cyclostationarity : Half a century of research. Signal Processing, 86(4) :639697, Apr. 2006. 17

[17] S. Xu, Z. Zhao, J. Shang, Spectrum Sensing Based on Cyclostationarity,Workshop on: Power Electronics and Intelligent Transportation System, 2008. PEITS 08, Aug. 2008. 16, 57

[18] Z. Khalaf, A.Nafkha, J. Palicot and M. Ghozzi, Hybrid Spectrum Sensing Architecture for Cognitive Radio Equipment , AICT, pp.46-51, 2010 Sixth Advanced International Conference on Telecommunications, Barcelona, Spain May 2010. 14

[19] Z. Khalaf, A.Nafkha and J. Palicot, Enhanced Hybrid Spectrum Sensing Architectures for Cognitive Radio Equipment, URSI GASS 2011, Istanbul, August 2011. 14

[20] Z. Khalaf, A.Nafkha and J. Palicot, Blind Spectrum Detector using Compressed Sensing and Symetry Property of the Second Order Cyclic Autocorrelation, The 7th International Conference on Cognitive Radio Oriented Wireless Networks, IEEE CROWNCOM, June 2012 Stockholm, Sweden. 16

[21] Z. Khalaf, Contributions à letude de détection des bandes libres dans le contexte de la radio intelligente, Ph.D dissertation, February 2013 14

[22] Official Web Page. European telecommunications standards institute. http ://www.etsi.org. 18

[23] A. Goldsmith. Wireless Communications. Cambridge Univ. Press, New York, 2005 19

[24] SENDORA FP7 project, Deliverable 3.1, Spectrum Sensing Algorithm Evaluation, version 1.1, May 2010. xi, 22

[25] Thai Q., S. Reisenfeld, S. Kandeepan, M.G. Maggio, Energy-Efficient Spectrum Sensing Using Cyclostationarity, Proc. of IEEE VTC, May 2011. 22

[26] Qualcomm products and services - the snapdragon platform. Qualcomm Inc. [Online]. Available: http://www.qualcomm.com/products services/chipsets/snapdragon.html 22

[27] L. Gwennap. (2010, July) Two-headed snapdragon takes fight: Qualcomm samples dual-cpu mobile processor at 1.2ghz. [Online]. Available: http://www.qualcomm.com/documents/?les/linleyreport-dual-core-snapdragon.pdf 22

[28] G. Ganesan and Y. Li. Cooperative spectrum sensing in cognitive radio networks. In IEEE Int. Symposium on New Frontiers in Dynamic Spectrum Access Networks, pages 137143, Baltimore, Maryland, USA, Nov. 2005. 24

[29] E. Visotsky, S. Kuffner and R. Peterson. On collaborative detection of tv transmissions in support of dynamic spectrum sharing. In IEEE Int. Symposium on New Frontiers in Dynamic Spectrum Access Networks, pages 338345, Baltimore, Maryland, USA, Nov. 2005. 24

[30] H. Tang. Some physical layer issues of wide-band cognitive radio systems. In IEEE Int. Symposium on New Frontiers in Dynamic Spectrum Access Networks, pages 151159, Baltimore, Maryland, USA, Nov. 2005. 24

[31] W. Guibene, A. Hayar and M. Turki, Distribution discontinuities detection using algebraic technique for spectrum sensing in cognitive radio networks, CrownCom'10, 5th International Conference on Cognitive Radio Oriented Wireless Networks and Communications, June 9-11 2010, Cannes, France.

[32] B. Zayen, W. Guibene and A. Hayar, Performance comparison for low complexity blind sensing techniques in cognitive radio systems, CIP'10, 2nd International Workshop on Cognitive Information Processing, June 14-16 2010, Elba Island, Tuscany, Italy.

[33] W. Guibene, M. Turki, A. Hayar and D. Slock, A Complete Framework for Spectrum Sensing based on Spectrum Change Points Detection for Wideband Signals, 2012 IEEE 75th Vehicular Technology Conference: VTC-Spring'12, 6-9 May 2012, Yokohama, Japan. 33

[34] W. Guibene, M. Turki, B. Zayen and A. Hayar, Spectrum sensing for cognitive radio exploiting spectrum discontinuities detection, EURASIP Journal on Wireless Communications and Networking, 2012. 33

[35] H. Moussavinik, W. Guibene, A. Hayar, Centralized collaborative compressed sensing of wideband spectrum for cognitive radios, ICUMT'10, International Conference on Ultra Modern Telecommunications, October 18-20 2010, Moscow, Russia.

[36] W. Guibene, H. Moussavinik and A. Hayar, Combined compressive sampling and distribution discontinuities detection approach to wideband spectrum sensing for cognitive

radios, ICUMT'11, International Conference on Ultra Modern Telecommunications, October 5-7 2011, Budapest, Hungary.

[37] W. Guibene and A. Hayar, Joint time-frequency spectrum sensing for cognitive radio, CogART'10, 3rd International Workshop on Cognitive Radio and Advanced Spectrum Management, November 07-10 2010, Rome, Italy, **Best Student Paper Award**.

[38] Z. Tian, and G. B. Giannakis, A Wavelet Approach to Wideband Spectrum Sensing for Cognitive Radios CROWNCOM, Mykonos, Greece, June 2006

[39] Z. Quan, S. Cui, A.H. Sayed and H. V. Poor, Optimal Multiband Joint Detection for Spectrum Sensing in Cognitive Radio Networks, IEEE Transactions on Signal Processing, VOL. 57, NO. 3, March 2009 27

[40] B.F-Boroujeny, Filter Bank Spectrum Sensing for Cognitive Radios, IEEE Transactions on Signal Processing, VOL. 56, NO. 5, MAy 2008 27

[41] M. Kim, J. Naganawa, and J. Takada, Multichannel Spectrum Sensing using Polyphase DFT Filter Bank for. Opportunistic Cognitive Radios, The Institute of Electronics, Information and Communication Engineers, IEICE Tech. Rep., vol. 109, no. 61, SR2009-19, pp. 121-127, May 2009. 27, 34

[42] E. Wofsey, The Weierstrass Approximation Theorem, Mathcamp 2009, online: http://www.math.harvard.edu/ waffle/wapproxt.pdf 29

[43] E. J. Cands, Compressive sampling, in Proceedings of the Interna- tional Congress of Mathematicians, (Madrid, Spain), 2006. 43, 45, 85

[44] E. Candes, J. Romberg, and T. Tao, Stable signal recovery from incomplete and inaccurate measurements, math/0503066, Mar. 2005. 43, 46

[45] E. Candes and T. Tao, Decoding by linear programming, math/0502327, Feb. 2005. 43, 88

[46] E. J. Candes and T. Tao, Near-Optimal signal recovery from random projections: Universal encoding strategies, IEEE Transactions on Information Theory, vol. 52, no. 12, pp. 54065425, 2006. 43

[47] E. Candes and M. Wakin, An introduction to compressive sampling, IEEE Signal Processing Magazine, vol. 25, no. 2, pp. 2130, 2008 43, 44

[48] Z. Tian and G. Giannakis, Compressed sensing for wideband cognitive radios, in Acoustics, Speech and Signal Processing, 2007. ICASSP 2007. IEEE International Conference on, vol. 4, pp. IV1357IV1360, 2007. 43, 44, 49

[49] M. A. Davenport, M. B. Wakin, and R. G. Baraniuk, Detection and estimation with compressive measurements, technical, Rice University, 2007. 43

[50] M. Duarte, M. Davenport, M. Wakin, and R. Baraniuk, Sparse signal detection from incoherent projections, in Acoustics, Speech and Signal Processing, 2006. ICASSP 2006 Proceedings. 2006 IEEE International Conference on, vol. 3, p. III, 2006. 43, 46

[51] W. Guibene, D. Slock, *Signal Separation and Classification Algorithm for Cognitive Radio Networks*, ISWCS12, The 9th International Symposium on Wireless Communication Systems, August 28-31, 2012, Paris, France 57

[52] Panaitopol, D; Bagayoko, A; Mouton, C; Delahaye, P; Abril, G; *Primary User Identification when Secondary User is Transmitting without using Quiet Period*, 12th International Symposium on Communications and Information Technologies (ISCIT 2012), Gold Coast, Australia, October 2012 57

[53] SACRA FP7 project, Deliverable 2.2, "Spectrum and Energy Efficiency through multi-band Cognitive Radio," version 1.1, Jan. 2012. 57

[54] Contribution to learning and decision making under uncertainty for Cognitive Radio, Ph.D dissertation, June 15 2012, Supelec Rennes. 57

[55] W. Jouini, C. Moy, J. Palicot. Decision making for cognitive radio equipment: analysis of the first 10 years of exploration, EURASIP Journal on Wireless Communications and Networking 2012, 2012:26. 57

[56] S. Chaudhari, V. Koivunen, H. V. Poor, Autocorrelation-Based Decentralized Sequential Detection of OFDM Signals in Cognitive Radios," *IEEE Trans. Sig. Proc.*, vol. 57, no. 7, pp. 2690–2700, July 2009. 63, 76

[57] M. Naraghi-Pour and T. Ikuma. *Autocorrelation-based spectrum sensing for cognitive radios*. IEEE Transactions on Vehicular Technology, 59(2), Feb. 2010 16, 18, 64

[58] A. Al-Habashna, A. O. Dobre, R. Venkatesan, C. D. Popescu, "Second-Order Cyclostationarity of Mobile WiMAX and LTE OFDM Signals and Application to Spectrum Awareness in Cognitive Radio Systems," *IEEE J. Sel. Topics Signal Process.*, vol. 6, no. 1, pp. 26–42, Feb. 2012. 62

[59] A. V. Dandawate and G. B. Giannakis, *Statistical tests for presence of cyclostationarity*, IEEE Trans. Signal Process., vol. 42, no. 9, pp. 23552369, Sep. 1994 63, 71

[60] M. Gautier, V. Berg, D. Noguet, *Wideband frequency domain detection using Teager-Kaiser energy operator*, IEEE 5th International Conference on Cognitive Radio Oriented Wireless Networks and Communications (Crowncom'12), Stockholm, Sweeden 2012 64

[61] D. Danev, "On signal detection techniques for the DVB-T standard", *Proc. ISCCSP*, March 2010. 66

[62] Final draft ETSI EN 300 744 V1.5.1 (2004-06), "Digital Video Broadcasting (DVB): Framing structure, channel coding and modulation for digital terrestrial television", June 2004. 66

[63] 3GPP TR 36.913 V8.0.1 (Release 8), Requirements for further advancements for E-UTRA, March 2009. 66

[64] LTE Simulator, http://www.nt.tuwien.ac.at/ltesimulator/ 66

[65] C. Mehlfuhrer, M. Wrulich, J. C. Ikuno, D. Bosanska, M. Rupp, âSimulating the Long Term Evolution physical layer,â *Proc. EUSIPCO*, Aug. 2009 66

[66] D. Birru, K. Challapali, and B. Dong, Detection of the presence of television signals embedded in noise using cyclostationary toolbox, in US Patent 2010/0157066, 2010 71

[67] D. Panaitopol, A. Bagayoko, P. Delahaye, and L. Rakotoharison, Fast and Reliable Sensing Using a Background Process for Noise Estimation, in In Proc. CrownCom, 2011 71

[68] 73, 76

R. C. Gonzalez, R. E. Woods, S. L. Eddins, "Morphological Reconstruction," *Digital Image Processing using MATLAB*, MathWorks, 2010, Available online: http://www.mathworks.co.uk/

[69] C. Smith, R. Black, M. Magee, âÃÃ¶âÃâ«Computer Vision for Improved Single-Sensor Spectrum Sensing," *Proc. SSPD*, London, UK, Sept. 2012. 73

[70] W Guibene, D Slock, A combined spectrum sensing and terminals localization technique for cognitive radio networks, Wireless and Mobile Computing, Networking and Communications (WiMob), 2012 IEEE 8th International Conference on, Barcelona, Spain, October 8-10, 2012 85

[71] W Guibene, D Slock, A compressive sampling approach for spectrum sensing and terminals localization in cognitive radio networks, Computer Aided Modeling and Design of Communication Links and Networks (CAMAD), 2012 IEEE 17th International Workshop on, Barcelona, Spain, September 17-19, 2012 85

[72] Xue. L; Qian H.; Chakravarthy, V.; Zhiqiang Wu, Joint spectrum sensing and primary user localization for cognitive radio via compressed sensing, IEEE Military Communications Conference, 2010 - MILCOM 2010, Oct 31- Nov 3, 2010, San Jose, California, USA.

[73] Mumtaz, S., Bastos, J., Rodriguez, J., Verikoukis, C. Adaptive beamforming for OFDMA using positioning information. In Wireless Advanced (WiAd), 2011 (pp. 7-14). IEEE, 20-22 June 2011, London 85

[74] WHERE2 Consortium, Location-aided PHY/MAC layer design for advanced cognitive radios 85

[75] P. Cheraghi, Y. Ma, and R. Tafazolli, Frequency-domain differential energy detection based on extreme statistics for OFDM source sensing,", Proc. IEEE VTC-SPRING, May 2011, Budapest, Hungary. 85

[76] W. Guibene, D. Slock, Degrees of Freedom of Downlink Single- and Multi-Cell Multi-User MIMO Systems with Location based CSIT, 2013 IEEE 77th Vehicular Technology Conference: VTC2013-Spring, 2-5 June 2013, Dresden, Germany 85

[77] B. Zayen, Sspectrum Sensing and Resource Allocation Strategies for Cognitive Radio, PhD Thesis, Telecom PariTech, November 2010

[78] D. Needell, Topics in Compressed Sensing, Ph.D Thesis University of California Davis, 2009

[79] S. Muthukrishnan. Data Streams: Algorithms and Applications. Now Publishers, Hanover, MA, 2005. 86

[80] J. A. Tropp and A. C. Gilbert. Signal recovery from random measurements via orthogonal matching pursuit. IEEE Trans. Info. Theory, 53(12):46554666, 2007. 87

[81] D. L. Donoho, Y. Tsaig, I. Drori, and J.-L. Starck. Sparse solution of underdetermined linear equations by stagewise Orthogonal Matching Pursuit (StOMP). Submitted for publication, 2007 87

[82] M. Fornasier and H. Rauhut. Iterative thresholding algorithms. Preprint, 2007 87

[83] T. Blumensath and M. E. Davies. Iterative hard thresholding for compressed sensing. Preprint, 2008. 87

[84] D. Needell and J. A. Tropp. CoSaMP: Iterative signal recovery from incomplete and inaccurate samples. ACM Technical Report 2008-01, California Institute of Technology, Pasadena, July 2008 87

[85] D. Needell and R. Vershynin. Uniform Uncertainty Principle and Signal Recovery via Regularized Orthogonal Matching Pursuit. Springer Foundations of Computational Mathematics June 2009, Volume 9, Issue 3, pp 317-334 87

[86] Urban transmission loss models for mobile radio in the 900 and 1800 MHz bands, 1991. 93

[87] E.J. Candes, The Restricted Isometry Property and Its Implications for Compressed Sensing, Elsivier Theory of Signals/Mathematical Analysis, Volume 346, Issues 910, May 2008, Pages 589592 88

[88] J. Mitola and G. Maguire, "Cognitive radio: making software radios more personal," *Personal Communications, IEEE*, vol. 6, no. 4, pp. 13–18, 1999.

[89] Yuan, G., Zhang, X., Wang, W., & Yang, Y. (2010). Carrier aggregation for LTE-advanced mobile communication systems. Communications Magazine, IEEE, 48(2), 88-93.

[90] Sacra consortium, "SACRA scenario study and system definition", SACRA D1.1v2.0, Delivered 01/07/2011.

[91] Sacra consortium, "Integration specification", SACRA D6.2v2.0, Delivered 13/04/2012.

[92] Sacra consortium, "Integration specification", SACRA D6.2v2.0, Delivered 13/04/2012.

[93] Official Web Page. OpenAirInterface. http ://www.openairinterface.org.

[94] Sacra consortium, "Validation report of integrated functionality, SACRA D4.4v1.0, Delivered 30/09/2012.

[95] A. Hekkala, I. Harjula, D. Panaitopol, T. Rautio, and R. Pacalet, "Cooperative spectrum sensing study using Welch periodogram," 11th International Conference on Telecommunications (ConTEL 2011). Graz, Austria, 15-17 June 2011, pp. 67-74.

[96] Sacra consortium, "Preliminary Report on Sensing and Access Techniques Design", SACRA D2.1v1.0, Delivered 30/12/2010.

[97] D. Danev, "On signal detection techniques for the DVB-T standard", in Proceedings of the 4th International Symposium on Communications, Control and Signal Processing, March 2010.

APPENDIX A

Resume en Francais

A.1 Introduction

Au cours des dernières décennies, nous avons assisté à de grands progrès et à un besoin croissant de systèmes de communication sans fil en raison de la demande des clients de disposer de dispositifs plus souples, sans fil, plus petits, plus intelligents et pratiques expliquant les marchés envahis par les smartphones, les assistants numériques personnels (PDA), tablettes et netbooks. Le spectre des fréquences radioélectriques (RF) est l'un des domaines d'attention pour relever ce défi. Alors que presque tout le spectre RF est attribué [1], il est en grande partie inutilisé ou sous-utilisé [1]. Le processus actuel d'attribution de spectre pour les communications sans fil est très inefficace, ce qui entraîne une sous-utilisation importante du spectre face à une croissance explosive de la demande. Par exemple, en juin 2010, l'administration Obama a ordonné à la NTIA de collaborer avec la Commission fédérale de la communication (FCC) "pour mettre à disposition un total de 500 MHz de spectre fédéral et non fédéral au cours des dix prochaines années pour l'utilisation large bande sans fil fixe et fixe "[2]. En conséquence, la NTIA, la FCC et d'autres organisations examinent de près l'attribution et l'utilisation actuelles du spectre RF pour identifier les bandes de spectre candidates à la réallocation, au partage et à l'accès dynamique au spectre (DSA).

Historiquement, la radio cognitive (RC) a été introduite par Mitola [3, 4], en tant qu'un des moyens possibles qui pourrait être déployé en tant qu'appareils ou systèmes en réseau sans fil et offrant un accès dynamique au spectre et au partage du spectre. Tel que défini à l'origine, un CR est un appareil conscient et autonome qui peut s'adapter aux changements de l'environnement sans fil. De tels dispositifs permettent de modifier facilement les paramètres sans fil d'un réseau et d'adapter leurs paramètres radio aux nouvelles opportunités détectées.

L'UIT-R a donné une autre définition intéressante des systèmes de radiocommunication cognitifs dans [5]: Â«un système de radiocommunication utilisant une technologie qui permet au système de connaître son environnement opérationnel et géographique, ses politiques établies et son état interne; à ajuster de manière dynamique et autonome ses paramètres d'exploitation et ses protocoles en fonction de ses connaissances acquises afin d'atteindre des objectifs prédéfinis; et d'apprendre des résultats obtenus ".

Les fonctions principales des radios cognitives sont [6,7]:

1. Détection du spectre: ce qui est une exigence importante pour la mise en œuvre et la faisabilité de la radiocommunication, car celle-ci détecte les opportunités de spectre disponibles (également appelées Spectrum Holes or Spectrum White Spaces). Trois stratégies existantes existent pour effectuer la détection du spectre: Détection d'émetteur (impliquant la détection de PU techniques), la détection coopérative (impliquant des systèmes centralisés et distribués) et la détection basée sur les interférences.

2. Gestion du spectre: qui capture les opportunités de spectre les plus satisfaisantes afin de satisfaire à la fois la qualité de service (QoS) des unités de traitement (PU) et de la SU (utilisateurs secondaires).

3. Spectrummobilité: ce qui implique des mécanismes et des protocoles autorisant la fréquence des sauts de fréquence et l'utilisation du spectre dynamique.

4. Partage du spectre: vise à fournir une stratégie de partage juste du spectre afin de desservir un maximum de SU.

Une autre définition du système a été donnée par FCC dans [8]. Dans cette définition, FCC considère une radio comme étant cognitive lorsqu'elle présente les fonctionnalités suivantes:

1. Agilité de fréquence: capacité d'une radio à modifier sa fréquence de fonctionnement afin d'optimiser son utilisation dans certaines conditions.

2. Sélection dynamique de fréquence: possibilité de détecter les signaux d'autres émetteurs proches afin de choisir un environnement de fonctionnement optimal

3. Emplacement Attention: possibilité pour un pays de déterminer son emplacement et l'emplacement d'autres émetteurs, ce qui aiderait à sélectionner les paramètres de fonctionnement appropriés, tels que la puissance d'émission et les fréquences autorisées à cet emplacement donné.

4. Utilisation négociée: incorpore un mécanisme qui permettrait le partage du spectre selon les termes d'un accord préalable conclu entre un utilisateur autorisé (utilisateur principal) et des utilisateurs non agréés (utilisateur secondaire).

5. Modulation adaptative: capacité de modifier et d'adapter les caractéristiques de transmission et les formes d'onde afin d'exploiter les possibilités d'utilisation du spectre.

6. Contrôle de la puissance de transmission: permet une transmission à pleine puissance lorsque nécessaire

L'objectif principal de ce travail est de fournir quelques contributions aux fonctions les plus importantes permettant la reconnaissance des technologies de pointe: la détection de spectres, la reconnaissance du spectre et la découverte de réseaux grâce à la détection et à la localisation coopératives de PU.

A.2 Structure et contributions

Les travaux présentés dans cette thèse 1 s'inscrivent dans le contexte des mécanismes de détection / détection du spectre et de découverte du réseau.

1. Le chapitre 1 est consacré à rappeler certaines définitions et paradigmes utiles de la radio cognitive. Nous commençons par présenter les objectifs et plusieurs problèmes de détection du spectre, puis nous introduisons des algorithmes de détection de pointe. Parmi ces algorithmes, nous sélectionnons des algorithmes de référence à étudier et à simuler en termes de performances, de caractéristiques de fonctionnement du récepteur, de courbes d'efficacité énergétique et d'étude de la complexité. Ensuite, nos contributions sont présentées comme suit:

2. Au chapitre 2 [J1, C8-9, C14-15], nous proposons d'étudier une nouvelle technique de détection du spectre multibande basée sur une banque de filtres reconfigurable. L'algorithme proposé localise certaines fréquences importantes dans le spectre RF caractérisé par des transitions à partir de bandes utilisées. La transmission des PU est ainsi localisée et la détection est effectuée au moyen d'un algorithme de détection d'énergie amélioré. De la même manière que ce qui a été présenté parTianand et Giannakis dans le contexte du capteur pressé à large bande,

3. chapitre 3 [C11-12], nous présentons un algorithme de détection compressé à large bande combinant notre algorithme de localisation de bord de fréquence à la détection comprimée du malisme. Le principal avantage de notre approche est que, contrairement à l'approche en ondelettes de Tian et al., Notre algorithme de localisation des fronts de fréquence est un algorithme non itératif, en ligne (de fonctionnement image par image).

4. Au chapitre 4 [C3, C7], nous proposons de traiter le problème de la classi?cation des signaux dans des systèmes cognitifs hétérogènes. L'approche est un algorithme en deux étapes: tout d'abord, au moyen d'une séparation aveugle des sources, nous séparons le mélange du signal reçu au niveau du CR, puis, grâce à une architecture hybride, nous sommes en mesure de discriminer aveuglément le présent. standard dans une bande détectée (signaux LTE, DVB-T ou PMSE).

5. Au chapitre 5 [C1], nous proposons d'aller plus loin dans l'analyse de la connaissance du spectre en proposant une autre contribution pour la coexistence de normes différentes dans le même cas de bande. Ce cas se produit lorsque l'unité centrale réapparaît dans ses bandes pendant que le SU communie. Dans ce contexte, nous proposons un système cyclostationnaire assisté par Computer-Vision. Algorithme de détection (CV-CFD) ca-

pable de détecter les signaux DVB-T ou PMSE lorsqu'un système LTE transmet dans un intervalle de temps considérablement réduit.

6. Au chapitre 6 [J2, C5-6], nous proposons de mettre l'accent sur un autre aspect principal de la technologie CR, à savoir la connaissance de l'emplacement. Dans ce chapitre, nous analysons les équations liées à la détection du spectre et à l'estimation de l'emplacement des unités centrales en tenant compte de la limitation matérielle dont souffrent souvent les terminaux CR: Convertisseurs analogiques-numériques acquérant des signaux à une vitesse inférieure à Nyquist. Dans ce chapitre, nous établissons un lien entre la localisation, la détection du spectre et la détection comprimée. Dans ce cadre, nous proposons d'étudier la détection / localisation à l'aide de la poursuite de base (BP), de la poursuite d'appariement orthogonal (OMP) et de la poursuite de correspondance par échantillonnage compressif (CoSaMP). Les simulations effectuées dans une topologie de réseau réaliste témoignent de l'efficacité du formalisme proposé.

7. Enfin, au chapitre 7, nous concluons sur le travail présenté, soulignons ses limites et suggérons de nouvelles orientations de recherche.

A.3 Détecteur multibande basé sur banc de filter reconfigurable

Ce chapitre présente une nouvelle technique de détection du spectre basée sur une nouvelle caractérisation des signaux PU dans les communications à large bande. Nous devons d'abord rappeler que, dans les systèmes CR, la première tâche à exécuter par le SU consiste à détecter et à identifier les trous du spectre dans l'environnement sans fil. Ce chapitre résume les progrès de l'approche algébrique. Nous présentons les résultats et le cadre complet de la technique proposée basée sur un détecteur multibande reposant sur une banque de ? ltres recon ? gurable. Le spectre sur une large bande de fréquence est décomposé en blocs élémentaires de sous-bandes bien caractérisées par des irrégularités de fréquence locales. En tant qu'outil mathématique puissant pour l'analyse des singularités et des arêtes, le cadre algébrique est utilisé pour détecter et estimer la structure spectrale irrégulière locale, qui contient des informations importantes sur les emplacements de fréquence et les densités spectrales de puissance des sous-bandes détectées.

Dans ce chapitre, nous avons mis au point une nouvelle technique de détection basée sur une banque de filtres pour les radios cognitives à large bande. La première étape consistait à localiser dans le spectre RF détecté des fréquences spécifiques portant des informations précieuses (transmission entre canaux vacants et canaux occupés). Deuxièmement, nous avons dérivé des filtres adaptés à ces bandes qui nous ont aidés à réduire le bruit d'acquisition et à améliorer la détection d'énergie sur les différentes bandes. Enfin, nous avons montré à travers divers réglages de simulation et données réelles la performance et la robustesse de la technique proposée.

A.4 Détection comprimée pour les radios cognitives à large bande

Récemment, l'échantillonnage à détection / compression comprimée (CS) a été considéré comme une technique prometteuse pour améliorer et mettre en œuvre des systèmes de radio cognitive (CR). En radio large bande, on peut ne pas être en mesure d'acquérir un signal au taux d'échantillonnage de Nyquist en raison des limitations actuelles de la technologie du convertisseur analogique-numérique (CAN) [43]. La détection par compression permet de reconstruire un signal épars en prenant moins d'échantillons que l'échantillonnage de Nyquist. La détection du spectre à large bande est donc réalisable par CS. Un signal épars ou compressible est un signal qui dépend essentiellement d'un nombre de degrés de liberté inférieur à la dimension du signal échantillonné à la fréquence de Nyquist. En général, les signaux d'intérêt pratique peuvent n'être que presque rares [43]. De plus, généralement, les signaux sans fil dans les réseaux ouverts sont rares dans le domaine des fréquences car, en fonction de l'emplacement et parfois du pourcentage d'occupation du spectre, les fréquences radio inactives sont faibles [3, 48].

Dans CS, un signal avec une représentation fragmentée sur une certaine base peut être récupéré à partir d'un petit ensemble de mesures linéaires non adaptatives [49]. Une matrice de détection effectue peu de mesures du signal et le signal original peut être reconstruit avec précision et parfois avec précision à partir d'observations incomplètes et contaminées en résolvant un simple problème d'optimisation convexe [43,44]. Dans [45] et [46], on introduit sur cette matrice de détection des conditions suffisantes pour récupérer le signal d'origine de manière stable. Et remarquablement, une matrice aléatoire remplit les conditions avec une probabilité élevée et effectue une détection efficace [47,49].

Outre la reconstruction du signal d'origine, la détection est plus nécessaire et intéressante dans le contexte de la radio cognitive. En règle générale, il n'est pas nécessaire, pour la détection, de reconstruire le signal d'origine, mais une estimation des statistiques suffisantes pour le problème en question suffit. Ceci conduit à moins de mesures requises et à une complexité de calcul inférieure [50]. Nous souhaitons ignorer l'estimation du signal original et utiliser directement les mesures à des fins de détection, afin de réduire autant que possible la complexité du système.

Dans [48], une approche de détection par ondelettes utilisant CS pour identifier les trous du spectre est introduite. Pour trouver les limites de bande de fréquences, ils développent une formulation d'optimisation convexe selon laquelle la solution donne les limites de bande du spectre sans qu'il soit nécessaire de reconstruire le signal d'origine.

En particulier, développez une combinaison d'échantillons ou de spectres de spectre avec une technique de détection basée sur une méthode algébrique pour la tâche de détection consistant à identifier les trous du spectre. Le détecteur algébrique proposé est un détecteur linéaire et

nous souhaitons alimenter directement l'algorithme avec les mesures comprimées. À cette fin, nous trouvons une matrice de détection appropriée qui permet d'alimenter directement le détecteur algébrique avec les mesures.

Nous présentons dans ce travail une nouvelle technique de détection combinant échantillonnage compressif et méthode algébrique pour détecter les trous du spectre. Dans une première étape, nous avons conçu une matrice de détection comprimée, qui conserve les propriétés linéaires du signal primaire échantillonné. Ensuite, nous avons appliqué les mesures comprimées au détecteur algébrique pour localiser les discontinuités du spectre et identifier les trous du spectre. L'analyse de la complexité de la technique proposée montre qu'elle peut être considérablement réduite lorsque l'ordre des modèles du détecteur algébrique augmente. La comparaison des performances à différentes fréquences d'échantillonnage montre que le nouveau schéma conçu offre de meilleures performances que les détecteurs d'énergie, tout en préservant une faible complexité de calcul.

A.5 Identification de spectre pour les systèmes de radio cognitive basés sur la modulation OFDM

Les travaux présentés dans ce chapitre s'inscrivent dans le contexte de la détection du spectre / du partage du spectre pour les réseaux CR et plus précisément de la détection / identification d'un nœud unique. En rapport avec ce travail, de nombreuses approches statistiques pour la partie détection de spectre ont été développées. Comme indiqué précédemment, l'une des techniques de détection les plus performantes est la détection de caractéristiques cyclostationnaires [7,17]. Le principal avantage de la détection de cyclostationnarité est qu'elle peut faire la distinction entre un signal de bruit et des données transmises par PU. En effet, le bruit n'a pas de corrélation spectrale alors que les signaux modulés sont généralement cyclostationnaires avec une corrélation spectrale non nulle due à la redondance intégrée dans le signal transmis. La technique de détection de référence est le détecteur d'énergie [7], car c'est la technique de détection la plus facile à mettre en œuvre et la moins complexe. D'autre part, certains articles ont été consacrés à la partie relative à l'identification du signal [51–53] et à la prise de décision [54,55], l'accent étant mis sur l'identification de la norme utilisée par les PU plutôt que sur la simple détection de leur présence. Dans ce chapitre, nous présentons une technique de classification robuste basée sur des techniques de séparation de signaux mixtes et de détection de spectre parallèle afin de combiner les caractéristiques de détection / classification du CR.

Dans ce chapitre, nous avons présenté un nouveau schéma de classi?cation robuste. Le cas d'utilisation considéré est un projet de ? guration de con ? guration en réseau wasaheterogen qui, sans perte de généralité, peut être étendu à tout autre scénario de réseau cognitif. La robustesse du classificateur proposé réside dans le choix de l'algorithme de détection pour chaque norme. Dans ce cas, l'AD a été choisi pour le DVB-T parce qu'il était supposé être le meilleur détecteur exploitant les propriétés OFBD DVB-T et l'authentique choix de CDF pour le standard ODF, mais nous avons opté pour l'exploitation de la propriété de bande de ces signaux.

A.6 Une approche de la classification des signaux basée sur la computer vision pour les applications de radio cognitive

Le premier objectif de ce chapitre est d'identifier les méthodes de classification de différents systèmes avec des paramètres et des caractéristiques de signal spécifiques, fonctionnant dans les espaces blancs du téléviseur. Les émetteurs considérés dans notre scénario sont identifiés et caractérisés ci-dessous:

1. Un utilisateur principal (UP) DVB-T qui utilise la modulation OFDM. Comme on le verra plus tard, il existe plusieurs configurations DVB-T, en fonction de

   (a) la largeur de bande (5 MHz, 6 MHz, 7 MHz, 8 MHz) du canal utilisé,

   (b) la modulation (QPSK / QAM / 16-QAM / 64-QAM) utilisée par les sous-porteuses à partir du symbole OFDM,

   (c) les symboles utiles et les périodes de garde: les caractéristiques du système sont prédéfinies par des normes, ainsi que des valeurs ? xes connues pour la période utile TU et TG de garde (cette dernière est également appelée période de préfixe cyclique).

2. Un utilisateur secondaire LTE (SU) utilisant la modulation OFDM (en DL) et SC-FDMA (en UL) associé à BPSK / QAM / 16-QAM / 64-QAM. Les caractéristiques du système avec symboles et périodes de garde fixes (TU et TG) sont prédéfinies par les activités de normalisation 3GPP.

3. Un PMSE PU utilisant la modulation QPSK (bande passante de 400 KHz) ou FM (200 KHz). Hormis la bande passante, les caractéristiques du système ne sont pas très bien définies pour PMSE. Ces dispositifs seront discutés plus en détail dans les dernières sections.

Le deuxième objectif de ce chapitre est de définir les spécifications des algorithmes de classification des signaux à utiliser par les radios cognitives. La classification dans le contexte CRS a pour but de faire la distinction entre plusieurs systèmes émettant en même temps, dans la même bande de fréquences. Parmi tous les scénarios de discrimination possibles (c'est-à-dire entre les SU, entre les SU et les PU, entre les PU), nous avons en outre sélectionné un seul (c.-à-d. Entre les SU et les PU), qui semble être le plus pertinent.
Même si la coexistence entre SU (SU / SU) est un cas très intéressant, la coexistence LTE ne devrait être traitée que dans le contexte de coexistence entre opérateurs. Cette déclaration est justifiée par le fait que les opérateurs existants peuvent aisément être gérés par une entité

supérieure qui gère la gestion des ressources (les eNodeB sont connectés via des interfaces X2 et peuvent facilement gérer l'allocation de ressources intra-opérateur). L'opérateur utilisera son propre spectre de fréquences sans recourir à aucune technique de classification. Par conséquent, seule la coexistence entre opérateurs peut justifier la classi ? cation, mais elle sort du cadre de ce travail.
La coexistence de différentes PU (coexistence PU / PU) semble peu réaliste, car, par définition, une PU occupe une bande de fréquences sous licence et 2 unités données ne partagent pas la même bande de fréquences sous licence.
En ce qui concerne la coexistence entre les SU et les PU (c'est-à-dire la coexistence SU / PU), nous supposons que le SU devrait viser le point de vue opportuniste et ensuite le PU commencer à émettre. Cependant, pour que la détection fonctionne avant d'accéder au spectre de façon opportuniste, le scénario de classification unique est valide lorsque la PU n'est pas présente (ou n'est pas détectée), le système SU commence à communiquer avec TVWS et, à l'heure inconnue, à un UP, il transmet une communication pour le premier temps. Dans ce scénario, le système SU doit procéder à une classification afin de discriminer les signaux provenant de son propre système et de ses transmissions PU.
La classification est donc nécessaire pour un SU afin de faire la distinction entre son propre réseau et un PU qui commençait à utiliser le même spectre à un moment donné et sans aucune période de repos établie par le système du SU.
L'objectif de cette étude était de détecter lors de la réception et du décodage des données (contrainte très forte), mais dans ce cas, le choix du temps de détection n'affectera pas la qualité de service. L'avantage d'utiliser la classification au lieu de QP est que le temps de classification peut être (théoriquement) aussi long que possible.
Notre conclusion est également que les exigences proposées par la FCC en matière de détection peuvent être adaptées à la classi ? cation. Veuillez également noter que l'exigence de classification dépend des paramètres suivants:

1. Temps de détection;
2. NF (figure de bruit de la chaîne d'amplification de LTE Rx);
3. Configuration LTE - qui donne la fréquence d'échantillonnage utilisée et la taille de BW de détection;
4. La quantité de DVB-T / PMSE capturée dans le BW analysé.

Pour une largeur de bande de 10 MHz (bande très large), le temps de classification est considérablement réduit de 250 ms à 125 ms afin de répondre aux exigences du système en matière de détection DVB-T.

A.7 Détection spectrale et localisation coopératives dans la radio cognitive

La radio cognitive est un concept de communication intelligente sans fil capable de promouvoir l'efficacité de l'utilisation du spectre en exploitant les bandes de fréquence libres du spectre, à savoir les trous de spectre [3,4].

La détection des trous dans le spectre est l'une des premières étapes de la mise en œuvre d'un système de radiocommunication cognitif. Elle est appelée détection de spectre.

Le problème majeur qui se pose dans le domaine de la radio à large bande est le fait qu'il est possible que l'on ne puisse pas acquérir un signal au-dessus de la sélection d'un échantillonnage en utilisant les limites actuelles de la technologie du convertisseur analogique-numérique (ADC) [43]. La détection par compression permet de reconstruire un signal épars en prenant moins d'échantillons que l'échantillonnage de Nyquist. La détection à spectre large bande est donc réalisable par Compressed Sensing (CS). Un autre aspect de la faisabilité et de la mise en œuvre concrète des systèmes de communication reconnus est le problème de la connaissance de la localisation [70, 71]. Ce problème se pose lorsque nous envisageons un scénario réaliste dans les systèmes hybrides superposition / sous-couche, lorsque ces possibilités de spectre permettent aux radios cognitives de transmettre en deçà du seuil de tolérance des utilisateurs principaux. Dans ce cas, la radio cognitive doit vérifier de manière fiable que les utilisateurs principaux se trouvent dans le réseau pour adapter sa fonction de puissance de transmission à l'emplacement estimé dans le réseau. La connaissance des informations de position dans CRS facilite également la formation de faisceaux en fonction de la localisation, comme indiqué dans [73] et dans le projet ICT-WHERE2, un ensemble complet de techniques de localisation de PHY / -MAC aidées par la localisation [74] avec de nouvelles techniques de simulation de la perspective informations [75], vers des systèmes MIMO multicellules et multi-utilisateurs avec CSIT basé sur la localisation [76].

Dans notre approche1, nous proposons d'analyser tous ces problèmes. Lors de la formulation du problème et en analysant plus en profondeur les équations liées à chaque question, nous établirons le lien entre la formulation de la détection du spectre, la connaissance de la localisation et la limitation matérielle en décrivant ces problèmes dans un formalisme de détection compressé unique.

Ce travail présente un premier regard vers une tâche combinée de détection du spectre et de localisation. Ces deux tâches sont fondamentales pour permettre la connaissance dans les réseaux sans fil. Avec la combinaison des deux tâches, nous avons également pris en compte une contrainte d'acquisition de données réaliste, qui est faible en raison des limites de la technologie ADC. Les résultats de simulation de la technique proposée montrent des résultats prometteurs et intéressants pour les techniques de détection comprimées appliquées

à ce formalisme.
Le formalisme que nous avons élaboré dans ce chapitre est le point de départ de tout un lieu, grâce à la connaissance du cadre de travail, au développement du projet FP7WHERE-2. Dans ce cadre, une fois que la carte radio est construite grâce aux demandes de détection et de localisation, les CR sont donc en mesure de communiquer dans les bandes disponibles dans les directions disponibles. Le cadre proposé est donc un élément clé de l'accès multiple par division (SDMA). systèmes. Et ce formalisme peut également être exploité pour la communication D2D (appareil à appareil), car les CR peuvent communiquer directement les uns avec les autres tandis que le centre de fusion peut jouer le rôle d'entité de contrôle dans le réseau.

A.8 Résumé

Dans ce travail, nous avons abordé plusieurs aspects liés à la technologie de la radio cognitive:

Tout d'abord, nous avons présenté un nouveau détecteur multibande capable de localiser à l'aveugle les limites de la communication PU dans le spectre RF, permettant ainsi une utilisation plus efficace du spectre en exploitant toutes ses parties fragmentées, ses intervalles de garde, etc. L'architecture proposée est également intéressante car les filtres proposés prennent en compte la réduction du bruit et permettent ainsi de multiples applications du cadre proposé. Nous avons montré à travers divers scénarios de simulation et mesures réelles l'efficacité et la performance du détecteur d'énergie amélioré proposé, associé à ce cadre.

La deuxième contribution est également liée à la détection du spectre compressé à large bande. L'amélioration par rapport aux techniques de pointe réside dans le fait que l'algorithme de localisation de bord de fréquence proposé est un algorithme non itératif, unique et en ligne. La performance de cette technique a été comparée à la technique de pointe et présente quelques améliorations.

La troisième contribution est liée à la sensibilisation au spectre. Dans cette contribution, nous avons développé une nouvelle technique de classification dans un scénario radio cognitif hétérogène. Ce classi ? cateur est basé sur la séparation de signaux mixte et de multiples techniques de détection parallèle pour les signaux DVB-T, LTE et PMSE. Chaque détecteur a été sélectionné afin d'optimiser la détection par rapport à un standard donné. Une règle de fusion a été dérivée comme une combinaison de ratios de vraisemblance permettant de mettre en évidence à chaque fois une norme unique.

Une autre contribution à la connaissance du spectre a été proposée en tant que technique interdisciplinaire de la classification des signaux héritant de certains outils de traitement d'images. Nous avons dérivé plusieurs applications de la technique proposée. Tout d'abord, en tant que technique de détection du spectre, nous avons montré à quel point cette technique était performante, avec des améliorations de près de 50% par rapport à la technique originale CFD. Une deuxième application concernait la classification du signal. Ici, l'usage ciblé détecte le système PU (DVB-T, PMSE) pendant que SU transmet (LTE). Nous avons montré à quel point la technique proposée est performante en termes de réduction de la période de classification tout en tenant compte des recommandations standard en termes de niveau de bruit.

La dernière contribution présentée est un mécanisme semblable à la découverte de réseau pour les systèmes de radiocommunication cognitifs basé sur la détection comprimée (CS). Dans ce chapitre, nous avons formulé la détection du spectre et la localisation d'émetteurs PU dans un formalisme CS. La densité est exploitée dans les deux sens: pour la détection du spectre, la faible densité est due au fait que les CAN ne sont généralement pas en mesure d'acquérir des signaux à la vitesse de Nyquist et cette acquisition de signaux incomplète /

inexacte peut être récupérée au moyen d'une détection comprimée. Un deuxième aspect de la clarté est pris en compte pour la localisation. En effet, lors de la construction de la carte des émetteurs PU à l'aide d'un modèle d'affaiblissement de trajet, la matrice dérivée caractérisant les transmissions PU est une matrice creuse au sens où seules quelques entrées sont non nulles. Nous pouvons donc appliquer le même algorithme pour récupérer ces positions.

A.9 Limites

Bien que certains résultats intéressants aient été présentés dans les contributions, certaines limitations existent également.

Dans la première contribution, nous voyons clairement que l'amélioration de la détection du spectre des banques de filtres classiques entraîne des coûts supplémentaires. Ceci est dû au calcul des limites de fréquence et des extra-filtres que nous dérivons afin d'aider à la réduction du bruit. L'ef ? cacité énergétique est également perdue lorsque nous utilisons des polynômes d'ordre élevé dans le modèle de spectre par bande.

Dans le formalisme CS qui a été présenté, la limitation est sous la forme de la matrice dérivée, car elle est très spécifique pour cette application et ce contexte et nous perdons trop en général car la matrice CS est déterministe.

L'algorithme de séparation et de classification de signaux mixtes proposé au chapitre 5 est basé sur l'algorithme FastICA, qui est une tâche itérative, consommant beaucoup de temps, consomme de l'énergie et fonctionne de manière flexible. L'autre hypothèse majeure retenue ici est que le terminal cognitif a suffisamment de degrés de liberté pour effectuer cette séparation.

Au chapitre 6, il est vrai que le temps requis pour la classification est presque divisé par deux, ce qui représente un progrès considérable, mais la complexité introduite par les outils de Vision par Ordinateur utilisés est également importante et prend beaucoup de temps.

Dans le chapitre 7, le cadre utilisé est évidemment une configuration LOS dans laquelle la PU se trouve dans sa zone de protection et les terminaux cognitifs évitent de transmettre dans les bandes de la PU. Le problème est que dans les systèmes du monde réel, les unités centrales et les unités d'organisation ne sont pas distribuées de cette manière. Certains cas d'utilisation des communications D2D ou M2M pourraient encore exploiter ce cadre. L'autre problème est que les émetteurs primaires sont supposés être des infrastructures ? xées. Alors, comment savoir comment exploiter davantage ce cadre pour répondre au moins à la mobilité des piétons?

A.10 Directions futures

Encore quelques problèmes et quelques idées peuvent compléter le travail présenté:

Détection du spectre: L'avenir de la détection du spectre dans les systèmes de radiocommunication cognitifs réside dans les techniques aveugles à haute efficacité énergétique qui complèteront la détection du spectre basée sur des bases de données de géolocalisation. Pour ces architectures hybrides, nous avons un travail en cours sur un algorithme de sélection de modèle aveugle utilisant Variational Bayes.

Sensibilisation au spectre: Certains problèmes restent en suspens dans la sensibilisation au spectre, notamment en ce qui concerne la réduction du temps de détection de la transmission par l'opérateur historique. Dans les techniques proposées, il y a une certaine amélioration du temps de détection mais au prix d'ajouter de la complexité à l'ensemble du système.

Vers des communications vertes: Une autre direction intéressante qui ramène Cognitive Radio à la lumière des projecteurs est la communication (cognitive) verte. Les algorithmes de couche PHY, en plus des mécanismes MAC, sont étudiés sous réserve de la minimisation de la consommation d'énergie. Cet aspect est assez intéressant à voir car ces contraintes d'économie d'énergie (en particulier du côté de l'équipement utilisateur) sont les paramètres clés pour voir les terminaux cognitifs envahir les marchés dans un proche avenir.

APPENDIX B

Considered Signals Physical Parameters

B.1 LTE System considerations

The LTE system considerations are useful for 2 distinct reasons:

1. The classification device has to classify PU signals, without erroneously classifying LTE SU instead. For this purpose, one has to know the LTE symbol period and the LTE useful period.

2. The classification device has to be a User Equipment, which means that the clock frequency and the bandwidth configurations are LTE compliant. As we will further show in the next paragraphs, each system configuration has distinct parameters. The most important ones are the sampling frequency (for a given sensing time, the number of samples impacts the classification) and the system bandwidth (which impacts the total amount of noise captured by the classification device).

B.1.1 LTE Physical Parameters

As being specified by 3GPP, the LTE system can be configured to different frequency bands: 1.4 MHz, 3 MHz, 5 MHz, 10 MHz, 15 MHz, 20 MHz. Corresponding to these frequency bands to be used, the IFFT lengths are: 128, 256, 512, 1024, 1536, and 2048 respectively. Similarly, for reasons related to the legacy with UMTS, the sampling frequency is multiple of UMTS chip period: 3.84/2 MHz, 3.84 MHz, 2x3.84 MHz, 4x3.84 MHz, 6x3.84 MHz, and 8x3.84 MHz respectively.
It is important to mention that IFFT length is a multiple of 2 for practical implementation issues, but the system itself will not use all the subcarriers. Corresponding to different system configurations, the number of subcarriers being used is: 73, 181, 301, 601, 901 and 1201 respectively, with the middle one called DC subcarrier (and which normally has less energy).
As the LTE system bandwidth increases, the total number of the resources increases as well. Therefore, according to the LTE bandwidth being used, the number of resource blocks per

symbol is: 6, 30, 50, 100, 150 and 200 respectively. Modulations used by the LTE systems are QPSK, 16-QAM, and 64-QAM. Depending on the channel, LTE system has the following modulation schemes:

Physical channel	Modulation schemes
PDSCH	QPSK, 16QAM, 64QAM
PMCH	QPSK, 16QAM, 64QAM
PHICH	BPSK
PUCCH	BPSK, QPSK, BPSK+QPSK

Table B.1: LTE Modulation Schemes

Related to the frame structure, there are 20 slots of 0.5 ms in one frame. It is also important to mention that the OFDM symbol is composed from a useful period and a cyclic prefix (see D2.1 for further explanations). However, different from DVB-T, for LTE systems the useful period is constant (T_U=1/(15 KHz)=66,66 μs) but cyclic prefix is not. There are several configurations described below:

1. Normal CP (7 symbols per slot)
   (a) T_{CP}=5.21 μs for the first OFDM symbol from one slot;
   (b) T_{CP}=4.69 μs for the last 6 OFDM symbols from one slot.
   (c) Extended CP (6 symbols per slot): T_{CP}=16.67 μs.
   (d) MBSFN only (7.5 kHz subcarrier spacing), the OFDM useful symbol has T_U=133.33 μs, and the cyclic prefix has T_{CP}=33.33 μs – R9 feature (3 symbols per slot)

B.1.2 Cyclic Prefix (CP) in LTE

As stated in the previous section, for the normal CP configuration, the CP is not constant. The figure below resumes the impact of having distinct CPs and different sampling rates for different LTE BW configurations.
This configuration, of course, will impact the classification properties of LTE systems. Please note that based on this configuration, we have developed an LTE signal generator (for normal and extended CP), and we have used this configuration for different simulations results presented in this chapter.

B.2 Primary User Considerations

This section describes the DVB-T and PMSE (QPSK and FM) signal parameters. The parameters described in this chapter have been further used for classification purposes. However,

Figure B.1: LTE cyclic prefix and symbol length in number of samples

please note that the classification has to be implemented in the UE LTE device, which means that the PU signals have to be sampled at LTE frequency rate. We have therefore developed primary user signal generators, and we have used these generators for different simulations presented in this chapter.

B.2.1 DVB-T Physical Parameters

The guard interval precedes every OFDM symbol and it helps mitigating the inter-symbol interference. Echoes of the previous symbol should abate within the guard interval. Otherwise the echoes would disturb the following OFDM symbol and increase the Bit Error Ratio (BER). Therefore, the required length of the guard interval depends on the application to be covered. An OFDM symbol is composed of two parts: a useful part with duration T_U and a guard interval with a duration T_{CP}. The guard interval consists in a cyclic continuation of the useful part, T_U, and is inserted before it. A longer guard interval could compensate longer echoes [18]:

- lengthening the guard interval without changing the absolute duration of the useful interval would accordingly decrease the channel capacity, thus reducing the deliverable bit rate;
- alternatively, lengthening both the guard interval and the useful interval would not bring any penalty to the channel capacity, but would make the signal processing more difficult because of the higher number of carriers that would result from the larger symbol duration.

In summary, the following parameters can be chosen in the DVB-T system:

- code rate of inner error protection: 1/2, 2/3, 3/4, 5/6, 7/8.
- carrier modulation: QPSK – 2 bit per carrier; 16-QAM – 4 bit; or 64-QAM – 6 bit.

- guard interval length: 1/4, 1/8, 1/16, 1/32.
- modulation parameter ?1 for non-hierarchical; 2 or 4 for hierarchical.
- FFT length which can be related to the number of carriers:
  - 2k mode with 1 705 carriers,
  - 4k mode with 3409 carriers (DVB-T handheld),
  - 8k mode with 6 817 carriers.
- T_U/T_S: 4/5, 8/9, 16/17 or 32/33 depending on guard interval.

According to [19] the useful symbol period T_U of DVB-T is:

- For 8 MHz DVB-T channel:
  - 896 μs (8k mode),
  - 448 μs (4k mode),
  - 224 μs (2k mode)
- For 7 MHz DVB-T channel:
  - 1024 μs (8k mode),
  - 512 μs (4k mode),
  - 256 μs (2k mode)
- For 6 MHz DVB-T channel:
  - 1194,667 μs (8k mode),
  - 597,333 μs (4k mode)
  - 298,6667 μs (2k mode)
- For 5 MHz DVB-T channel (normative):
  - 1433,6 μs (8k mode),
  - 716,8 μs (4k mode),
  - 358,4 μs (2k mode).

DVB-T Cyclic Prefix can be: 1/4, 1/8, 1/16 or 1/32. In our simulations we have considered 8 MHz DVB-T with useful symbol 224 μs and CP 1/4 (T_{CP}=T_U/4).

B.2.2 PMSE Signal Parameters

The following documents provide technical information on Radio microphones: ERC Report 42 [20] and ERC Report 88 [21]. During 1991, ETSI was requested to update T/R 20-06 and this work has resulted in three standards [20]:

1. ETS 300 422 Radio Equipment and Systems (RES); Technical characteristics and test methods for radio microphones in the 25 MHz to 3 GHz frequency range

2. ETS 300 454 Radio Equipment and Systems (RES); Wide band audio links; Technical characteristics and test methods

3. ETS 300 445 Radio Equipment and Systems (RES); Electro-Magnetic Compatibility (EMC) standard for radio microphones and similar Radio Frequency (RF) audio link equipment

Also, another interesting report useful for the PMSE information regarding the standardization is [9] on PU protection for TVWS. In this report it can be found that PMSE can be analogical or digital, with different frequency bandwidths.